Inducible mRNA degradation tools to study transcriptional adaptation in mammalian systems

Dissertation
zur Erlangung des Doktorgrades
der Naturwissenschaften

Vorgelegt beim Fachbereich 15
der Johann Wolfgang Goethe-Universität
in Frankfurt am Main

Von
Gabrielius Jakutis
aus Vilnius, Litauen

Frankfurt 2023
(D30)

Vom Fachbereich Biowissenschaften (FB15) der Johann Wolfgang Goethe-Universität als Dissertation angenommen.

Dekan: **Prof. Dr. Sven Klimpel**

Gutachter: **Prof. Dr. Didier Y. R. Stainier**

Prof. Dr. Ingo Ebersberger

Datum der Disputation: **15.03.2024**

Reviewers

Prof. Dr. Didier Y. R. Stainier
Department of Developmental Genetics
Max Planck Institute for Heart and Lung Research
Bad Nauheim, Germany

and

Prof. Dr. Ingo Ebersberger
Institute of Cell Biology and Neuroscience
Applied Bioinformatics
Frankfurt am Main, Germany

Life is a mystery looking forward and a science looking back

TABLE OF CONTENTS

LIST OF COMMONLY USED ABBREVIATIONS

Abbreviation	Description
ASO	Antisense oligonucleotide
ATAC-seq	Assay for Transposase-Accessible Chromatin using sequencing
BSA	Bovine serum albumin
BCS	Bovine calf serum
cDNA	Complementary DNA
CRISPR	Clustered regularly interspaced short palindromic repeats
crRNA	Crispr RNA
DNA	Deoxyribonucleic acid
DSB	Double-strand break
dsRNA	Double-stranded RNA
EJC	Exon junction complex
FACS	Fluorescence-activated cell sorting
GCR	Genetic compensation response
GWAS	Genome-wide association study
HEK cells	Human embryonic kidney 293 cells
HR	Homologous recombination
lncRNA	Long non-coding RNA
LOF	Loss of function
miRNA	Micro RNA
mRNA	Messenger RNA
NGD	No-go decay
NGS	Next-generation sequencing
NHEJ	Non-homologous end joining
NMD	Nonsense-mediated decay

NSD	Non-stop decay
PBS	Phosphate-buffered saline
PCR	Polymerase chain reaction
PAM	Protospacer adjacent motif
PTC	Premature termination codon
PuroR	Puromycin resistance gene
qPCR	Quantitative real time PCR
RBP	RNA-binding protein
RNA	Ribonucleic acid
RNAa	RNA activation
RNA-seq	RNA sequencing
saRNA	Small activating RNA
sgRNA	Single-guide RNA
siRNA	Small interfering RNA
TA	Transcriptional adaptation
TSS	Transcription start site
UTR	Untranslated region
WT	Wild-type

1. INTRODUCTION

Parts of this chapter have been published as an article in *Annual Review of Genetics* (Gabrielius Jakutis and Didier Y.R. Stainier, *Annu. Rev. Genet.* 2021; https://doi.org/10.1146/annurev-genet-071719-020342). My contribution to the article is described as follows: conceptualization, literature analysis, visualization, writing (original draft, reviewing and editing).

A number of recent genome-wide association studies (GWAS) have revealed that a surprisingly high number of individuals in the common population carry complete loss-of-function (LOF) mutations, yet display no obvious phenotype or disease (GenomeAsia, 2019; Karczewski et al., 2020; Sulem et al., 2015; Yang et al., 2003). E.g., almost 8% of Icelandic population are homozygotes or compound heterozygotes for one or more LOF mutations (Sulem et al., 2015). A different study even reported that each human genome could contain approximately 100 LOF variants, among which approximately 20 genes are completely inactivated (MacArthur et al., 2012). The reason behind not developing any burden or disease in these instances is, likely, genetic robustness, an inherent property of biological systems to withstand various perturbations, including genetic mutations (Kitano, 2007). For many decades, the field of genetic robustness remained relatively uneventful, with periodic emergence of new examples in different animal models. Most of these instances fell under the scope of well-established underlying modes of robustness until a novel mechanism conferring robustness was identified in 2015 (Rossi et al., 2015). The mechanism was termed transcriptional adaptation (TA) and this dissertation will focus on elucidating the previously unknown temporal, as well as mechanistic features of this phenomenon.

1.1 Gene perturbations as a foundation of genetics

The sequencing of the human genome stands as one of the most pivotal milestones in genetics over the past few decades. Not only did it provide the complete sequence of every human gene, but it also revealed the intricate sequences within the vast intergenic regions. These intergenic regions play a significant role in the transcriptional output of our genome, harboring essential regulatory elements such as promoters, enhancers, and noncoding RNAs. Furthermore, this monumental project led to a revision of the estimated number of human genes, shedding light on their structural organization and laying the groundwork for the omics revolution (Lander et al., 2001). It also facilitated the identification of candidate genes associated with various diseases (Moraes & Goes, 2016). Only several years after the completion of the Human Genome Project, in 2007, next-generation sequencing (NGS) technology was developed by Illumina. The 1,000 Genomes Project, initiated in 2008, aimed to sequence the genomes of 2,500 individuals. By 2010, sequencing systems with enhanced throughput capabilities emerged, generating more data points efficiently and expediting the process. Finally, in 2014, crucial improvements across the sequencing chain, including chemistry, imaging, optics, software, and analytics led to the development of high-efficiency dual system imaging sequencers, doubling sequencing output without affecting the costs, ultimately unlocking endless opportunities to sequence any desired genome.

However, despite the passage of 20 years since the Human Genome Project's initial publication and this massive improvement in sequencing technology, a substantial portion, approximately a third, of human genes still lack comprehensive characterization, leaving their physiological importance largely unknown (Stoeger, Gerlach, Morimoto, & Nunes Amaral, 2018). Likewise, approximately one fifth of proteins across all eukaryotic species remain functionally undefined (Wood et al., 2019). The exploration of gene function is primarily facilitated by introducing mutations into an organism's genome and studying the resulting phenotypes. Historically at first, the

understanding of gene function relied on forward genetics, wherein phenotypes were identified first and then linked to specific mutations and loci of interest (Moresco, Li, & Beutler, 2013; Schneeberger, 2014). However, in the 1980s, a reverse genetics approach started to become more prevalent. Although more eukaryotic genomes were being sequenced, the field still lacked precise tools to target specific loci. A significant breakthrough came with the discovery of RNA interference (RNAi) by Fire, Mello, and colleagues (Fire et al., 1998), following the identification of the first microRNA, lin-4 (R. C. Lee, Feinbaum, & Ambros, 1993). Their work in *Caenorhabditis elegans* (*C. elegans*) demonstrated that exogenous double-stranded RNAs (dsRNAs) could selectively silence genes with sequence similarity to the injected dsRNA, offering a targeted approach to rapidly decipher gene function. Nonetheless, similar to other antisense approaches, RNAi often resulted in partial LOF phenotypes (Eisen & Smith, 2008) and carried a probability, ranging from 5% to 80% in various organisms, of off-target effects (Jackson & Linsley, 2010; Qiu, Adema, & Lane, 2005). Consequently, researchers persisted in developing tools for precise genome modification.

The quest for making precise modifications to the genome has long captivated the scientific community. In the late 1970s to early 1980s, the discovery of DNA repair mechanisms hinted at the possibility of targeted genome engineering by inducing DNA breaks (Lindahl, 1974; A. L. Lu, Clark, & Modrich, 1983; Sancar & Rupp, 1983). This led to the development of various techniques, starting with chemical DNA recognition methods such as complementary oligonucleotides, peptide nucleic acids, and cleavage reagent-linked polyamides, as well as self-splicing introns and homing endonucleases. Subsequently, more sophisticated approaches emerged, including zinc finger nucleases (ZFNs) and transcription activator-like effector nucleases (TALENs) (Bibikova, Golic, Golic, & Carroll, 2002; Christian et al., 2010; Doudna & Charpentier, 2014). These techniques allowed for site-specific modifications by inducing double-strand breaks that often resulted in small insertions or deletions causing frameshift mutations (Carlson et al., 2012). However, ZFNs

and TALENs required intricate design, synthesis, and validation processes; therefore naturally, the field of mutant generation saw a significant boost with the discovery of type II CRISPR-Cas systems, particularly the CRISPR-Cas9 technology. Initially identified in 1987 (Ishino, Shinagawa, Makino, Amemura, & Nakata, 1987) and later recognized as a bacterial adaptive defense system against viral infections (Makarova, Grishin, Shabalina, Wolf, & Koonin, 2006), clustered regularly interspaced palindromic repeats with associated helicase and nuclease domain-containing proteins, or CRISPR-Cas systems, were shown to be guided by mature CRISPR RNAs (crRNAs) (Brouns et al., 2008) and comprised at least three different types (I, II, and III), based on their unique nucleic acid recognition and cleavage mechanisms (Makarova, Aravind, Wolf, & Koonin, 2011). At the moment, there are at least six types of CRISPR-Cas systems (I through VI), belonging to two large classes based on whether Cas effectors contain multiple subunits (class 1; types I, III, and IV) or are single large proteins (class 2; types II, V, and VI) (Makarova et al., 2020). Landmark papers published in 2012 demonstrated that CRISPR-Cas9-crRNA complexes could be programmed for specific sequence recognition and DNA cleavage (Gasiunas, Barrangou, Horvath, & Siksnys, 2012; Jinek et al., 2012). Since then, CRISPR-Cas9 has become the go-to tool for genome editing, and its toolbox has expanded to include additional Cas enzymes like Cas3, Cas12, Cas13, and the Cascade complex, each offering unique target recognition sequences and cutting properties, unlocking vast possibilities for genome editing. Furthermore, the development of super-precise CRISPR systems, such as cytosine and adenine base editors fused to a catalytically impaired Cas9 protein, has enabled recognition of noncanonical protospacer adjacent motifs (PAMs) and minimized off-target mutations, enhancing the precision and versatility of targeted genome editing (Doman, Raguram, Newby, & Liu, 2020; Miller et al., 2020). However, it is worth noting that manipulating the same gene using different approaches can yield diverse phenotypic outcomes.

1.1.1 Gene function disruption by knockdown approaches

Within the scope of techniques to disrupt gene function, the knockdown approach typically involves silencing gene expression at the transcriptional or translational level, without introducing modifications to the genome. A widely utilized method for knockdown is RNA interference (RNAi), which operates through a conserved pathway where small noncoding RNAs and associated proteins regulate gene expression (Carthew & Sontheimer, 2009). RNAi encompasses three major modes: (a) microRNAs (miRNAs), prevalent in eukaryotes, which govern numerous biological processes including cell growth, tissue differentiation, and disease progression (Wilson & Doudna, 2013); (b) small interfering RNAs (siRNAs), either endogenous or exogenous inducers of RNAi, utilized for targeted gene repression (Snead & Rossi, 2010); and (c) animal-specific PIWI-interacting RNAs (piRNAs). Distinct from miRNAs and siRNAs, piRNAs are produced independently of the endoribonuclease Dicer and are specifically expressed in the germline (Klattenhoff & Theurkauf, 2008). However, piRNAs still play a crucial role in gene regulation by promoting heterochromatin assembly, DNA methylation, and the suppression of transposable elements and viral infections (Ozata, Gainetdinov, Zoch, O'Carroll, & Zamore, 2019).

siRNA offers a significant advantage in that the cellular machinery responsible for silencing is present in a wide range of eukaryotic cells (Shabalina & Koonin, 2008). Moreover, in plants and *C. elegans*, RNAi silencing exhibits heritability, as nematode hermaphrodites treated with siRNA produce progeny with depleted target mRNAs from both the maternal and zygotic sources (Grishok, Tabara, & Mello, 2000). In *Drosophila*, siRNAs are frequently employed in tissue-specific screens and analyses (Dietzl et al., 2007). Additionally, the convenience of siRNA treatment lies in the absence of prior modifications required for the cells of interest, and the delivery of RNAi agents is relatively straightforward. The specificity of siRNAs can be finely tuned to target specific mRNA isoforms or disease-specific alleles (Aagaard & Rossi,

2007). Furthermore, the ability to induce partial LOF phenotypes enables the study of genes essential for viability.

miRNAs also play a crucial role in zebrafish development, as evidenced by the phenotype observed in *dicer* mutants, which cease development at 10 days post-fertilization (Wienholds, Koudijs, van Eeden, Cuppen, & Plasterk, 2003). Nevertheless, the siRNA approach has not been widely adopted in the zebrafish field, primarily due to the interference between injected siRNAs and the biogenesis and activity of essential endogenous miRNAs (Zhao, Fjose, Larsen, Helvik, & Drivenes, 2008), as well as the activation of the innate immune response (Seok, Lee, Jang, & Chi, 2018). Instead, the most prevalent method for gene knockdown in zebrafish utilizes morpholino antisense oligomers. Morpholinos are chemically synthesized oligomers consisting of a 25-nucleotide chain with a morpholine ring in place of a ribose ring. They target mRNAs through complementary binding, preventing their splicing or translation (Corey & Abrams, 2001). The unique structure of morpholinos enhances their stability by protecting them from nuclease activity, distinguishing them from other antisense reagents. Moreover, the absence of a negatively charged backbone in morpholinos reduces the likelihood of interactions with other cellular components, thereby mitigating their toxicity to some degree (Eisen & Smith, 2008). However, since morpholinos typically do not induce target RNA degradation, assessing knockdown efficiency can be challenging, especially when employing translation-blocking morpholinos that do not affect splicing patterns (Pauli, Montague, Lennox, Behlke, & Schier, 2015).

Antisense oligonucleotides (ASOs) present an alternative approach in the arsenal of gene knockdown techniques. They consist of synthetic DNA (or RNA) oligomers or single-stranded RNA-DNA hybrids known as gapmers. ASOs elicit the catalytic degradation of complementary cellular RNAs through the action of ribonuclease H (RNase H). To enhance their stability, ASOs are commonly designed with phosphorothioate bonds, while 2'-*O*-methyl RNA modifications provide resistance against nuclease activity (Ideue, Hino, Kitao, Yokoi, & Hirose,

2009). The central DNA region, modified with phosphorothioate, activates RNase H, while the flanking ribonucleotides enhance the binding affinity with the target RNA. ASOs have found utility in gene function studies and are also explored as therapeutic agents for disorders stemming from toxic gain-of-function mutations (Aguti, Marrosu, Muntoni, & Zhou, 2020).

Off-target effects pose a major significant concern in antisense technology. In the case of siRNAs, off-target effects can be categorized as either sequence specific, caused by the complementary binding to non-target mRNAs, or non-sequence specific, arising from interference between miRNA and siRNA processing pathways. The introduction of exogenous dsRNAs can displace endogenous miRNAs from the RNA-induced silencing complex (RISC), leading to disruption of gene expression regulated by these miRNAs (Khan et al., 2009). Furthermore, theoretical calculations indicate that injected morpholinos can surpass target mRNAs at a ratio of thousands to one (Schulte-Merker & Stainier, 2014), inevitably resulting in significant off-target effects that give rise to phenotypic artifacts (Boer, Jette, & Stewart, 2016; Gerety & Wilkinson, 2011) and p53-dependent apoptosis (Robu et al., 2007). While p53 activity can be suppressed, such drastic measures can hinder the evaluation of resulting phenotypes (Schulte-Merker & Stainier, 2014). Additionally, certain animals injected with morpholinos exhibit dose-dependent upregulation of interferon-stimulated genes (*isg15* and *isg20*), the cell death pathway gene *casp8*, and various cellular stress response genes (Lai, Gagalova, Kuenne, El-Brolosy, & Stainier, 2019). Another challenge lies in the variable efficiency of different knockdown reagents, often leading to divergent phenotypes even when targeting the same gene, thereby complicating the unified interpretation of results.

1.1.1.1 Using CRISPR-Cas13 to induce gene knockdown

Although CRISPR-Cas systems are typically brought up when scientists discuss generating mutations in the genome and thus knockout alleles, certain members

of the CRISPR-Cas family can be also used to induce gene knockdowns. CRISPR-Cas13 is a class 2, type VI effector that contains two HEPN domains, which facilitate the RNase activity (B. Zhang et al., 2019). Similarly to other CRISPR-Cas effectors, it is guided by a sgRNA; however, targets, in a programmable fashion, exceptionally messenger RNAs without altering the DNA. The Cas13 effectors family comprises four subtypes (a-d), each with distinct properties and efficiency. Among these subtypes, Cas13d demonstrates superior efficiency and specificity in cleaving targeted RNA in the mammalian system (Gupta et al., 2022). Additionally, Cas13d exhibits distinct structural and functional advantages over other Cas13 variants, making it an exceptional and highly effective tool for RNA engineering and of particular value to studying transcriptional adaptation. A significant drawback of Cas13d and Cas13 family in general is their collateral activity. Evolutionarily, Cas13 effector arose to target the transcripts of bacteria-invading DNA genomes and possesses nonspecific RNase activity that is triggered by target recognition to induce dormancy in virus-infected bacteria (Makarova et al., 2020). The property of cleaving non-specific ssRNAs regardless of the perfect base-pairing of the crRNA is highly prevalent in bacterial systems; however, have conflicting reports in mammalian cells or plants, with some studies reporting no collateral cleavage at all (Abudayyeh et al., 2017; Xu et al., 2021), while others indicating broad collateral activity effects (Y. Li et al., 2023; Shi et al., 2023).

1.1.1.2 Mechanisms underlying CRISPR-Cas13-mediated mRNA degradation

In the context of TA and mRNA degradation, it is important to understand how CRISPR-Cas13 triggers mRNA degradation and whether this mechanism can resemble, in any way, one of the endogenous mRNA quality surveillance pathways. Cas13 proteins are typically activated through crRNA and cleave RNA after recognizing the target sequence complementary to that crRNA's spacer (Hillary & Ceasar, 2023). Cas13 possesses a dual-lobe architecture that consists

of a recognition (REC) and a nuclease (NUC) lobes, the latter of which contains two HEPN-endonuclease domains. Upon recognition, binding and loading of the target RNA molecule, Cas13 undergoes a conformational change, whereas the HEPN catalytic site of the activated Cas13 relocates on the outer surface, leading to cleavage of the target RNA outside of the binding region (Wolter & Puchta, 2018). It is worth mentioning that in nonsense-mediated mRNA decay (NMD) surveillance pathway, the predominant decay mechanism is also endonucleolytic cleavage (Boehm et al., 2021), which occurs in close proximity to a premature termination codon (PTC). Furthermore, Cas13 binding of the target RNA can hypothetically impede the progression and promote stalling of translating ribosomes, as demonstrated by several recent studies that have utilized a nuclease-inactive dCas13d (Apostolopoulos, Tsuiji, Shichino, & Iwasaki, 2023; Charles et al., 2021), potentially simulating the no-go decay (NGD) pathway and promoting RNA degradation.

1.1.2 Gene function disruption by knockout approaches

The knockout approach involves disrupting gene function by introducing deleterious mutations into the genome. For a mutation to be considered deleterious, it must negatively affect the function of the gene or regulatory element (Morris, 2015). Such mutations can arise from single-base changes or larger modifications, such as insertions or deletions. Single-base changes often have a neutral impact and result in a protein variant that functions similarly to the wild-type protein, unless they create a PTC. Currently, the preferred method to introduce harmful mutations is by inducing double-strand breaks in the genome, which triggers the DNA damage response. During this response, internal cellular mechanisms detect double-strand breaks through the ATM kinase and the MRE11-RAD50-NBS1 (MRN) complex, initiating a phosphorylation cascade that activates cell cycle checkpoints and DNA repair processes (Vitor, Huertas, Legube, & de Almeida, 2020). Double-strand break

repair can occur through either homologous recombination (HR) or non-homologous end joining (NHEJ) mechanisms.

HR necessitates a template with a homologous DNA sequence, with the sister chromatid being the most commonly utilized template rather than the homologous chromosome (Johnson & Jasin, 2000). Recombination between homologous chromosomes can lead to loss of heterozygosity or other chromosomal abnormalities; thus, HR primarily occurs during the S and G2 phases of the cell cycle while being suppressed in the G1 phase when sister chromatids are not available for repair (Fugger & West, 2016). Furthermore, postreplicative chromatin favors HR by recruiting the Tonsoku-like-Methyl methanesulfonate-sensitivity protein 22-like (TONSL-MMS22L) complex to DNA lesions (Saredi et al., 2016). HR is a precise and accurate repair pathway, which makes it less desirable for generating gene knockouts. However, it can be employed for creating small knock-ins that can result in null alleles. NHEJ directly rejoins the two broken ends, which can lead to insertion and/or deletion events, causing frameshifts, premature termination, and LOF (Chang, Pannunzio, Adachi, & Lieber, 2017). It is worth mentioning that recent research reported instances of precise NHEJ, as observed in Drosophila *Mcm*^{5A7} mutants (Hatkevich, Miller, Turcotte, Miller, & Sekelsky, 2021). In these mutants, the repair of programmed meiotic double-strand breaks is initiated by HR but completed by NHEJ, resulting in accurate repair outcomes.

Frameshift mutations often result in altered protein sequences or premature termination codons (PTCs), triggering the NMD pathway (Kurosaki & Maquat, 2016). NMD has a role in endogenous gene regulation (Lykke-Andersen & Jensen, 2015), but is particularly relevant for generating mutants using sequence-specific nucleases. Pre-mRNAs undergo several maturation steps, including polyadenylation, capping, and splicing, with capping and splicing playing key roles in NMD. Exon junction protein complexes (EJCs) are assembled and deposited at exon junctions during splicing, and EJCs, along with the cap-binding protein (CBP) heterodimer CBP80-CBP20, mark newly

synthesized mRNAs (Maquat, Tarn, & Isken, 2010). PTC encounters lead to ribosome termination, leaving EJCs bound to the mRNA, initiating rapid degradation mediated by NMD proteins UPF1, UPF2, and UPF3 (Lopez-Perrote et al., 2016; Maquat et al., 2010). Besides NMD, NGD and nonstop decay (NSD) pathways can also generate strong mutant alleles by degrading aberrant mRNAs with stacks of ribosomes stalled internally or lacking a stop codon at the terminal end (Shoemaker & Green, 2012). Stalled ribosomes in NGD can result from various factors such as stable intramolecular or intermolecular secondary RNA structures, rare codons, enzymatic cleavage or collisions, leading to ribosome pausing and potential degradation (Navickas et al., 2020). NSD targets truncated mRNAs or those lacking stop codons but containing a poly(A) tail. In NSD, ribosomes pause after incorporating in the nascent polypeptide several positively charged amino acids (lysines or arginines) that electrostatically interact with the negatively charged exit channel of the ribosome, inhibiting further ribosome progression (J. Lu & Deutsch, 2008; Shoemaker & Green, 2012). NSD can be employed to create a strong allele, by incorporating *loxP* sites surrounding the exon containing the stop codon and initiating Cre-mediated recombination (Theodosiou et al., 2016), or by using CRISPR-Cas targeting to delete the ultimate exon (El-Brolosy et al., 2019).

The sequence-specific nuclease technology raises concerns regarding its off-target effects, which have the potential to introduce genomic instability and interfere with the function of non-target sites, complicating the interpretation of phenotypes and potentially affecting mutant viability. Even with up to five base mismatches, the 5' end of the single guide RNA (sgRNA) exhibits tolerance for errors, allowing it to bind unintended genomic loci and trigger off-target DNA cleavage by directing Cas9 (Hsu et al., 2013).

1.1.3 Studying gene function by creating inducible knockdown and knockout systems

Inducible gene expression and perturbation systems can serve as attractive alternatives to stable expression or mutant systems in a wide range of research fields, including functional genomics, gene therapy, tissue engineering, biopharmaceutical protein production, drug discovery, and, perhaps most importantly, generating genetic perturbations on demand (Kallunki, Barisic, Jaattela, & Liu, 2019). These systems offer greater flexibility and reversibility as well as they generally exhibit higher efficiency and fewer undesirable effects, such as cell death or impaired growth, in comparison to constitutive expression methods. Such advantages can open a time window to study lethal mutations or assess what impact gene perturbations have on cell physiology immediately after their occurrence.

Over the years, numerous approaches have been refined to regulate gene expression in a temporal and spatial manner. Many of these strategies have originated from genetic tools established in organisms such as flies and mice, including the UAS-Gal4 system and the Cre-Lox recombination system. In addition, inducible systems based on prokaryotic operons offer a solution for controlling gene expression without genetic modification, with one of the most versatile options being the tetracycline inducible system (Tet-Off and Tet-On) developed by Gossen and colleagues (Gossen & Bujard, 1992).

Several other prokaryotic operons-based inducible systems have been developed in the past years; e.g., a vanillic acid-inducible system (Sunter, 2016), a cumate-inducible system (F. J. Li et al., 2017), as well as an inducible system based on an insect steroid hormone 20-OH ecdysone, where a chimeric protein composed of the VP16 activation domain fused to an ecdysone receptor with altered DNA-binding specificity has been tailored for use in mammalian cells (Oehme, Bosser, & Zornig, 2006). These inducible systems remain as alternatives or add-ons; however, have not surpassed the popularity of the tetracycline inducible system. The major drawback of inducible gene expression

systems is the lack of absolute expression control, also known as 'leakiness' (Hosoya, Chung, Ansai, Takeuchi, & Miyaji, 2021; Y. Zhou, Lei, & Zhu, 2020). In addition, some cell types, such as Chinese Hamster Ovary (CHO) cells, have a significant reduction in proliferation and culture viability when maintained in media supplemented with Doxycycline, even at concentrations commonly reported (Costello et al., 2019). Even with significant upgrades; e.g., by screening and selecting reverse tetracycline-controlled transactivator (rtTA) mutants that are more sensitive to doxycycline and thus require lower concentrations for induction (X. Zhou, Vink, Klaver, Berkhout, & Das, 2006), or optimizing the TRE promoter to obtain lower background expression of the Tet-On system and higher induction of target gene expression (Loew, Heinz, Hampf, Bujard, & Gossen, 2010), the absolute tight control has not been achieved to date. Nevertheless, the less popular, alternative inducible approaches can be used in tandem with the tetracycline-inducible system to increase tightness or control several genes at the same time.

1.2 Discrepancies between knockdown and knockout phenotypes

The abundance of gene knockout tools, particularly the CRISPR-Cas9 technology, has significantly expanded the repertoire of genetic manipulation techniques in the field of genetics, resulting in the generation of numerous mutant organisms. Interestingly, in many instances, knockdown approaches designed to achieve a similar reduction in gene expression often exhibit more pronounced phenotypic effects (Kok et al., 2015). For instance, studies have documented cases such as *Ppara* knockout and knockdown mice, where *Ppara* mutants display hypoglycemia and hypertriglyceridemia following fasting, while animals treated with siRNA targeting *Ppara* exhibit the same abnormal blood glucose and triglyceride profiles even in the absence of fasting (De Souza et al., 2006). Similarly, in *klf2a* knockout and knockdown zebrafish, *klf2a* mutants show unaffected cardiovascular development (Novodvorsky et al., 2015), while embryos injected with morpholinos (morphants) targeting *klf2a*

exhibit severe cardiovascular defects (J. S. Lee et al., 2006; Nicoli et al., 2010). Similar discrepancies between knockout and knockdown phenotypes have been reported in *Arabidopsis* (Gao et al., 2015), *Drosophila* (Yamamoto et al., 2014), *C. elegans* (Akay et al., 2019; Firnhaber & Hammarlund, 2013), and human cell lines (Evers et al., 2016; Morgens, Deans, Li, & Bassik, 2016).

Phenotypic differences observed between morphants and mutants can potentially be attributed to dose-dependent off-target effects and the toxicity of the antisense reagents. For instance, a high dose of a morpholino targeting *foxc1a* led to complete loss of somite boundaries in zebrafish embryos, while a lower dose resulted in a milder phenotype more comparable to *foxc1a* mutants with only mild somite defects (Topczewska et al., 2001). Zimmer et al. (Zimmer, Pan, Chandrapalan, Kwong, & Perry, 2019) found that a 4-nanogram dose of *rhcgb* ATG morpholino produced the same phenotype as CRISPR-Cas9-generated *rhcgb* mutants, without additional morphological defects. However, higher doses of *rhcgb* morpholino induced additional trunk and tail curving and body axis deviation, which were also observed in high-dose-morpholino-injected *rhcgb* mutants. Similarly, Jiang et al. (Jiang, Carlantoni, Allanki, Ebersberger, & Stainier, 2020) compared zebrafish *tek* morphants and mutants and demonstrated that while the morphants exhibited severe vascular defects, *tek* mutants, regardless of the mutation type, including a full locus deletion, reached adulthood without obvious cardiovascular malformations. Further experiments showed that the *tek* morpholino induced the same phenotype in wild-type embryos and *tek* mutants lacking the morpholino binding site, highlighting the off-target effects of the morpholino. Additionally, the contribution of maternal mRNA could explain why morphants often exhibit more severe phenotypes than mutants. Zygotic mutants produce the target protein from maternal stores, whereas translation-blocking morpholinos and siRNAs can knock down both maternal and zygotic transcripts, revealing phenotypes that are only observed in maternal zygotic mutants (Zimmer et al., 2019).

1.3 The concept of genetic robustness

However, not all instances of phenotypic discrepancy can be attributed to such straightforward explanations. Genetic robustness, which refers to an organism's ability to maintain its phenotype despite genetic perturbations (Kitano, 2007), also plays a significant role in gene perturbation studies. Biochemical and network-level mechanisms responsible for robustness include dosage compensation (Brockdorff & Turner, 2015), gene duplication providing redundancy (Masel & Siegal, 2009), and changes in gene regulatory network architecture, such as redundant wiring of transcription factors (Macneil & Walhout, 2011) or regulatory compensation within gene networks (Peng, Song, & Acar, 2016). A classic example of robustness due to dosage compensation is sex chromosome dosage compensation, which in *Drosophila* involves transcriptional upregulation of X chromosomal genes in males (Gelbart & Kuroda, 2009), while in *C. elegans*, it entails downregulation of genes on each of the two X chromosomes in hermaphrodites (Meyer, 2005), both aiming to equalize gene expression between sexes. In mammals, sex chromosome dosage compensation was traditionally thought to be achieved solely by the complete inactivation of one of the two X chromosomes in females; however, recent reports indicate that a twofold upregulation of some X chromosomal genes also occurs in males (Deng et al., 2013; Deng et al., 2011).

Robustness resulting from paralogous genes, where a family member with a similar function is upregulated in response to gene loss, has been widely observed in mouse (O'Leary et al., 2013), *C. elegans* (Longman, Johnstone, & Caceres, 2000), zebrafish (Dooley et al., 2019), and other model organisms. On the other hand, robustness arising from gene network rewiring is a more intricate phenomenon that does not solely rely on gene duplicates. For instance, transcription factors can converge onto different genes through redundant shadow enhancers, distant from primary enhancers, or multiple transcription factors from one family can bind the same regulatory DNA element. Similarly, TFs from different families can interact with a regulatory module containing

several elements (Macneil & Walhout, 2011). Protein network architecture also contributes to compensation, even when mutations occur in genes encoding structurally or functionally unique proteins. In yeast, enzymes catalyzing different chemical reactions can compensate for recessive mutations in genes encoding functionally unrelated enzymes, sustaining an optimal turnover of metabolites (Wagner, 2000). Additionally, Hsp90 can buffer against mutations in multiple unrelated genes in yeast and other organisms (Zabinsky, Mason, Queitsch, & Jarosz, 2019). Moreover, large metabolic networks can buffer against the complete loss of function of one or more enzymes by utilizing alternative metabolic routes (Edwards & Palsson, 1999).

1.4 Genetic compensation and the understanding of genotype-phenotype relations

Massively parallel sequencing and deep mutational scanning techniques enable the comprehensive analysis of numerous mutations and their corresponding phenotypes, leading to the development of predictive models and aiding in the differentiation of harmful and benign genetic variants (Kemble, Nghe, & Tenaillon, 2019; Livesey & Marsh, 2020). So far, most of these studies have focused on yeast and individual genes. For instance, Hietpas et al. (Hietpas, Jensen, & Bolon, 2011) explored the fitness landscape for all possible point mutations in a nine-amino-acid region of Hsp90. Another study utilized a complementary DNA (cDNA) library containing all 9,595 possible single amino acid substitutions in PPARγ, a gene associated with lipodystrophy and type 2 diabetes, to assess the tolerance level for each amino acid substitution in human macrophages (Majithia et al., 2016). These examples illustrate that achieving a comprehensive understanding of the connections between genotype and phenotype is not as straightforward as solving a simple single-variable equation. Phenotypes usually arise from intricate interactions among multiple genes or combinations of different mutations. Moreover, frequently, the phenotypic outcome of a mutation is influenced by the presence of other

variants in the genome (Lehner, 2011). A well-known illustration in human genetics is observed in the case of cystic fibrosis, a single-gene disorder resulting from a mutation in *CFTR*. However, the clinical phenotypes can vary due to the involvement of at least seven different modifier loci (Badano & Katsanis, 2002).

The complexity of genotype-phenotype relationships is further compounded by time-dependent effects of genetic robustness on evolvability. Evolvability refers to a biological system's capacity to generate heritable and adaptive phenotypic variation through genetic mutations (Elena & Sanjuan, 2008; Payne & Wagner, 2019). Mutational robustness, in short, leads to cryptic genetic variation, which may manifest as novel, heritable phenotypes under specific environmental conditions (Masel & Trotter, 2010). In the short term, genetic robustness can impede evolvability by reducing selection intensity, but in the long term, it allows populations to accumulate a greater diversity of genotypes, thus promoting evolutionary innovation (Elena & Sanjuan, 2008). In addition, LOF mutations can transform neutral genotypes into adaptive ones (Masel & Trotter, 2010). This phenomenon is commonly observed with genetic robustness through paralogous genes or gene network buffering, which generally exhibit positive effects in various biological contexts. For instance, studies on paralogous genes in multiple model organisms have demonstrated their lower essentiality compared to singleton genes due to functional redundancy (Blomen et al., 2015; Gu et al., 2003; Kamath et al., 2003; White et al., 2013). To gain further insights into genotype-phenotype relationships, scientists have employed synthetic lethality screens, where the disruption of individual genes has no impact on fitness, but simultaneous disruption of multiple genes proves lethal. Essentiality measurements in human genes have yielded similar insights (Wang et al., 2015) and revealed that close paralogs are less likely to be involved in human disease, as genes with close homologs (at least 90% sequence identity) show three times fewer pathogenic mutations compared to genes with diverged homologs (Hsiao & Vitkup, 2008).

As the genotype-phenotype relations are already difficult to interpret and understand, one can imagine how much more puzzling they became once TA was introduced first as a robustness-promoting mechanism and later revealed to have a whole range of effects on mutant phenotypes. The following chapters describe in-detail the discovery of TA, the mechanisms it employs, and outlines knowledge gaps and open questions that require careful investigations to in order to be answered.

1.5 Transcriptional adaptation: a case for facilitating robustness or a novel gene regulation pathway

TA was first discovered as scientists were investigating the role of the *EGF-like-domain, multiple 7* (*egfl7*) gene in zebrafish vascular development. Using both knockdown and knockout approaches, Rossi and colleagues realized that while zebrafish *egfl7* morphants exhibited severe vascular tube malformations, no vascular phenotype was observed in zebrafish *egfl7* mutants (literature data confirmed similar occurrences in *Xenopus* and mouse *egfl7* morphants and mutants, respectively) (Rossi et al., 2015). Initially, the discrepancy between the mutant and morphant phenotypes raised questions about the possibility of morpholino off-target effects, the presence of hypomorphic mutant alleles, or other factors. However, further evidence indicated that the zebrafish mutant represented a severe allele and that the phenotypic differences were not due to off-target effects. The mechanism by which zebrafish overcame the genetic alteration, but not the antisense reagent, became clearer through proteomic and transcriptomic analyses of mutant and morphant embryos. A specific extracellular matrix protein called Emilin3a was found to be upregulated in mutants but not morphants, and transcriptomic analysis revealed upregulation of several *emilin* genes in mutants (Rossi et al., 2015). The compensatory role of increased Emilin expression in response to Egfl7 loss was supported by injecting wild-type *Emilin* mRNA into *egfl7* morphants, which do not upregulate any of the *emilin* genes, resulting in only mild vascular phenotypes.

Initially recognized as a robustness-conferring mechanism, the understanding what role TA can play in biological systems changed with additional studies and an in-depth literature analysis. Contrary to the notion that genetic robustness primarily exerts positive effects on the fitness and survival of various mutants, the impact of TA on mutant phenotypes can range from beneficial outcomes (observed in zebrafish *egfl7* (Rossi et al., 2015) and *capn3a* mutants (Ma et al., 2019), as well as in nematode (Serobyan et al., 2020), zebrafish (Sztal, McKaige, Williams, Ruparelia, & Bryson-Richardson, 2018), and mouse cell line (El-Brolosy et al., 2019) *actin* mutants) to apparently neutral (in zebrafish *vegfaa* mutants (El-Brolosy et al., 2019)), or potentially even detrimental effects (in mouse *Lgr6* (Huang et al., 2017) and zebrafish *marcksb* mutants (Ye et al., 2019) (Table A)). The review by Kontarakis and Stainier provides a comprehensive overview of these cases (Kontarakis & Stainier, 2020). Intriguingly, since TA is only triggered by PTC-causing mutations, it is plausible that different mutations, those that induce TA and those that do not, can result in similar phenotypic outcomes, as exemplified by zebrafish *vegfaa* mutants. This paradox adds a new layer of complexity to our understanding of how genetic robustness influences the relationship between genotype and phenotype. Additionally, TA has implications for how we understand haplosufficiency. It has been demonstrated that in heterozygous cells and zebrafish, TA leads to upregulation of the wild-type allele (El-Brolosy et al., 2019), potentially resulting in normalization of protein levels. This challenges the prevailing model of haplosufficiency, which posits that half of the protein activity encoded by a single functional allele is sufficient to maintain a wild-type phenotype. In cases where TA is active, the single functional allele is actually upregulated. Finally, these observations also invite a reassessment of classical models of robustness that attribute compensation responses to increased expression of paralogs in response to protein loss; perhaps an overlooked mutant mRNA degradation and TA may be involved.

Positive effects (reduced severity of a phenotype)	Neutral effects	Detrimental effects (more severe phenotype)
egfl7 mutant zebrafish (Rossi et al., 2015)	*vegfaa* mutant zebrafish (El-Brolosy et al., 2019)	*Lgr6* KO mice (predisposition to squamous cell carcinoma due to upregulation of *Lgr5*) (Huang et al., 2017)
Some *Actin* mutants in zebrafish (*actc1b*) (Sztal et al., 2018), worms (*act-5*) (Serobyan et al., 2020), mouse cells (*Actb*) (El-Brolosy et al., 2019)	*Actg1* mutant mouse cells (El-Brolosy et al., 2019)	*marcksb* mutant zebrafish (upregulation of MARCKS-family members leads to a ventralization phenotype) (Ye et al., 2019)
capn3a mutant zebrafish (Ma et al., 2019)	*nid1a* mutant zebrafish (Ma et al., 2019)	
Some *clh-1* alleles in worms (on the body size phenotype) (Fernandez-Abascal, Wang, Graziano, Johnson, & Bianchi, 2022)	Some *clh-1* alleles in worms (on the nose touch insensitive phenotype) (Fernandez-Abascal et al., 2022)	

Table A. Phenotype-influencing effects of transcriptional adaptation in different mutant models.

However we look at it, TA presents a complex case where multiple genes become dysregulated, and the fact that restoring wild-type phenotypes is rarely the main objective of TA, one can pin-point TA's main function as an additional layer of gene regulation.

1.5.1 Models and mechanisms

The precise mechanism underlying TA remains to be uncovered; however, a few recent studies had hinted at several major requirements, as well as proposed working models for TA (El-Brolosy et al., 2019; Ma et al., 2019). El-Brolosy and colleagues conducted a thorough analysis involving mutant zebrafish and mouse

cells in culture, revealing a correlation between TA, premature termination codons (PTCs) in mutant mRNAs, and nonsense-mediated mRNA decay (NMD). The researchers demonstrated the necessity of mutant mRNA degradation in initiating TA by observing that RNA-less alleles, promotor- or full-locus deletions, do not exhibit TA. They also knocked out or knocked down mRNA processing factors involved in NMD, namely UPF1, SMG6, and XRN1, further supporting the requirement of mutant mRNA degradation for TA (El-Brolosy et al., 2019). Additionally, epigenetic remodeling was observed during the TA response. This was evident through the enrichment of both WDR5, a component of the COMPASS complex responsible for histone H3K4 methylation, and the H3K4me3 histone mark, indicating active and accessible chromatin, at the transcription start site (TSS) of upregulated genes in several mouse cell line TA models (El-Brolosy et al., 2019). Furthermore, as became evident from various mutant alleles generated by El-Brolosy and colleagues, as well as *Rfx*Cas13d-directed mRNA targeting research in zebrafish (Kushawah et al., 2020), multiple forms of mRNA degradation (NMD, NGD, NSD, *Rfx*Cas13d-mediated) can trigger TA and the upregulation of adapting genes (Figure 1).

Notably, Ma and colleagues reported a similar phenomenon termed genetic compensation response (GCR). They observed increased mRNA levels of related genes, particularly *capn8* and *capn12*, in zebrafish *capn3a* mutants (Ma et al., 2019). Knockdown and knockout experiments targeting various NMD factors revealed a significant role for *Upf3a*, but not *Upf1*, *Upf2*, or *Upf3b*, in mediating GCR. Building upon previous findings suggesting the suppression of NMD by UPF3a under certain conditions and its direct interaction with the WDR5-COMPASS complex, which is crucial for the GCR response, Ma et al. proposed that mRNAs bearing PTCs, rather than mutant mRNA degradation intermediates, guide these components to the TSS region of related genes to enhance their transcription (Ma et al., 2019).

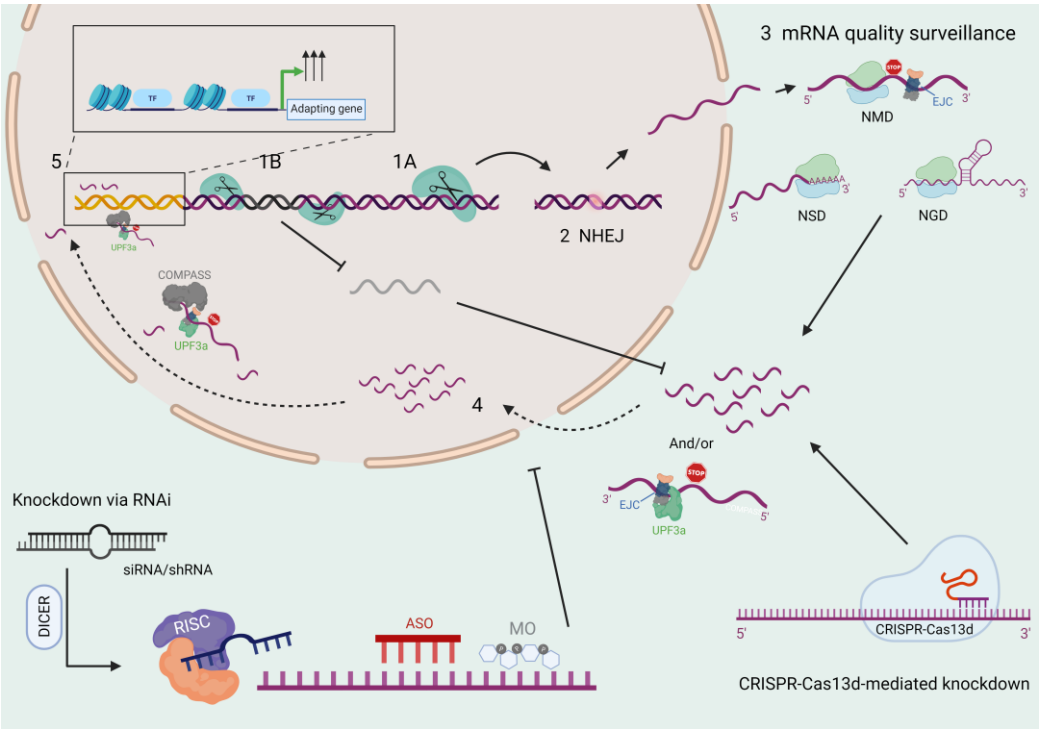

Figure 1. Various techniques for manipulating genes can either induce or avoid TA. The initiation of DSBs using sequence-specific nucleases (1A) prompts DNA repair mechanisms, such as NHEJ (2), leading to indels with or without frameshifts. Aberrant mRNAs are detected by mRNA quality control pathways (NMD, NGD, or NSD) (3), resulting in mutant mRNA degradation. The current model of TA suggests that fragments of mutant mRNAs or mRNAs with PTCs may translocate back into the nucleus (4). Here, they interact with the WDR5-COMPASS complex, impacting the TSS and modulating the expression of the adapting gene(s) (5). Gene knockout achieved through large deletions, such as promoter or full-locus deletions (1B), eliminates mRNA expression, effectively preventing TA. Although RNA-targeting techniques such as RNAi using siRNAs or shRNAs, ASOs, and morpholinos have not been shown to trigger TA, mRNA cleavage using CRISPR-Cas13d can initiate mRNA degradation which leads to TA. Adapted from (Jakutis & Stainier, 2021).

Subsequently, TA was also documented in the nematode *C. elegans* (Serobyan et al., 2020), highlighting its evolutionary conservation and emphasizing the need to consider it when generating knockout alleles in diverse model organisms. The research in *C. elegans* not only validated the participation of several NMD genes, namely *smg-2* (ortholog of *Upf1*), *smg-4* (ortholog of *Upf3*), and *smg-6* (ortholog of *Smg6*), in the TA response but also unveiled the

involvement of factors associated with small RNA biogenesis. This included the AGO proteins ERGO-1 and NRDE-3, as well as Dicer, suggesting potential overlap between TA and RNA interference (RNAi) mechanisms to some extent. Additionally, the study revealed the necessity of the RNA-dependent RNA polymerase RRF-3, implying a potential role in amplifying mutant mRNA degradation fragments or generating small RNA derivatives such as the 26G RNAs, which are implicated in the TA response (Serobyan et al., 2020).

1.5.2 Knowledge gaps

New experiments are necessary to gain an evolutionary perspective on TA and elucidate its origin and potential spread. At present, TA can be regarded as an outcome resulting from two fundamental processes: (a) mRNA quality surveillance and (b) gene regulation mediated by small RNAs (sRNAs). These two independent processes, each selected for their positive impact on genetic information transmission, appear to contribute equally to the emergence of TA by (a) generating mRNA fragments that undergo further processing into sRNAs and (b) by modulating the expression of the related genes. A potential mechanistic explanation for the role of these sRNAs in TA can be drawn from the phenomenon known as RNA activation (RNAa). This phenomenon involves 21-bp RNA duplexes that enhance transcription from target promoters by modifying repressive histone methylation (L. C. Li et al., 2006).

Nevertheless, this is still a very vague understanding of TA and many open questions had remained ever since reporting TA for the first time. Those questions primarily relate to how widespread the phenomenon is, as well as try to address every aspect of TA's mechanism.

1) Does TA represent an intricate form of genetic robustness that enhances genetic variation specifically in a limited set of genes? Alternatively, could it be a specialized mechanism of gene regulation linked to genome duplication events that subsequently converged into pathways promoting

robustness? Currently, only a handful of TA instances have been documented (Table B), and most mutants with small indels, as reported in the literature, exhibit discernible phenotypes. This raises questions regarding the actual number of gene families capable of exhibiting functional compensation through TA and how many instances of TA may have been overlooked, given the tendency to underreport negative data. A comparative analysis of the phenotypes displayed by alleles with and without TA is necessary as one line of experiments. Similarly, studies designed for unbiased detection of novel TA models are needed to determine how prevalent TA is.

2) Alongside the evolutionary aspect, numerous mechanistic aspects of TA remain unknown. What are the characteristics of the degradation products derived from mutant mRNAs and what roles do they play? Is it possible to isolate or capture those fragments in high-depth sequencing experiments? Effort needs to be put into analyzing different mRNA degradation pathways and whether they all produce similar degradation fragments; if not – how does that influence the landscape of TA?
3) Which proteins are involved at each step of the TA process? It is widely known that RNAs, whether long or short, do not re-enter the nucleus on their own; therefore, inevitably certain RNA-binding proteins (RBPs) have to be involved in the TA response. Likewise, proteins that modify histone marks and are responsible for writing the epigenetic code could be as important in TA.
4) How much sequence similarity is required for TA, and does the crucial similarity reside in specific regions of the adapting genes?
5) How does TA impact the transcriptome of mutant cells? What are the direct targets of TA, and can it also result in reduced transcription of certain genes?
6) Lastly, can TA be harnessed for therapeutic purposes in the treatment of human genetic disorders?

Model organisms		
Zebrafish	**Murine cells in culture**	***Caenorhabditis elegans***
• *hbegfa (hbegfb), vcla (vclb), hif1ab (epas1b), vegfaa (vegfab), egfl7 (emilin3a)* (El-Brolosy et al.) • *alcama (alcamb)* (Jiang et al.) • *capn3a (capn8, capn12)* (Ma et al.) *nid1a (nid1b, nid2a)* (Zhu et al.) • *actc1b (actc1a)* (Sztal et al.)	• *Actb (Actg1, Actg2), Actg1 (Actb), Fermt2 (Fermt1) Rela (Rel)* (El-Brolosy et al.)	• *act-5 (act-3) unc-89 (sax-3)* (Serobyan et al.) • *clh-1* (different *clh* genes, depending on which exons are deleted in distinct *clh-1* alleles) (Fernandez-Abscal et al.)

Table B. The up-to-date in literature reported instances of transcriptional adaptation; mutated gene listed first with reported adapting genes listed in the brackets.

2. AIM OF THE DISSERTATION

The global aim of this dissertation is to shed further light on the molecular mechanism of transcriptional adaptation and elucidate how TA affects the global transcriptome of a cell. Recognition that the expression of decay-prone mutant mRNAs can instigate the transcriptional adjustments of other genomic loci and genes through TA, emphasizes the necessity of delving deeper into comprehending cellular response mechanisms to diverse gene perturbations. As a recently discovered phenomenon, TA still lacks a clear understanding of the extent to which genes or gene families can display it as well as what are the primary (direct) and secondary (indirect) targets of the adaptation response.

I hypothesize that transcriptional adaptation is a stochastic process which relies on more than one endogenous pathway of mRNA degradation and involves different adapting genes depending on a given mRNA degradation context. In order to further our understanding of the effects of TA on cells' transcriptome and the molecular rules of this process, the dissertation's work revolves around three specific aims:

Aim1: Studying various mRNA degradation and transcriptional adaptation-inducing tools.

I aim to explore other avenues of triggering TA, primarily study how it can be achieved without introducing DNA lesions. I will utilize CRISPR-Cas13d tool that can directly degrade target mRNAs and investigate whether such mean of mRNA degradation results in TA.

Aim 2: Creating an inducible model of transcriptional adaptation in mouse cell lines.

Having established another tool for triggering TA, I will try to develop an inducible TA system that will allow studying TA from its earliest onset. I will do it using two different approaches: 1) by overexpressing NMD-prone transgenes and 2) by directly knocking-down mRNA in a time-dependent manner.

Aim 3: Revealing the temporal profile of transcriptional adaptation and identifying the genes whose expression is directly upregulated during the transcriptional adaptation response.

I will perform transcriptomic analyses in order to identify how TA affects the cellular transcriptome over time: from the earliest onset of TA until the saturation time point.

Having successfully achieved the aforementioned aims, the results of the dissertation project(s) will significantly contribute to current fundamental understanding of genetic compensation via transcriptional adaptation.

3. MATERIALS AND METHODS

3.1 Materials

3.1.1 Antibiotics

Table 1: List of antibiotics used and their respective working concentration.

Antibiotic	Working concentration
Ampicillin	100 µg/mL
Doxycycline	100 ng/mL
G418	0.5 µg/mL or 2 mg/mL
Kanamycin	50 µg/mL
Penicillin	100 µg/mL
Puromycin	8 µg/mL
Streptomycin	100 µg/mL

3.1.2 Bacterial strains

Table 2: List of bacterial strains used and their purpose.

Bacterial strain	Purpose
DH5α	Competent cells for transformation

3.1.3 Buffers and solutions

Table 3: List of buffers and solutions and their composition.

Buffer/Solution	Composition
10X TBE	121 g Tris 62 g Boric Acid 7.4 g EDTA 1 L distilled H_2O
20X SSC	175.3 g NaCl 88.2 g Sodium Citrate Dissolve in 800 mL distilled H_2O Adjust pH to 7 Up to 1 L with distilled H_2O

PBS	8 g NaCl 0.2 g KCl 1.44 g Na_2HPO_4 0.24 g KH_2PO_4 Dissolve in 900 mL distilled H_2O Adjust pH to 7.4 Up to 1 L with distilled H_2O
ChIP low salt buffer	0.1% SDS 1% Triton X-100 2 mM EDTA 20 mM Tris-HCl pH 8.1 150 mM NaCl
ChIP high salt buffer	0.1% SDS 1% Triton X-100 2 mM EDTA 20 mM Tris-HCl pH 8.1 500 mM NaCl
ChIP LiCl buffer	10 mM Tris-HCl pH 8.0 250 mM LiCl 1% NP-40 1% deoxycholic acid 1 mM EDTA
ChIP elution buffer	1% SDS 100 mM $NaHCO_3$

3.1.4 Centrifuges

Table 4: List of centrifuges and their respective supplier.

Centrifuge	Supplier
Centrifuge 5415D (1.5-2 mL tubes)	Eppendorf
Centrifuge 5417 R (200 µL tubes)	Eppendorf

Centrifuge 5418 (1.5-2 mL tubes)	Eppendorf
Centrifuge 5810 R (15-50 mL tubes)	Eppendorf

3.1.5 Chemicals and reagents

Table 5: List of chemicals and reagents used and their respective supplier.

Chemical/reagent	Supplier
2-Mercaptoethanol	Gibco™
10x NEBuffer 2.1	NEB
10x NEBuffer 3.1	NEB
Acetone, anhydrous	VWR
Agarose	Peqlab
Bovine calf serum (BCS)	HyClone
Bovine serum albumin (BSA)	Sigma
Chloroform	Merck
CutSmart buffer	NEB
DAPI	Thermo Fisher Scientific
DMEM high glucose + pyruvate	Thermo Fisher Scientific
DMSO	Sigma
Doxycycline	Sigma
DNA ladder (100 bp and 1 kb)	Thermo Fisher Scientific
dNTP mix	Thermo Fisher Scientific
Ethanol	Roth
Fetal bovine serum (FBS)	HyClone
FuGENE 6	Promega
FuGENE HD	Promega
Gel loading dye	Thermo Fisher Scientific
Glycerol	Sigma
Isopropanol	Roth
LB agar	Roth
Lipofectamine 3000	Thermo Fisher Scientific

Lipofectamine MessengerMax	Thermo Fisher Scientific
Lipofectamine RNAiMax	Thermo Fisher Scientific
Methanol	Roth
Mineral oil	Sigma
Nuclease-free water	Ambion
Paraformaldehyde (PFA)	Sigma
PBS	Lonza
Penicillin-Streptomycin	Thermo Fisher Scientific
Phenol-chloroform-isoamyl alcohol	Thermo Fisher Scientific
Proteinase K	Roche
SYBR Safe	Thermo Fisher Scientific
SOC medium	Thermo Fisher Scientific
T4 ligase buffer	NEB
Tris	Sigma
Triton-X	Sigma
Trizol	Ambion
Trypsin-EDTA	Thermo Fisher Scientific
Tween-20	Sigma

3.1.6 Enzymes

Table 6: List of enzymes used and their respective supplier.

Enzyme	Supplier
DyNAmo ColorFlash SYBR Green PCR mix	Thermo Fisher Scientific
DNase I	Qiagen
KAPA 2G fast DNA polymerase	Kapa Biosystem
Phire Hot Start II DNA polymerase	Thermo Fisher Scientific
Proteinase K	Roche
Restriction enzymes: AfeI, AgeI AleI, ApaI, BamHI, BbsI-HF, Bpu10I,	NEB

BsmBI, EcoRI, EcoRV, FseI, HindIII, KpnI, NcoI, NdeI, NotI-HF, SacI, SacII, SfiI, XbaI, XhoI, XmaI	
RQ1 RNase-free DNase	Promega
SeqAmp DNA polymerase	Takara
Sp6 RNA polymerase	Promega
T4 DNA ligase	NEB
T7 RNA polymerase	Promega
TrypLE™ Express Enzyme	Thermo Fisher Scientific
PrimeStar max DNA polymerase	Takara

3.1.7 Growth media

Table 7: List of growth media used and their composition.

Growth medium	Composition
E. coli SOC medium	Tryptone 2% Yeast extract 0.5% NaCl 0.05% KCl 0.0186% Dissolve in distilled H_2O, adjust pH to 7, and then add: $MgCl_2$ 10 mM D-glucose 20 mM Then autoclave
NIH-3T3 culture medium	DMEM high glucose, pyruvate 10% Bovine Calf Serum 1% Penicillin/Streptomycin
HEK293T culture medium	DMEM high glucose, pyruvate 10% Fetal Bovine Serum 1% Penicillin/Streptomycin

3.1.8 Kits

Table 8: List of kits used and their respective supplier.

Kit	Supplier
Amaxa® Cell Line Nucleofector® Kit V	Lonza
Amaxa® Cell Line Nucleofector® Kit R	Lonza
GeneJET Gel extraction kit	Thermo Fisher Scientific
GeneJET PCR purification kit	Thermo Fisher Scientific
GeneJET Plasmid miniprep kit	Thermo Fisher Scientific
In-Fusion® HD Cloning Kit	Takara
Maxima First Strand cDNA Synthesis kit	Thermo Fisher Scientific
MEGAshortscript T7 kit	Ambion
mMESSAGE mMACHINE kit (Sp6)	Ambion
mMESSAGE mMACHINE kit (T3)	Ambion
mMESSAGE mMACHINE kit (T7)	Ambion
Nextera DNA Sample Preparation Kit	Illumina
pGEM-T-easy vector kit	Promega
PureLink™ RNA Mini Kit	Thermo Fisher Scientific
RNA Clean and Concentrator kit	Zymo Research
Super Script III Reverse Transcriptase	Invitrogen
truChIP Chromatin Shearing Kit with Formaldehyde	Covaris
Wizard® Genomic DNA Purification Kit	Promega

3.1.9 Laboratory equipment

Table 9: List of laboratory equipment used and their respective supplier.

Equipment	Supplier
4D-Nucleofector ® System	Lonza
Bacterial incubator	Heraeus
Bacterial incubator shaker	Infors HAT
BD FACSAria™ III sorter	BD Biosciences
Cell culture CO_2 incubators	Thermo Fisher Scientific
Cell culture laminar flow hoods	Thermo Fisher Scientific
CFX connect real time PCR detection system	Bio-Rad
ChemiDoc MP	Bio-Rad
Eco Real-time PCR system with HRMA	Illumina
Electrophoresis power supply	Bio-Rad
Gel Doc EZ system	Bio-Rad
Heating blocks	VWR
LUNA-II automated cell counter	Logos Biosystems
Microscale	Novex
Microwaves	Bosch
NanoDrop 2000 c	Thermo Fisher Scientific
Next Advance Bullet Blender Homogenizer	Scientific Instrument Services
NextSeq 500 platform	Illumina
Nucleofector™ Transfection 2b Device	Lonza
PCR mastercycler Pro	Eppendorf
Weighing balance	Sartorius

3.1.10 Laboratory supplies

Table 10: List of laboratory supplies and their respective supplier.

Laboratory supply	Supplier
Bacterial culture tube	Sarstedt
Beakers (100 mL, 600 mL, 1000 mL)	VWR
CELLSTAR cell culture dishes (35 mm, 60 mm, 100 mm, 145 mm)	Greiner bio-one
CELLSTAR cell culture flasks (T25, T75, T125)	Greiner bio-one
CELLSTAR cell culture multi-well plates (96-well, 48-well, 24-well, 12-well, 6-well)	Greiner bio-one
Centrifuge tubes (1.5 mL, 2 mL)	Sarstedt
Conical flasks (100 mL, 500 mL)	VWR
Falcons (15 mL, 50 mL)	Greiner bio-one
Forceps	Dumont
Glass bottles (100 mL, 250 mL, 500 mL, 1000 mL, 2000 mL)	Duran
Glass bottom dish	MatTek
Laboratory film	Parafilm
Latex gloves	Roth
Magna ChIP Protein A+G Magnetic Beads	Milipore
Microloader pipette tips	Eppendorf
Nitrile gloves	VWR
PCR tubes (200 µL)	Sarstedt
Petri dish (35 mm, 60 mm, 90 mm)	Greiner bio-one
Pipetboy	Integra
Pipette filter tips	Greiner bio-one

Pipettes (2 µL, 20 µL, 100 µL, 200 µL, 1000 µL)	Gilson
Pipette tips	Greiner bio-one
Scalpel	Braun
Serum pipette	Greiner bio-one

3.1.11 Mammalian cell lines

Table 11: List of mammalian cell lines used and their source.

Cell line	Source
Inducible *Actb*^{PTC}/*Actb*^{WT} transgene-expressing NIH3T3 cells	This study
Inducible *Actg1*^{PTC}/*Actg1*^{WT} transgene-expressing NIH3T3 cells	This study
Stable *Actg1*^{PTC}/*Actg1*^{WT} transgene-expressing HEK293T cells	This study
Cas13d-expressing NIH3T3 cells	This study
Cas13d-NLS-expressing NIH3T3 cells	This study
Cas13d-expressing HEK293T cells	This study
WT NIH-3T3 cells	(El-Brolosy et al., 2019)
WT HEK293T	Prof. T. Braun (Max Planck Institute for Heart and Lung Research, Bad Nauheim, Germany)

3.1.12 Oligonucleotides

3.1.12.1 Common sequencing primers

Table 12: List of common sequencing primers used.

Primer	Sequence (5' to 3')
CMV F	CGCAAATGGGCGGTAGGCGTG
F1ori F	GTGGACTCTTGTTCCAAACTGG
hU6-F	GAGGGCCTATTTCCCATGATT

M13 F	GTAAAACGACGGCCAGT
Puro R	GTGGGCTTGTACTCGGTCAT
SP6 F	ATTTAGGTGACACTATAG
SV40pA R	GAAATTTGTGATGCTATTGC
T3 F	GCAATTAACCCTCACTAAAGG
T7 F	TAATACGACTCACTATAGGG

3.1.12.2 Genotyping primers

Table 13: List of oligonucleotides used for genotyping and their targets.

Target	Sequence (5' to 3')
***Actg1*^{PTC}/*Actg1*^{WT} transgene in NIH3T3 cells *Hipp11* locus**	F: CAAGGGTGGTCTTAGTAG R: GTCTTGTAGTTGCCGTCGTC
***Ctnna1*^{PTC}/*Ctnna1*^{WT} transgene in NIH3T3 cells *Hipp11* locus**	F: CAAGGGTGGTCTTAGTAG R: GTCTTGTAGTTGCCGTCGTC
***Nckap1*^{PTC}/*Nckap1*^{WT} transgene in NIH3T3 cells *Hipp11* locus**	F: CAAGGGTGGTCTTAGTAG R: GTCTTGTAGTTGCCGTCGTC
Cas13d/Cas13d-NLS in NIH3T3 cells *Hipp11* locus	F: CAAGGGTGGTCTTAGTAG R: GTCTTGTAGTTGCCGTCGTC

3.1.12.3 qPCR primers

Table 14: List of oligonucleotides used for quantitative RT PCR and their targets.

Organism	Target gene	Sequence (5' to 3')
	Actb mRNA	F: CTGTATTCCCCTCCATCGTG R: CTCGTCACCCACATAGGAGTC
	Actg1 mRNA	F: CCGCGGTCGGTCTCAC R: TACGATGGAAGGGAACACGG
	Actg1 pre-mRNA	F: CACACATCACATTTGTGG R: ATGACAATGCCAGTGG
	Actg1 Transgene mRNA	F: CATCGTCCACCGCAAATG R: TAGAAGGCACAGTCGAGG

Mouse	*Actg2* mRNA	F: CGAGTAGCACCAGAAGAGCA
		R: CCATCCCCCGAATCCAGAAC
	Actg2 pre-mRNA	F: CATGGGAAGTGGATATGG
		R: AACATACATGGCAGGG
	Ctnna1 mRNA	F: GAGGAGCTTGTGGTTG
		R: CATGTTGCCTCGCTTC
	Ctnnal1 mRNA	F: GACTGGAGATCAGGACG
		R: CTGAATCGCTTGCAGG
	Ctnna2 mRNA	F: GTGAACAGATCGCTAAGG
		R: ACTCTGAGGAGGCAATC
	Ctnna3 mRNA	F: GGGAGATGATTGCTAAGG
		R: CGTCTGTAAATCTCTCAGC
	Gapdh mRNA	F: GCACAGTCAAGGCCGAGAAT
		R: GCCTTCTCCATGGTGGTGAA
	Hprt mRNA	F: TTTACTGGCAACATCAACAG
		R: AGGGATTTGAATCACGTTTG
	Nckap1 mRNA	F: GACCAGATGGCTGCACTCTT
		R: TCTTGTGCCAATGACCGGAA
	Hem1 mRNA	F: TGATGCCTGCCAGTGTCATT
		R: GGTCCTCAATCCGTGACAGG
	Nckap5 mRNA	F: TTCCAACAGCGAGTCAGACC
		R: CAAGGCAGGGGTTCCTGATT
	Nckap5l mRNA	F: CAGCTAGCCGGCATGTATCA
		R: CACTGGCTGGAAATCCCCAT
Human	*ACTB* mRNA	F: TGAGGCACTCTTCCAGCCTTC
		R: CGGCAATGCCAGGGTACATG
	ACTG1 mRNA	F: CCCAAGGCCAACAGAGAGAAG
		R: CATGACAATGCCAGTGGTGC
	ACTG2 mRNA	F: GCCAGATGGGCAGGTTATCAC
		R: AGTCCTTACGGATGTCAATGTCAC

	GAPDH mRNA	F: TGTTGCCATCAATGACCCCTT R: CTCCACGACGTACTCAGCG
	TOP1 mRNA	F: ATGGGCATGCTGAAGAGACG R: TGCCGGACTTCTTTCCACTT

3.1.12.4 sgRNAs

3.1.12.4.1 CRISPR-Cas9

Table 15: List of oligonucleotides used for CRISPR-Cas9 mutagenesis and their targets.

Target DNA	Sequence (5' to 3'), variable oligonucleotide
Actg1	CGTAATACGACTCACTATAGGGCCAGAAAGACTCATACGGTTTTA GAGCTAGAAATAGCAAG
GFP	CGTAATACGACTCACTATAGGTGCCCATCCTGGTCGAGCGTTTTA GAGCTAGAAATAGCAAG

3.1.12.4.2 CRISPR-Cas13d

Table 16: List of oligonucleotides used for CRISPR-Cas13 knockdowns and their targets.

Target RNA	Sequence (5' to 3'), variable oligonucleotide
Actg1	1. CAGGGCCGTGTTCCCTTCCATCGGTTTCAAACCCCGACCAGTT GGTAGGGGTTCCTATAGTGAGTCGTATTACG 2. CGGGGCTACAGCTTTACCACCACGTTTCAAACCCCGACCAGTT GGTAGGGGTTCCTATAGTGAGTCGTATTACG 3. CTGGGCATGGAGTCCTGTGGTATGTTTCAAACCCCGACCAGTT GGTAGGGGTTCCTATAGTGAGTCGTATTACG 4. CTGGGACGACATGGAGAAGATCTGTTTCAAACCCCGACCAGTT GGTAGGGGTTCCTATAGTGAGTCGTATTACG 5. CTGGGCGCACCACTGGCATTGTCGTTTCAAACCCCGACCAGTT GGTAGGGGTTCCTATAGTGAGTCGTATTACG

	6. ACGGGCAGGTGATCACCATTGGCGTTTCAAACCCCGACCAGTT GGTAGGGGTTCCTATAGTGAGTCGTATTACG 7. TCCTGACTGAACGGGGCTACAGCGTTTCAAACCCCGACCAGTT GGTAGGGGTTCCTATAGTGAGTCGTATTACG
Ctnna1	1. AAGGGGGATAAAATTGCAAAAGAGTTTCAAACCCCGACCAGTT GGTAGGGGTTCCTATAGTGAGTCGTATTACG 2. CTGGGGAGTTTGCAGATGATCCAGTTTCAAACCCCGACCAGTT GGTAGGGGTTCCTATAGTGAGTCGTATTACG 3. GTGGGGCTGCCCTGATGGCTGACGTTTCAAACCCCGACCAGTT GGTAGGGGTTCCTATAGTGAGTCGTATTACG 4. GGGGATGGCTTCCTTGAACCTTCGTTTCAAACCCCGACCAGTT GGTAGGGGTTCCTATAGTGAGTCGTATTACG 5. GAGAACATGGATCTTTTTAAAGAGTTTCAAACCCCGACCAGTT GGTAGGGGTTCCTATAGTGAGTCGTATTACG 6. ATGGGACCCCAAAAGTCTGGAGAGTTTCAAACCCCGACCAGTT GGTAGGGGTTCCTATAGTGAGTCGTATTACG 7. CCCGGGCGATCATGGCTCAGCTTGTTTCAAACCCCGACCAGTT GGTAGGGGTTCCTATAGTGAGTCGTATTACG 8. GGAGGCGGGATCCAGGATGGACAGTTTCAAACCCCGACCAGTT GGTAGGGGTTCCTATAGTGAGTCGTATTACG
Nckap1	1. CGGGGCTACAATAAACGTATTAAGTTTCAAACCCCGACCAGTT GGTAGGGGTTCCTATAGTGAGTCGTATTACG 2. AAGGGGAACCTGAAAGGGAAAAAGTTTCAAACCCCGACCAGTT GGTAGGGGTTCCTATAGTGAGTCGTATTACG 3. CGATCTCTCCATATTTTGTTTTTGTTTCAAACCCCGACCAGTTG GTAGGGGTTCCTATAGTGAGTCGTATTACG 4. ATGGGCCTGTCATGCAGAGGTACGTTTCAAACCCCGACCAGTT GGTAGGGGTTCCTATAGTGAGTCGTATTACG 5. GAGGGAGTATTTGACTTCTCATCGTTTCAAACCCCGACCAGTT GGTAGGGGTTCCTATAGTGAGTCGTATTACG

	6. TCGGGAAACTGATATGAAGGTTGGTTTCAAACCCCGACCAGTT GGTAGGGGTTCCTATAGTGAGTCGTATTACG
GFP	1. CCGGGGTGGTGCCCATCCTGGTCGTTTCAAACCCCGACCAGTT GGTAGGGGTTCCTATAGTGAGTCGTATTACG 2. GAGGGCGACACCCTGGTGAACCGGTTTCAAACCCCGACCAGTT GGTAGGGGTTCCTATAGTGAGTCGTATTACG 3. CTGGGGCACAAGCTGGAGTACAAGTTTCAAACCCCGACCAGTT GGTAGGGGTTCCTATAGTGAGTCGTATTACG

3.1.12.5 siRNAs

Table 17: List of siRNA used and their providers.

siRNA target	Sequence (5' to 3') or company code if pool	Provider
Control (Scr)	SIC001	Sigma
UPF1	GUUCCAUCCUCAUUGACGA[dt][dt]	Sigma
XRN1	Sc-61812	Santa Cruz

3.1.13 Plasmids

Table 18: List of plasmids used and their respective resistance, source, and purpose.

Plasmid	Resistance	Source	Purpose
AAVS1-TRE3G-EGFP	Ampicillin	Addgene	Donor vector for Tetracycline-inducible gene expression
pcDNA3.1	Ampicillin	Thermo Fisher Scientific	Mammalian expression vector
pCS2+	Ampicillin	Addgene	Vector for cDNA cloning under the T7 promoter
pGEM-T	Ampicillin	Promega	Vector for sequence cloning

pT3TS-RfxCas13d-HA	Ampicillin	Addgene	Plasmid to carry out IVT of RfxCas13d
pUC119-MCS	Ampicillin	Addgene	Vector with a multiple cloning site and T7 and SP6 promoters on each end
px330	Ampicillin	Addgene	Co-expression of spCas9 and a sgRNA in mammalian systems
px458	Ampicillin	Addgene	Co-expression of spCas9-P2A-GFP and a sgRNA in mammalian systems
px459	Ampicillin	Addgene	Co-expression of spCas9-P2A-PuroR and a sgRNA in mammalian systems

3.1.14 Software and databases

Table 19: List of software and databases used and their respective purpose, sources, and online links, if applicable.

Software/Database	Purpose	Source	Online link
ApE	Plasmid DNA sequence analysis	University of Utah	
BioRender	Creating illustrations and visualizations	BioRender	https://www.biorender.com/

BLASTn	Identifying sequence alignments and similarities	NIH	https://blast.ncbi.nlm.nih.gov/Blast.cgi
ChopChop	sgRNA design for CRISPR-Cas9 mutagenesis	University of Bergen	https://chopchop.cbu.uib.no/
Ensembl	Genomic sequence, gene loci arrangement analysis and BLAST	Ensembl	https://www.ensembl.org/
GraphPad Prism	Data analysis	GraphPad	
IGV	Genomic sequence and NGS data analysis	Broad Institute	
Microsoft Office	Writing, data analysis, image formatting	Microsoft	
OligoCalc	Oligonucleotide design	Northwestern University	http://biotools.nubic.northwestern.edu/OligoCalc.html
Primer3	Primer design	University of Massachusetts Medical School	https://www.bioinformatics.nl/cgi-bin/primer3plus/primer3plus.cgi
PrimerX	Design of mutagenic PCR primers for site-directed mutagenesis	Bioinformatics.Org	https://www.bioinformatics.org/primerx

R	Bioinformatics' analyses	R Foundation for Statistical Computing	
SnapGene	Plasmid DNA sequence analysis	SnapGene by Dotmatics	
USCS Genome browser	Genomic sequence, gene loci arrangement and NGS data analysis	University of California Santa Cruz	https://genome.ucsc.edu/

3.2 Methods

3.2.1 Agarose gel electrophoresis

Digested plasmid DNA, PCR reaction products, or RNA, were mixed with 6x gel loading dye and loaded on a 1-2%, depending on expected nucleic acid size differences, agarose gel, prepared with SYBR Safe to label DNA, along with the appropriate DNA ladder (100 bp or 1 kbp). Nucleic acids were run on electrophoresis gel at 120-160 volts for 20-45 minutes before analyzing the gel with a blue light transilluminator or taking a picture using UV light with a gel imager system.

3.2.2 ATAC-seq material extraction and library preparation

Cells were trypsinized and washed with PBS, then counted with MOXI Z Mini Automated Cell Counter Kit. ATAC library was prepared from 35,000 cells using the Tn5 transposase (Illumina). Cell pellet was resuspended in 50 µL PBS and 25 µL tagmentation DNA buffer, 2.5 µL Tn5, 0.5 µL 10% NP-40 and 22 µL water, then incubated at 50°C for 30 minutes with 500 nM EDTA, pH 8.0 for the recovery of digested DNA fragments. 100 µL of 50 nM $MgCl_2$ was added to neutralize EDTA and DNA fragments were purified using the MinElute PCR purification kit. Amplification and indexing of the library were performed as described in (Buenrostro, Giresi, Zaba, Chang, & Greenleaf, 2013). Equimolar ratios of libraries were then mixed and sequenced on a NextSeq 500 machine using v2 chemistry.

3.2.3 ATAC-seq analysis

FastQC (https://www.bioinformatics.babraham.ac.uk/projects/fastqc) was used to evaluate the sample quality. Trimmomatic v.0.3350 was used to trim reads after a quality drop below a mean of Q20 in a five nucleotides window. Only reads >30 nucleotides were cleared for further analysis. In order to normalize all samples to a similar sequencing depth, 27 million reads per sample were randomly selected for further analysis. STAR 2.5.2a (Dobin et al., 2013) was used to align the trimmed and filtered reads to the mm10 (GRCm38) Ensembl mouse genome version; only unique alignments were selected. To avoid PCR artefacts that could lead to multiple copies of the same original fragment, reads were additionally de-duplicated using Picard 1.136 (https://broadinstitute.github.io/picard/). For peak identification, MACS2 peak caller v.2.1.0 was used. Minimum q value was fixed to -1.5 and false discovery rate was set to 0.01. To determine thresholds for significant peaks, the data were inspected manually on the Integrated Genomics Viewer (IGV; (Robinson et al., 2011)). To compare peaks between different samples, final lists of new significant peaks were overlapped and unified to represent identical regions. Counts per unified peak per sample were computed with bigWigAverageOberBed (UCSC Genome Browser Utilities, https://hgdownload.cse.ucsc.edu/downloads) following conversion of binary alignment map (BAM) files to bigwig format with deep Tools bamCoverage (Ramirez, Dundar, Diehl, Gruning, & Manke, 2014). For normalization, raw counts for unified peaks were submitted to DESeq2 (Anders & Huber, 2010). Spearman correlations were produced using R to identify the degree of reproducibility between different samples. For normalized display of new peaks on IGV, the raw BAM files were normalized for noise level (number of reads inside peaks) and sequencing depth (number of mapped de-duplicated reads per sample). Two factors were computed and applied to the original BAM files, using bedtools genomecov (Quinlan & Hall, 2010), resulting in normalized bigWig files that can be visualized on IGV.

3.2.4 cDNA synthesis

Typically, 500-2000 ng of total RNA was used for reverse transcription using Maxima First Strand cDNA synthesis kit. PCR tubes with the reaction mix were placed in a thermocycler under following conditions:

Step	Temperature	Duration
1.	25°C	10 minutes
2.	50°C	30 minutes
3.	85°C	5 minutes

cDNA was then directly used for RT-qPCR analysis or stored at -20°C.

3.2.5 Cell culture

3.2.5.1 Cell line maintenance: NIH3T3 cells

NIH3T3 cells were maintained in DMEM high glucose + pyruvate medium, supplemented with 10% BCS and 1% penicillin-streptomycin. Cells were grown at 37°C, 5% CO_2, 9% humidity. Experiments were performed on cells under 20 passages, cells were grown in plates or dishes, and were split once they have reached 80-90% confluence. To split the cells, the old medium was aspirated, cells were washed by PBS and trypsinized (using TrypLE™ Express Enzyme) for 3-5 minutes at 37°C. Serum-containing medium was added to neutralize trypsin and cells were collected and centrifuged at 300 G for 5 minutes. After centrifugation, cells were resuspended in 1 mL fresh medium and split 1:20 to 1:10 depending on experimental needs in fresh plates or flasks. All cell lines were regularly tested for mycoplasma contamination.

3.2.5.2 Cell line maintenance: HEK293T cells

HEK293T cells were maintained in DMEM high glucose + pyruvate medium, supplemented with 10% FBS and 1% penicillin-streptomycin. Cells were grown at 37°C, 5% CO_2, 9% humidity. Experiments were performed on cells under 20 passages, cells were grown in plates or dishes, and were split once they have reached 70-80% confluence. To split the cells, the old medium was aspirated,

cells were trypsinized (using TrypLE™ Express Enzyme) for 1-3 minutes at 37°C. Serum-containing medium was added to neutralize trypsin and cells were collected and centrifuged at 300 G for 5 minutes. After centrifugation, cells were resuspended in 1-2 mL fresh medium and split 1:20 to 1:10 depending on experimental needs in fresh plates or flasks. All cell lines were regularly tested for mycoplasma contamination.

3.2.6 Creating knock-ins in mammalian cells

Two genomic sites, *Hipp11* and *Rosa26*, known as safe harbor loci that allow the expression of an inserted transgene without the risk of affecting surrounding endogenous genes were selected for targeted knock-ins in mammalian cells. Vector plasmids for both *Hipp11* and *Rosa26* loci were created to encode 800 base-pair length left and right homology arms and a multiple cloning site between them for integrating a knock-in cassette of interest. Homology arms were flanked with CRISPR cut-site sequences for an internal linearization of the template and thus higher knock-in efficiency. CRISPR-Cas9 technology was used for creating a targeted knock-in. Depending on what selection marker was included in the knock-in cassette, GFP-encoding (px458), PuroR-encoding (px459) or no selection marker containing (px330) Cas9 vector was used for co-transfection into the mammalian cells. Common cell cycle synchronizers, such as Nocodazole, were not used in this thesis to avoid cytotoxic effects. After transfections, cells were left to grow for 48-72 hours before proceeding to FACS or starting an antibiotic selection. Successful knock-ins were verified by genotyping and transgene expression (qPCR) analyses.

3.2.7 CRISPR-Cas9 mutagenesis: guide RNA assembly

DNA-targeting CRISPR site was selected using the ChopChop software. sgRNA(s) with the lowest off-target and the highest efficiency scores were selected, with lower off-target score being a higher priority. sgRNAs were then used in two ways: 1) for experiments where cells were transfected with Cas9-encoding vector, sgRNAs where ordered as two complementary oligonucleotides with

BbsI overhangs, annealed and then cloned into the same vector under the mammalian U6 promoter; 2) For experiments where mammalian cells were engineered to express Cas9 protein, sgRNAs were ordered as a constant T7 oligonucleotide and a variable long oligonucleotide, annealed, in vitro synthesized using a MEGAshortscript T7 kit, and then directly transfected into the cells. T7 oligonucleotide (5'_CGTAATACGACTCACTATAGG_3') consisted of a CG spacer, TAATACGACTCACTATA T7 promoter, and a starting GG for more efficient T7-driven synthesis. Variable long oligonucleotide (5'_AAAAGCACCGACTCGGTGCCACTTTTTCAAGTTGATAACGGACTAGCCTTATTTTAACTTGCTATTTCTAGCTCTAAAACXXXXXXXXXXXXXXXXXXXCCTATAGTGAGTCGTATTACG_3') consisted of reverse complements of a Cas9 sgRNA backbone with CRISPR site without PAM, and a T7 oligonucleotide.

3.2.8 CRISPR-Cas9 mutagenesis: guide RNA synthesis

The constant T7 and variable long oligonucleotides were mixed at equimolar concentrations in a total volume of 20 µL. Reaction mix was placed in a thermocycler, using the following program to anneal the two oligonucleotides:

Step	Temperature	Duration
1.	95°C	5 min
2.	95 to 85°C	-2°C/s
3.	85 to 25°C	-0.1°C/s

Annealed oligonucleotides were then used for sgRNA in vitro synthesis using the MEGAshortscript T7 kit from Ambion. 6 µL of the previous annealing mix was used per in vitro synthesis reaction, which was incubated at 37°C for 4 hours. With 15 minutes left, 1 µL of Turbo DNase was added to digest template oligonucleotides, and synthesized sgRNAs were then purified using the RNA Clean and Concentrator kit from Zymo Research.

3.2.9 CRISPR-Cas13d knockdowns: guide RNA assembly

RNA-targeting CRISPR site was selected using a custom-made CRISPR-Cas13d efficiency calculator. The most efficient sgRNA(s) were then screened with BLAST to eliminate those with potential off-target effects. sgRNAs were ordered as a constant T7 oligonucleotide and a variable long oligonucleotide, annealed, in vitro synthesized using a MEGAshortscript T7 kit, and then directly transfected into the mammalian cells. T7 oligonucleotide (5'_CGTAATACGACTCACTATAGG_3') consisted of a CG spacer, TAATACGACTCACTATA T7 promoter, and a starting GG for more efficient T7-driven synthesis. Variable long oligonucleotide (5'_XXXXXXXXXXXXXXXXXXXXXGTTTCAAACCCCGACCAGTTGGTAGGGGTTCC TATAGTGAGTCGTATTACG_3') consisted of reverse complements of an RfxCas13d sgRNA backbone with 23-bp RfxCas13d sgRNA specific sequence, and a T7 oligonucleotide, for visual representation see Figure 2.

3.2.10 CRISPR-Cas13d knockdowns: guide RNA synthesis

The constant T7 and variable long oligonucleotides were mixed at equimolar concentrations in a total volume of 20 µL. Reaction mix was placed in a thermocycler, using the following program to anneal the two oligonucleotides:

Step	Temperature	Duration
1.	95°C	5 min
2.	95 to 85°C	-2°C/s
3.	85 to 25°C	-0.1°C/s

Annealed oligonucleotides were then used for sgRNA in vitro synthesis using the MEGAshortscript T7 kit from Ambion. 6 µL of the previous annealing mix was used per in vitro synthesis reaction, which was incubated at 37°C for 4 hours (Figure 2). With 15 minutes left, 1 µL of Turbo DNase was added to digest template oligonucleotides, and synthesized sgRNAs were then purified using the RNA Clean and Concentrator kit from Zymo Research.

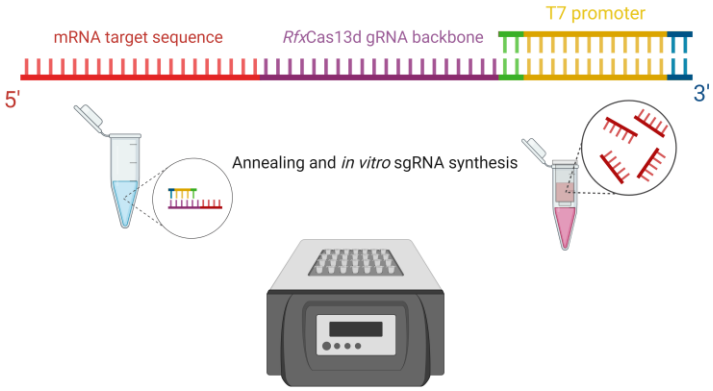

Figure 2. sgRNA preparation for mRNA-cleavage experiments using CRISPR-Cas13d.

3.2.11 DNA ligation

Ligation for DNA templates and DNA vectors digested with restriction enzymes that generate matching sticky 5' and 3' end overhangs was performed using the T4 DNA ligase as per manufacturer's instructions. Reaction mix consisting of the DNA template, linearized vector, T4 DNA ligase and T4 DNA ligase buffer was incubated either at 1 hour at room temperature, or at 16°C overnight (to increase the efficiency), then heat-inactivated at 65°C for 10 minutes, before being transformed into DH5α competent cells.

3.2.12 DNA purification from enzymatic reactions

DNA products from PCR and restriction digestion reactions were purified using the GeneJET PCR or GeneJET Gel extraction, if gel electrophoresis was needed to separate and isolate multiple DNA products, kits as per manufacturer's protocols.

3.2.13 DNA sequencing

Sanger (chain-termination) method was used to sequence plasmid DNA or PCR products of interest. 0.5-1 µg of a DNA sample was mixed with 10-12 µL water and 3 µM sequencing primer and sent to the SeqLab (Göttingen) facility. For longer DNA sequences, sequencing primers were designed every 600-800 bps to ensure overlapping and full coverage.

3.2.14 *E. coli* competent cell preparation

DH5α competent cells were inoculated in LB liquid medium at 37°C overnight. In the morning, 1 mL of the overnight culture was added to 200 mL of LB liquid medium and left in the shaker at 37°C for 4 hours. Then, the culture was placed on ice for 20 minutes, the cells were centrifuged at 4°C for 10 minutes, 4000 RPM. Supernatant medium was discarded and the pellet was left to dry, then it was resuspended in 5 mL cold 0.1M $CaCl_2$ and kept on ice for 5 minutes. The culture was centrifuged at 4°C for 5 minutes, 4000 RPM. Supernatant medium was discarded and the pellet was left to dry, then it was resuspended in a cold 0.1M $CaCl_2$ + 15% glycerol solution. Finally, 20 µL aliquots of resuspended cells were distributed in 1.5 mL tubes, snap-frozen, and stored at -80°C.

3.2.15 *E. coli* competent cell transformation

E. coli (DH5α) competent cells (20-40 µL) were thawed on ice for 2-5 minutes. Plasmid DNA or ligation mix, or linear PCR products after mutagenesis were added to competent cells and they were chilled on ice for 10 minutes. Heat shock at 42°C was applied for 60-90 seconds, followed by incubation on ice for 5 minutes. 100 µL of SOC medium was used to resuspend competent cells and transformed bacteria were plated on 30 mm Petri dish(es) prepared with LB agar containing ampicillin or kanamycin, or chloramphenicol and incubated at 37°C overnight.

3.2.16 Fluorescence-activated cell sorting (FACS)

Harvested (washed with PBS, detached from cell culture plates or flasks using trypsin (TrypLE™ Express Enzyme), centrifuged for 5 minutes at 300 G, and resuspended in DMEM medium) mammalian cells in culture, NIH3T3 cells or HEK293T cells, were passed through the 35 µm nylon mesh cell strainer into the glass FACS tubes and placed on ice to prevent clumping. DAPI was added to samples to distinguish between live and dead cells. Before running the samples on the sorter, negative controls (non-fluorescent WT cells) were sorted to

adjust the gate. A gate to distinguish cells from debris on a scatter plot of forward scatter (FSC-A) amplitude vs side scatter amplitude (SSC-A) was selected. Cells were sorted and collected using a BD FACSAria™ III machine. Cells were sorted into 96-well plates containing DMEM growth medium and transferred to the cell culture CO_2 incubators.

3.2.17 Gene abundance analysis by real-time quantitative qPCR

Synthesized cDNA was diluted 1:3 with nuclease-free water. For all performed experiments DyNAmo ColorFlash SYBR Green PCR mix was used as a dye, and samples were run on a CFX connect Real-time System (Biorad) under the following conditions:

Step	Temperature	Duration
Pre-amplification	95°C	7 minutes
Amplification (x39 cycles)	95°C	10 seconds
	60°C	30 seconds
Melting curve	60°C to 92°C	1°C increment every 5 seconds

Primer3 was used to design qPCR primers that amplify targets <200 bp in length. NCBI BLAST was used to validate the specificity of the designed qPCR primers. Only primers spanning introns or exon-exon junction were selected. Each biological replicate was derived from three technical replicates. Gene expression values were normalized using housekeeping genes: *Hprt* for mouse cell samples, *GAPDH* or *TOP1* for human cell samples. Fold change was calculated using the $2^{-\Delta\Delta Ct}$ method: the housekeeping gene's mean Ct value was deducted from the Ct values of the analyzed gene to obtain the ΔCt. ΔΔCt was then calculated by subtracting the average ΔCt of the control samples from ΔCts of the experimental condition samples.

3.2.18 Genomic DNA and total RNA isolation and purification

For genotyping different mutant (knock-out and knock-in) cell lines, cells were collected by trypsinization. After centrifugation, cell pellet was washed with PBS, spun down again, and processed using the Wizard® Genomic DNA Purification Kit (Promega). Isolated DNA was then used for PCR-based genotyping.

Total RNA was isolated using the cell lysis buffer (from PureLink™ RNA Mini Kit), supplemented with 1% 2-Mercaptoethanol (Gibco): 350 µL/well (12-well plate) or 500 µL/well (6-well plate). Cell lysate was mix with equal volume 70% ethanol and further purified using the PureLink™ RNA Mini Kit.

3.2.19 Genotyping

PCR followed by gel electrophoresis and sequencing was used to genotype mouse cell line mutants with large knock-ins. A primer pair constituted of one primer outside the knock-in cassette and one primer within the knock-in cassette as well as a primer pair constituted of both primers outside the knock-in cassette were used to differentiate wild-type, heterozygous and homozygous knock-in cell lines. Following PCR and gel electrophoresis, the wild types would display one short band (primer pair outside the knock-in cassette), heterozygous mutants would display two bands (both primer pairs used), and homozygous mutants would display one larger band (both primer pairs used). If necessary, Sanger (chain-termination) sequencing was used to validate the genotyping-PCR results.

3.2.20 Inducible system assembly

The inducible transgene expression approach was designed and cloned using the Tetracycline-inducible (TRE) promoter in conjunction with the Tet-On 3G transactivator, forming a TetON 3G system. The transgene sequence was fused with the TRE promoter, which allows for tight regulation of gene expression upon induction. The transactivator protein, which binds to the TRE in the presence of doxycycline, a tetracycline derivative, leading to activation of gene

expression, was placed under the control of a constitutive promoter. The fully assembled inducible transgene expression system was cloned into the knock-in destination vector containing homology arms, homologous for *Hipp11* safe harbor locus. The construct was verified by sequencing. The functionality of the inducible system was validated by assessing the transgene expression levels in the absence and presence of doxycycline using RT-qPCR.

3.2.21 Infusion cloning

Selected destination vectors were linearized with one or two restriction enzymes. Rarely, when linearization was not possible via restriction digestion, vectors were linearized using a PCR. Forward and reverse primers for PCR amplification of the desired insert were designed to contain 20 bp overhangs, homologous to the ends of the linearized destination vector. Following the PCR amplification of the insert, PCR products were run on the gel, the desired band was purified, mixed with a linearized vector and an InFusion enzyme. The reaction mix was then incubated at 50°C for 15 minutes, before being transformed into the DH5α competent cells.

3.2.22 In vitro transcription

Actb^{PTC} or *Actb*^{WT} transgene was cloned into a vector under the T7 or SP6 promoter. The vector was linearized by inducing a cut downstream of the transgene coding sequence. Transgenes were transcribed using a T7 or SP6 mMESSAGE mMACHINE kit as per manufacturer's instructions.
After annealing the short (T7) and long (sgRNA backbone with target sequence) oligos, Cas9 and Cas13d sgRNAs were in vitro transcribed using the MEGAshortscript T7 kit as per manufacturer's instructions.

3.2.23 Measurement of nucleic acid concentrations

DNA and RNA concentration was measured using a Nanodrop 2000 spectrophotometer. 1 µL of sample was loaded on the station, absorptions at 230, 260, and 280 nm were recorded, and the concentration numeric value was

calculated by the software as per Lambert-Beer law. The quality of DNA and RNA was evaluated based on the 260/280 (>1.8 for DNA and >2.0 for RNA) and 260/230 (approximately 2.0 to 2.2 for both DNA and RNA) ratios.

3.2.24 PCR amplification

PCR reactions were assembled with high-fidelity or non-high-fidelity polymerases, depending on experimental needs and downstream procedures, as per manufacturers' amplification protocols. Common thermocycler steps for the PCR reaction are as follows:

Step	Temperature	Time	Step description
1.	95-98°C	1-2 minutes, depending on polymerase used	Initial denaturation
2.	95°C	10-15 seconds	Denaturation
35-40 cycles	55-65°C, depending on primer melting temperature	15-30 seconds, depending on target complexity	Annealing
	68-72°C, depending on polymerase used	20-60 seconds per kbp, depending on polymerase used	Extension
3.	68-72°C	5-10 minutes	Final extension
4.	4°C	Indefinite	Hold

3.2.25 Plasmid DNA isolation

Following transformation and overnight incubation on agar plates, a single bacterial colony was inoculated in 5 mL LB medium supplemented with an appropriate antibiotic, and incubated overnight in a bacterial shaker at 37°C, 200 RPM. In the morning, the bacterial culture was centrifuged at 4000 RPM for 10 minutes. Supernatant was discarded and the bacterial pellet was

resuspended in a resuspension buffer. Plasmid DNA was then isolated using a GeneJet Plasmid MiniPrep kit as per manufacturer's instructions.

3.2.26 PTC-bearing transgene design

All PTC-bearing transgenes were designed to contain at least three introns downstream the PTC. For *Actb* and *Actg1* transgenes, given their relatively small genomic size (3.64 kb and 2.85 kb respectively), the whole WT genomic sequence was amplified and a nonsense mutation, a single-nucleotide change resulting in a PTC, was introduced using site-directed mutagenesis approach. For *Ctnna1* and *Nckap1* transgenes, given their genomic size (135.92 kb and 80.75 kb respectively) was too big for direct cloning, three parts of the transgene were amplified separately: 5'UTR-cDNA upstream introns, genomic DNA with exons and at least three shortest introns, downstream cDNA-3'UTR, and pieced together using the InFusion cloning technique. The 3'UTR was trimmed in order to be able to design qPCR primers for specific transgene recognition. A PTC was placed more than 55 nucleotides upstream of the last exon-exon junction for proper NMD recognition. The modified transgene was cloned into an appropriate expression vector, under an inducible TRE promoter.

3.2.27 Restriction digestion

1000 ng of given DNA templates (vectors, PCR amplicons, etc.) were mixed with 1U of the required restriction enzyme, 2 µL of the appropriate 10x digestion buffer, and H_2O to top up the reaction to 20 µL. Reaction mix was incubated for 1 hour at 37-65°C, depending on manufacturer's requirements for a specific restriction enzyme. Appropriate heat inactivation (65-80°C) followed if the digested DNA was not meant to be run on gel electrophoresis.

3.2.28 RNA sequencing (RNA-seq)

PureLink™ RNA Mini Kit was used to purify total RNA harvested from mouse cells in culture. Approximately 350,000 cells (1 well in a 12-well plate) were used per sample. DNase treatment was performed after RNA purification using

the RQ1 DNase kit from Promega. Another round of purification using the same PureLink™ RNA Mini Kit was applied afterwards. RNA and library integrity were verified on the LabChip Gx Touch 24 (Perkin Elmer). 1 µg of the total RNA was used as an input for the SMARTer Stranded Total RNA Sample Prep Kit-HI Mammalian. RNA sequencing was performed on a NextSeq 500 machine using v2 chemistry, generating on average 25-30 million reads per library, with a 1 x 75 bp single-end setup.

3.2.29 RNA-seq analysis

FastQC was used to evaluate the quality of raw reads, duplication rates, and adaptor content. To trim the reads after a quality drop below a mean of Q20 in a 10 nucleotides window, Reaper v.13-100 (Davis, van Dongen, Abreu-Goodger, Bartonicek, & Enright, 2013) was used. For subsequent analysis, only reads of at least 15 nucleotides were cleared. STAR 2.5.3a was used to align trimmed and filtered reads to the mm10 (GRCm38) Ensembl mouse genome version. featureCounts 1.6.0 was used to count the number of reads that aligned to various genes. Every read had to at least partially map to the exonic sequence; such reads were aggregated per gene. Reads mapping to multiple regions or genes were eliminated. DESeq2 v.1.14.1 (Love, Huber, & Anders, 2014) was used to identify differentially expressed genes. $P < 0.05$ (Wald test) was used to classify genes as significantly differentially expressed. Specific minimum or maximum threshold values for a fold change were not set.

3.2.30 Site-directed mutagenesis

PrimerX was used for automated design of mutagenic PCR primers, based on the input sequence. The desired mutation was then introduced using PCR amplification following the QuickChange protocol. Briefly, PCR reaction was prepared using a template plasmid and SeqAmp DNA polymerase. Whole plasmid was amplified using the following protocol.

Step	Temperature	Duration	
1.	95°C	2 minutes	Initial denaturation
2.	95°C	50 seconds	Denaturation
	60°C	30 seconds	Annealing
18 cycles	68°C	8-11 minutes, depending on the plasmid length	Extension
3.	68°C	10-15 minutes	Final extension
4.	4°C	Indefinite	Hold

Afterwards, PCR reaction was supplemented with NEB CutSmart buffer and DpnI restriction enzyme, which cleaves only when its recognition site is methylated; therefore, removing the WT template DNA from the reaction mix. The restriction enzyme was then heat-inactivated, and linear PCR product was used directly for transformation into the competent cells.

3.2.31 Statistical analysis

Statistical analyses were performed using GraphPad Prism (Version 6.07). A Gaussian distribution was tested for every sample group using the D'Agostino-Pearson omnibus normality test; experiments that passed the normality criterion were further analyzed using the Student's t-test for comparison of 2 samples, or one-way ANOVA test followed by correction for multiple comparisons with Dunn's Test for 3 or more samples. Experiments that did not pass the normality criterion were further analyzed using non-parametric tests: p-values were determined using the Mann-Whitney test for comparison of 2 samples, or the Kruskal-Wallis test followed by correction for multiple comparisons with Dunn's Test for 3 or more samples.

3.2.32 Transfection into mouse cell lines

NIH3T3 and HEK293T cells were transfected using identical protocols. The following table describes transfection reagent use based on the experimental setup, as well as amounts of transfected materials:

Transfection reagent	Transfected materials	Amount used (ng)
Lipofectamine 3000	Vector DNA	2000/12-well 5000/6-well
Lipofectamine MessengerMAX	mRNA, cDNA	1000/12-well 2000/6-well
Lipofectamine RNAiMAX	Cas9 and Cas13d sgRNAs	1000/6-well

For generating stable knock-in cell lines, when transfection of two vectors (Cas9+sgRNA and donor template) was needed, 1.5 µg of Cas9-carrying vector (px330, px458, or px459) and 3.5 µg of template DNA-containing vector were used per single well in a 6-well plate. 48 hours post transfection, a selection procedure using 2 µg/mL (for HEK293T cells) or 8 µg/mL (for NIH3T3 cell) Puromycin was initiated. If necessary, FACS was performed 72 hours post transfection.

4. RESULTS

4.1 Manipulation of inducible degradation-prone transgenes triggers TA

4.1.1 Assembly of a Tetracycline-controlled transcriptional activation system practical for studying the TA response

I have selected a Tetracycline-dependent Tet-On system, which employs an inducible TRE promoter and a transactivator rtTA (reverse tetracycline-controlled transactivator) that binds to the tetracycline operator (tetO) sequences in the TRE promoter in presence of Tetracycline or Doxycycline. Such setup allows keeping the transgene of interest transcriptionally inactive at all times, except for when the cells are treated with the inducer. Two versions of a selected transgene, either *Actb* or *Actg1*, the wild-type version (further denoted as Tg-*Actb*^{WT} or Tg-*Actg1*^{WT}) (Figure 3A, 3C) and the degradation-prone PTC-bearing version (further denoted as Tg-*Actb*^{PTC} or Tg-*Actg1*^{PTC}) (Figure 3B, 3D) were cloned under the inducible TRE promoter in a plasmid backbone which contained a transactivator rtTA, as well as two selection markers – GFP and PuroR – driven by two separate constitutive promoters, see plasmid maps (Figure 4A–B). PTCs in both transgenes were introduced via site-directed mutagenesis (Methods 3.2.30), by substituting one nucleotide in the *Actb* and *Actg1* coding sequences (Figure 3B, 3D). In conclusion, such vectors can be used in future experiments to swap in various degradation-prone transgenes and test whether they are capable of triggering TA.

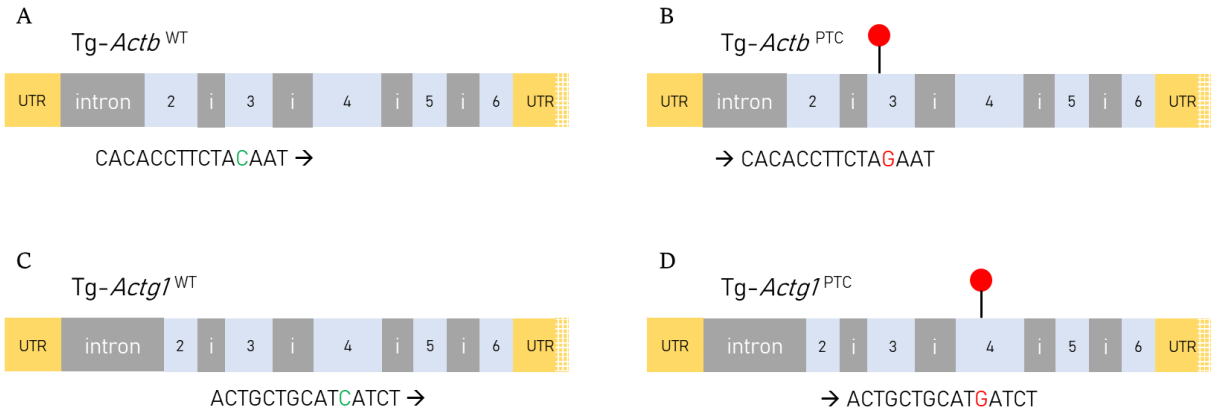

Figure 3. Schematics of different *Actin* transgenes used in this study.

A: Schematic of the wild-type *Actb* transgene (Tg-*Actb*^{WT}). B: Schematic of the degradation-prone *Actb* transgene (Tg-*Actb*^{PTC}), the UAG premature STOP codon is

introduced in the 3rd (2nd coding) exon. C: Schematic of the wild-type *Actg1* transgene (Tg-*Actg1*^{WT}). D: Schematic of the degradation-prone *Actg1* transgene (Tg-*Actg1*^{PTC}), the UGA premature STOP codon is introduced in the 4th (3rd coding) exon. Each transgene has a modified 3' UTR (dotted region) for transgene-specific qPCR primer design.

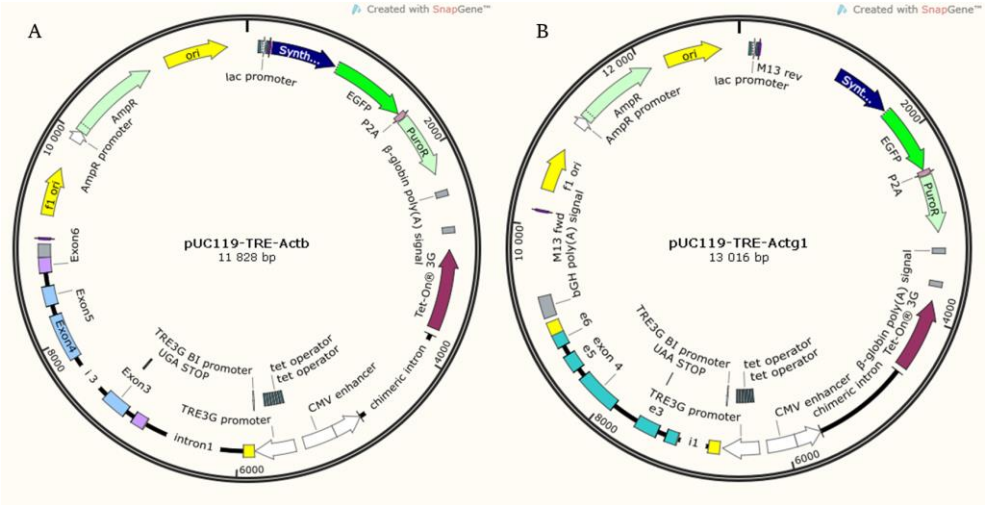

Figure 4. Plasmid backbones encoding the two Tet-On *Actin* transgene induction systems.

A: Plasmid encoding the *Actb* transgene, the Tet-On inducible gene expression system components: TRE3G promoter, transactivator rtTA, and two selection markers. B: Plasmid encoding the *Actg1* transgene, the Tet-On inducible gene expression system components, and two selection markers.

4.1.2 Engineering the *Hipp11* locus for a targeted knock-in of the PTC-containing *Actin* transgenes

The tetracycline-controlled transcriptional activation system was cloned into a new vector (Figure 5), which contained the homology arms for a precise knock-in in mouse *Hipp11* locus. *Hipp11* is a safe harbor locus, meaning that the integration of a transgene does not perturb endogenous gene activity; in addition, *Hipp11* does not contain an endogenous promoter (Hippenmeyer et al., 2010; Y. S. Li et al., 2019), unlike, e.g., *Rosa26*, making *Hipp11* particularly suitable for the inducible expression of transgenes. Guide RNA 5'GTCATGAGACTCATACTACG3' was used to initiate a DSB using a CRISPR-Cas9 effector. The engineered locus after a knock-in of WT and PTC+ transgenes is depicted in Figure 6. In conclusion, *Hipp11* homology arms-containing vectors

can be used in future experiments to create stable cell lines for various purposes, including studying transgenic means of triggering TA.

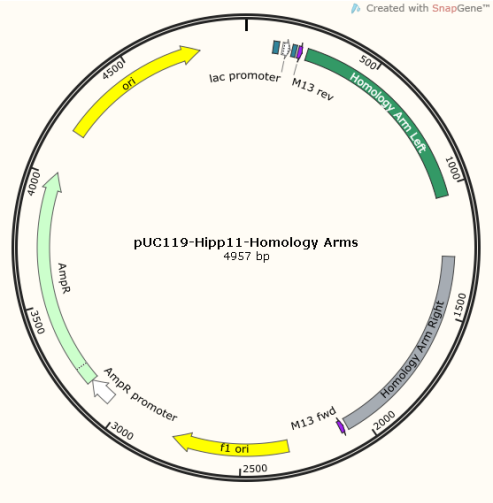

Figure 5. Plasmid backbone encoding left and right homology arms, homologous to the mouse *Hipp11* locus, and a multiple cloning site between them.

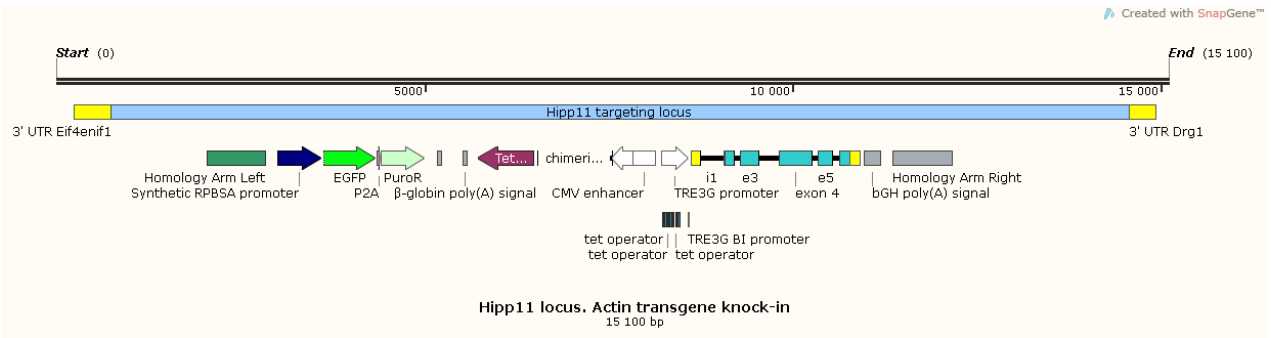

Figure 6. Map of the *Hipp11* safe harbor locus, lying between the *Eif4enif1* (at the 5' end) and *Drg1* (at the 3' end) genes. The knock-in is performed between two homology arms (dark green and grey in the map). The knock-in cassette includes an *Actin* transgene driven by the inducible TRE3G promoter, EGFP and PuroR selection markers driven by the synthetic RPBSA promoter, and a Tet-On transactivator driven by the CMV promoter.

4.1.3 NIH3T3 cells tolerate the Doxycycline treatment and efficiently express inducible *Actin* transgenes

First, I tested whether Doxycycline itself has any effect on the expression of *Actin* genes in WT NIH3T3 cells. The results indicated minimal and not significant influence on the expression of *Actb*, *Actg1* and *Actg2* (Figure 7).

Next, I induced the transgene-carrying NIH3T3 cells and measured the expression of Tg-*Actb*^{WT}, Tg-*Actg1*^{WT}, Tg-*Actb*^{PTC} and Tg-*Actg1*^{PTC}. RT-qPCR analyses indicated that all transgenes were efficiently expressed after treating cells with Doxycycline both at 24 and 48 hours after induction (Figure 8). In conclusion, these results demonstrate that it is safe to use Doxycycline in NIH3T3 cells while monitoring the expression of *Actin* genes. Additionally, *Actin* transgenes can be efficiently expressed from the *Hipp11* locus.

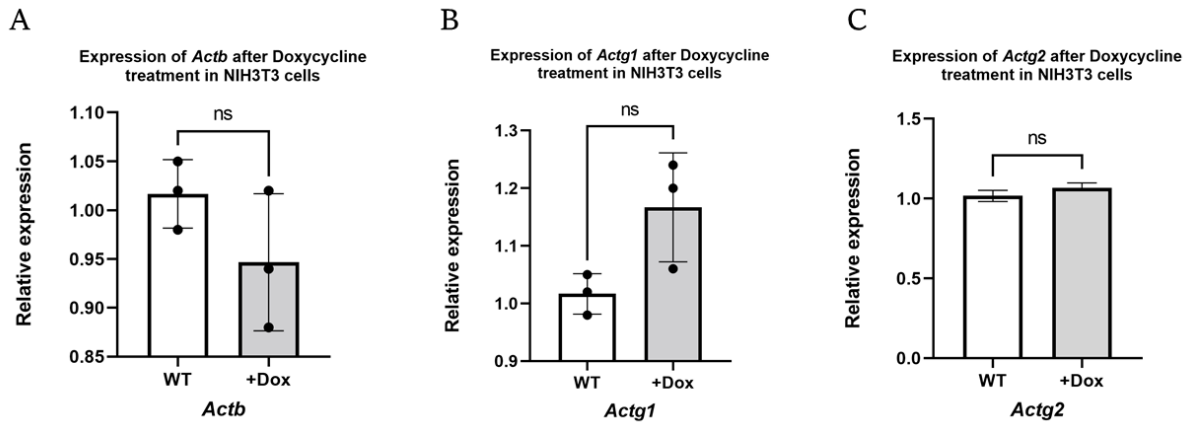

Figure 7. The effect of the Doxycycline treatment on the expression of endogenous *Actin* genes in wild-type NIH3T3 cells.

A: A change in *Actb* expression in response to Doxycycline treatment. B: A change in *Actg1* expression in response to Doxycycline treatment. C: A change in *Actg2* expression in response to Doxycycline treatment. Doxycycline was used at 1000 ng/mL working concentration, dissolved in water. Untreated WT NIH3T3 cells were used as a control.

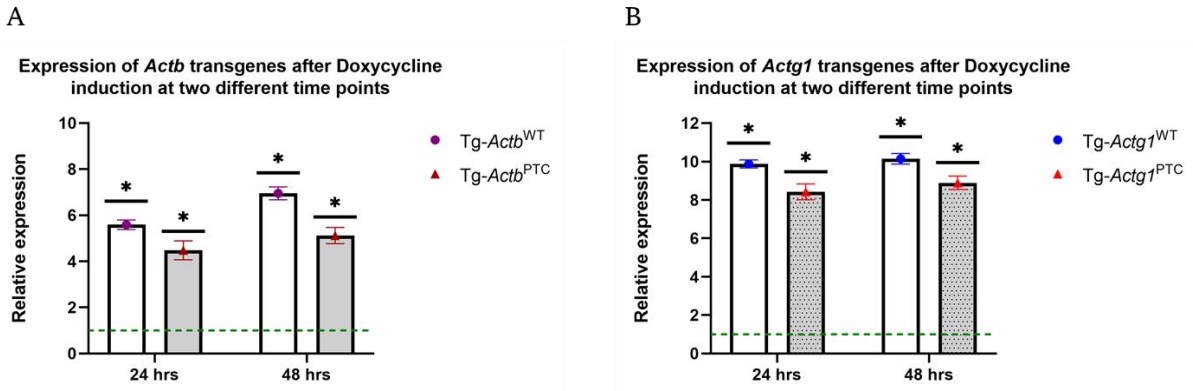

Figure 8. Doxycycline efficiently induces the expression of *Actin* transgenes.

A: *Actb* transgenes are approximately 4-6-fold upregulated after the induction with Doxycycline. B: *Actg1* transgenes are approximately 8-10-fold upregulated after the induction with Doxycycline. Doxycycline was used at 1000 ng/mL working

concentration, dissolved in water. Not induced transgene-carrying NIH3T3 cells were used as a control, set as 1 (green dashed line).

4.1.4 PTC-bearing transgenes become efficiently degraded consequent to their induction

After the evaluation of transgene expression, I tested whether the PTC-bearing transgenes (Tg-*Actb*^{PTC} or Tg-*Actg1*^{PTC}) are targeted by the mRNA surveillance machinery and are efficiently degraded. RT-qPCR analyses indicated that Tg-*Actb*^{PTC} and Tg-*Actg1*^{PTC} are downregulated in relation to their wild-type counterparts Tg-*Actb*^{WT} and Tg-*Actg1*^{WT} (Figure 9A, 9D). In the case of Tg-*Actb*^{PTC}, three different STOP codons (UAA, UAG, UGA) were tested; carrying any of the PTCs resulted in the degradation of the transgene (Figure 9A). In the case of Tg-*Actg1*^{PTC}, an additional, invisible to NMD, PTC in the last coding exon was also tested in order to verify that NMD is involved in the recognition of PTC-transgenes. Transgenes carrying this PTC were, as expected, not degraded within the cells (Figure 9D). In conclusion, these results suggest efficient degradation of the PTC-bearing transgenes, most likely via the NMD pathway.

4.1.5 Degradation of the PTC-bearing transgenes triggers TA

Next, I have tested whether the degradation of PTC-bearing transgenes results in the upregulation of the known *Actb* and *Actg1* adapting genes. RT-qPCR analyses revealed the upregulation of *Actg1* and *Actg2* in induced Tg-*Actb*^{PTC}-expressing cells (Figure 9B), and the upregulation of *Actg2* in induced Tg-*Actg1*^{PTC}-expressing cells (Figure 9E). In conclusion, these results suggest that overexpression of the PTC-bearing transgenes can trigger a TA response, which is independent of protein loss and manifests as upregulation of adapting paralogous genes.

4.1.6 Inducible Tet-On TA system demonstrates undesirable leakiness

Finally, I have tested the expression of adapting genes without the induction with Doxycycline to test whether the inducible TA system is ‘silent’ at baseline

conditions, and therefore is sensitive and accurate enough to study the temporal dynamics of TA. RT-qPCR analyses revealed that the adapting genes are upregulated in PTC-bearing transgene expressing cells without Doxycycline as compared to not induced WT transgene-expressing NIH3T3 cells (Figure 9C, 9F). In conclusion, these results suggest that despite its ability to trigger TA, the inducible system based on a Doxycycline-sensitive TRE promoter demonstrates undesired transgene activation and subsequent adapting gene upregulation without induction, rendering it unsuitable for studying the TA response from its earliest onset and TA's temporal effects on adapting gene expression.

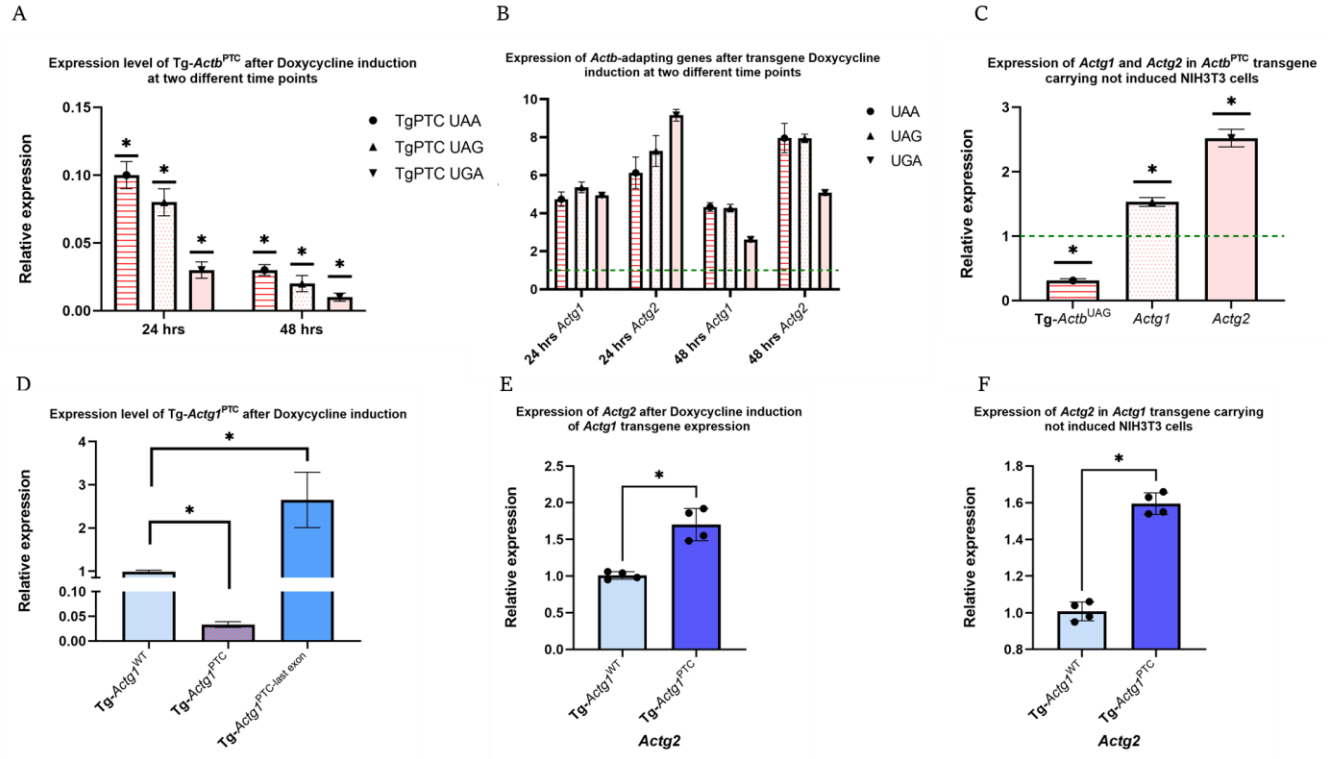

Figure 9. PTC-bearing transgenes are efficiently degraded and can induce the TA response; however, they are not sufficiently tightly regulated.

A: Three different *Actb*^{PTC} transgenes, carrying UAA, UAG, or UGA PTCs are significantly downregulated as compared to the *Actb*^{WT} transgene at 24 and 48 hours after induction. B: At 24 and 48 hours after induction, *Actg1* and *Actg2* are significantly upregulated in induced *Actb*^{PTC} transgene-carrying NIH3T3 cells, as compared to *Actb*^{WT} transgene control (green dashed line set as 1). C: Without Doxycycline treatment, *Actb*$^{PTC\text{-}UAG}$ transgene is significantly downregulated, and both *Actg1* and *Actg2* adapting genes are significantly upregulated, as compared to not induced *Actb*^{WT} transgene-carrying NIH3T3 cells (green dashed line set as 1). D: *Actg1*^{PTC} transgene is significantly downregulated, whereas *Actg1*^{PTC} transgene with the PTC located in the last coding exon,

thus not recognizable by the NMD machinery, is not downregulated as compared to the *Actg1*^{WT} transgene at 24 hours after induction. E: *Actg2* is significantly upregulated in induced *Actg1*^{PTC} transgene-carrying NIH3T3 cells, as compared to *Actg1*^{WT} transgene control. F: Without Doxycycline treatment, *Actg2* in the not induced *Actg1*^{PTC} transgene cell line is still significantly upregulated, as compared to not induced *Actg1*^{WT} transgene-carrying NIH3T3 cells. Doxycycline was used at 1000 ng/mL working concentration.

4.1.7 *ACTB*^{PTC} transgene overexpression triggers the TA response in a human HEK293T cell line

Despite the leakiness of the inducible transgene overexpression system, I have decided to test the usefulness of the transgene overexpression approach in human cells and to assess whether TA can be triggered in human cells using the latter approach. I have established two stable HEK293T cell lines, one expressing *ACTB* transgene with a UAA PTC (Tg-*ACTB*^{UAA}), and one with a UAG PTC (Tg-*ACTB*^{UAG}). Overexpression of any of the two transgenes resulted in the upregulation of *ACTG1*, *ACTG2*, and the endogenous *ACTB* gene (Figure 10), suggesting that TA occurs in human cells and that a transgenic approach can be a useful method to study the TA mechanisms in human cells.

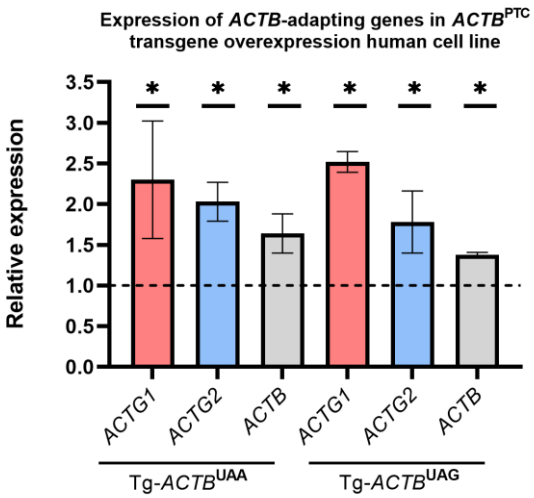

Figure 10. *ACTB* PTC-bearing transgenes trigger a TA response in HEK293T cells. Upregulation of *ACTB* adapting genes *ACTG1*, *ACTG2* and endogenous *ACTB* occurs in both Tg-*ACTB*^{UAA} and Tg-*ACTB*^{UAG} expressing cell lines, as compared to *ACTB*^{WT} transgene-carrying HEK292T cells (dashed line set as 1).

4.2 CRISPR-Cas13d-triggered mRNA degradation leads to a TA-like response

4.2.1 Engineering the *Hipp11* locus for a targeted knock-in of the CRISPR-Cas13d effector

The CRISPR-Cas13d effector driven by a constitutive EF-1alpha promoter was cloned into an aforementioned pUC119-*Hipp11*-HomologyArms vector, which contained the homology arms for a precise knock-in in mouse *Hipp11* locus (Figure 11). Guide RNA 5'GTCATGAGACTCATACTACG3' was used to initiate a DSB using a CRISPR-Cas9 effector. The engineered locus after a knock-in of CRISPR-Cas13d is depicted in Figure 12. In conclusion, *Hipp11* locus is a suitable genomic site for not only inducible, but also constitutive transgene expression.

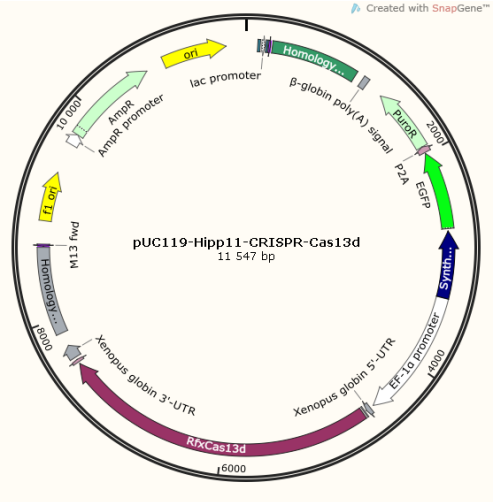

Figure 11. Plasmid backbone encoding two homology arms, left and right, homologous to the mouse *Hipp11* locus, a CRISPR-Cas13d effector, and two selection markers.

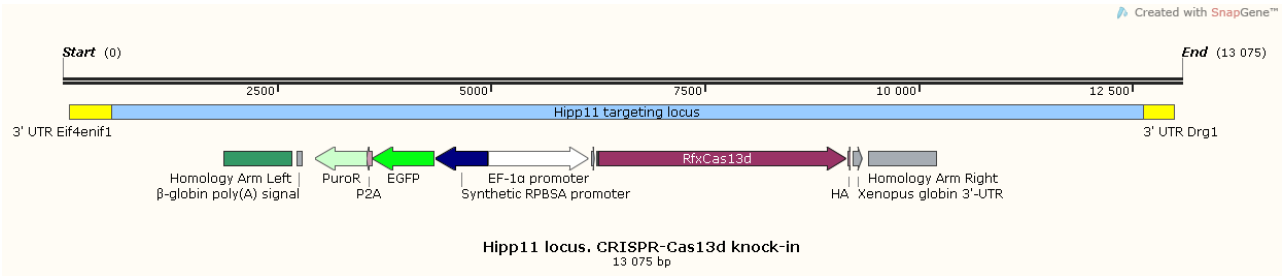

Figure 12. Map of the *Hipp11* safe harbor locus, lying between the *Eif4enif1* (at the 5' end) and *Drg1* (at the 3' end) genes. A knock-in is performed between two homology

arms (dark green and grey in the map). The knock-in cassette includes a CRISPR-Cas13d effector driven by the EF-1alpha promoter, and EGFP and PuroR selection markers driven by the synthetic RPBSA promoter.

4.2.2 NIH3T3 cells efficiently express the CRISPR-Cas13d effector

Prior to starting the cytoplasmic mRNA knockdown experiments, I have validated the expression of CRISPR-Cas13d and CRISPR-Cas13d-NLS effectors in NIH3T3 cells. Cells have been FACS-sorted and multiple single clones were expanded. Several clones were tested for Cas13d expression using RT-qPCR (Figure 13). In conclusion, CRISPR-Cas13d and CRISPR-Cas13d-NLS effectors can be efficiently expressed and do not cause harm for NIH3T3 cells.

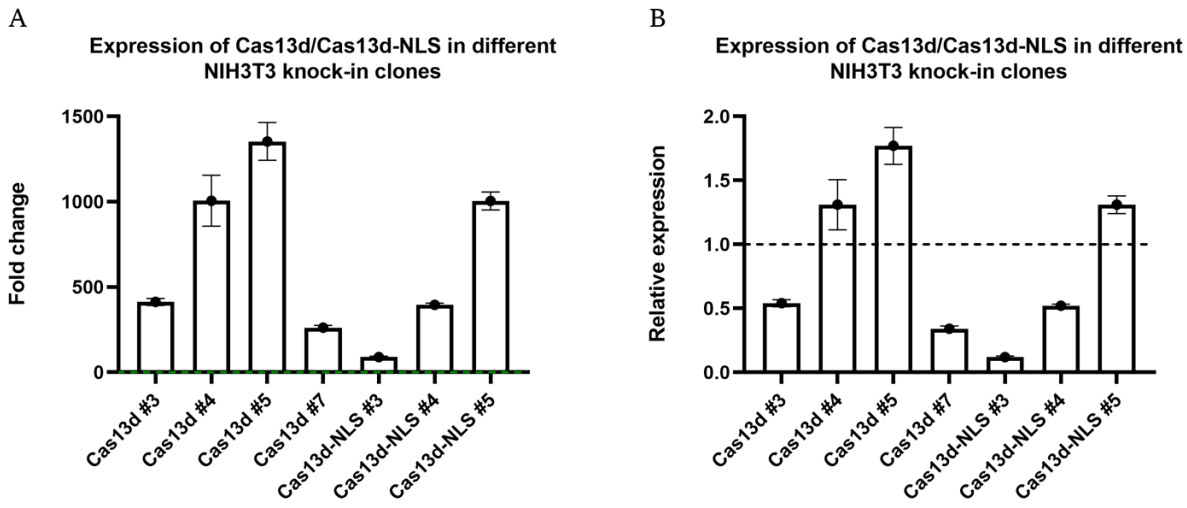

Figure 13. CRISPR-Cas13d and CRISPR-Cas13d-NLS effectors are efficiently expressed in NIH3T3 cells.

A: Expression of Cas13d and Cas13d-NLS effectors in NIH3T3 knock-in clones compared to WT NIH3T3 cells. B: Expression of Cas13d and Cas13d-NLS effectors in NIH3T3 knock-in clones, normalized to a Cas13d-expressing NIH3T3 cell line (dashed line set as 1).

4.2.3 CRISPR-Cas13d-mediated *Actg1* mRNA cleavage leads to transcriptional upregulation of *Actg2*

In order to investigate other potential means of triggering mRNA degradation and test whether they lead to TA, I transfected CRISPR-Cas13d-expressing NIH3T3 cells with sgRNAs targeting *Actg1* mRNA. Two different sets of sgRNAs

were used: a pool of six sgRNAs (sg_pool), which recognized both *Actg1* and *Actb* coding sequences, and a unique sgRNA (sg_uniq), which targeted specifically *Actg1* mRNA. Cleavage of *Actg1* with either sgRNA approach resulted in a significant downregulation of *Actg1* and an upregulation of *Actg2* within 24 hours (Figure 14). In conclusion, these results suggest that cytoplasmic mRNA degradation without a genomic lesion is sufficient to induce a TA-like response.

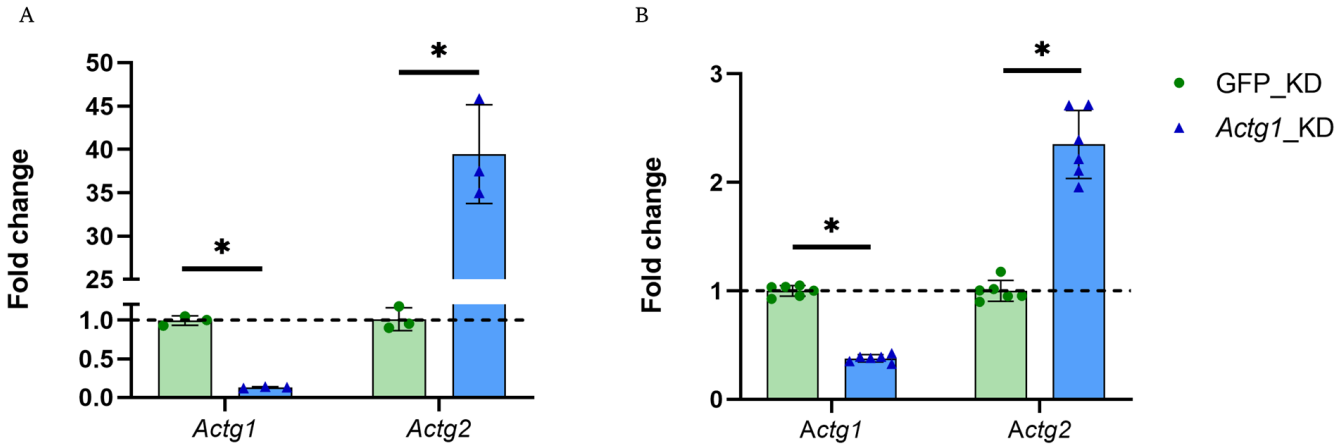

Figure 14. Cas13d-mediated cleavage of *Actg1* mRNA leads to transcriptional upregulation of *Actg2*.

A: CRISPR-Cas13d-mediated cleavage of *Actg1* using a pool of six sgRNAs (sg_pool) leads to compelling *Actg2* upregulation. B: CRISPR-Cas13d-mediated cleavage of *Actg1* using a single sgRNA (sg_uniq) leads to lower, but significant *Actg2* upregulation. Normalized to a GFP knockdown (dashed line set as 1).

4.2.4 CRISPR-Cas13d-mediated TA-like response is not limited to *Actin* genes

Moreover, I observed similar results using additional two gene models, where target genes have several high sequence-similarity paralogs. Namely, cleavage of *Ctnna1* mRNA resulted in transcriptional upregulation of *Ctnna2* and *Ctnna3* genes, as well as significant downregulation of *Ctnna1l* gene (Figure 15A), whereas cleavage of *Nckap1* (*Hem2*) mRNA led to transcriptional upregulation of *Hem1*, *Nckap5*, and *Nckap5l* genes (Figure 15B). In conclusion, these data suggest that Cas13d cleavage-induced TA-like response is not limited to the *Actin* gene family.

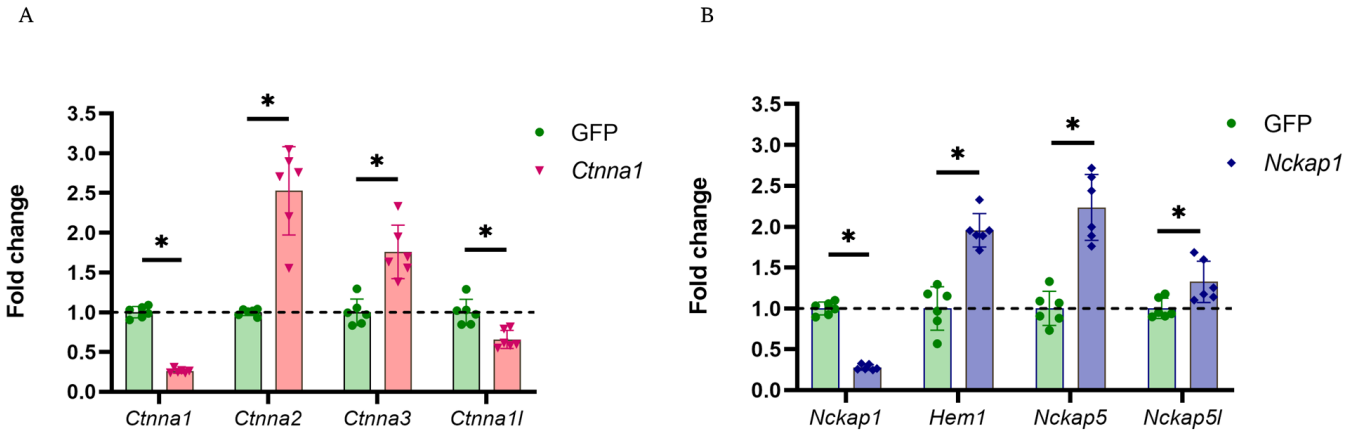

Figure 15. Cas13d cleavage-induced TA-like response is not limited to the *Actin* gene family.

A: CRISPR-Cas13d-mediated cleavage of *Ctnna1* mRNA leads to transcriptional upregulation of *Ctnna2* and *Ctnna3*, as well as downregulation of *Ctnna1l*. B: CRISPR-Cas13d-mediated cleavage of *Nckap1* mRNA leads to transcriptional upregulation of *Hem1*, *Nckap5*, and *Nckap5l*. Normalized to a GFP knockdown (dashed line set as 1).

4.2.5 Different mRNA degradation pathways trigger distinct TA responses

Next, I performed an RNA-seq experiment on CRISPR-Cas13d-expressing NIH3T3 cells treated with sgRNAs targeting *Actg1* mRNA versus sgRNAs targeting GFP mRNA as a control. I observed transcriptional upregulation of *Actg2* (Table 20); however little overlap between other differentially expressed genes in CRISPR-Cas13d RNA-seq experiment as compared to CRISPR-Cas9 *Actg1* KO RNA-seq dataset (Figure 16), obtained by our laboratory (unpublished data), suggesting that different mRNA degradation modes, potentially generating diverse mRNA degradation fragments, can lead to distinct TA responses. Similarly in line with these findings, Fernandez-Abascal and colleagues have demonstrated that different nonsense alleles upregulate different *clh* family genes, depending on which exons are removed from the *clh-1* gene in *C. elegans*, see Discussion for further consideration.

Ensembl gene	Mean reads: *Actg1*-KD; sg_uniq	Mean reads: *Actg1*-KD; sg_pool	Mean reads: Control; GFP-KD
Actg1	224	272	249
Actg2	**28**	**71**	**8**
Acta2	1012	1317	743
Acta1	133	217	62
Actb	1470	1616	1628

Table 20. Mean reads of different *Actin* genes in a CRISPR-Cas13d-mediated *Actg1* knockdown RNA-seq dataset.

Degradation (downregulation) of *Actg1* is not observed possibly due to high sequence similarity and a subsequent multi-mapping issue between the *Actg1* and *Actb* transcripts, resulting in most of the *Actg1* reads being eliminated from the analysis. Successful degradation is indicated by *Actg2* upregulation. *Acta1* and *Acta2* are also upregulated after *Actg1* mRNA cleavage.

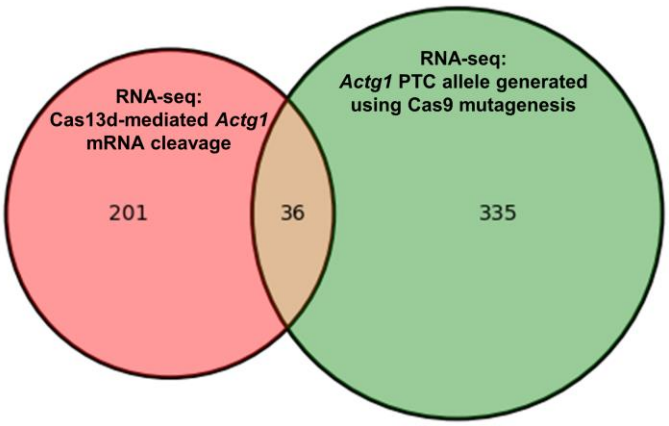

Figure 16. A Venn diagram of overlapping differentially expressed genes between CRISPR-Cas13d-mediated *Actg1* knockdown and CRISPR-Cas9-generated *Actg1* knockout allele.

36 common differentially expressed genes can be identified between two RNA-seq datasets: a Cas13d-mediated *Actg1* mRNA cleavage versus an *Actg1* PTC allele generated using Cas9 mutagenesis.

4.2.6 Transcriptional upregulation of *Actg2* after CRISPR-Cas13d-mediated *Actg1* mRNA cleavage is not associated with increased chromatin accessibility

Next, I investigated whether CRISPR-Cas13d-mediated *Actg1* mRNA degradation and the subsequent TA-like response leads to chromatin remodeling at the adapting *Actg2* gene locus. I designed an experiment, where CRISPR-Cas13d-expressing NIH3T3 cells where treated with sgRNAs targeting *Actg1* mRNA for three rounds of transfection, which were performed on the day of passaging cells. I maintained the Cas13d-mediated cleavage of *Actg1* for 10 days, routinely monitoring the upregulation of *Actg2* (Figure 17A), then discontinued sgRNA transfections and investigated whether *Actg2* expression is altered once *Actg1* mRNA levels have been restored. Notably, I observed a moderate upregulation of *Actg2* even in the absence of *Actg1*-targeting sgRNAs (Figure 17B), which is dependent on increased transcription, rather than increased mRNA stability, as demonstrated by *Actg2* pre-mRNA expression levels (Figure 17C). These data suggest that cytoplasmic mRNA degradation could produce intermediaries, capable of persistent modulation at the adapting gene loci.

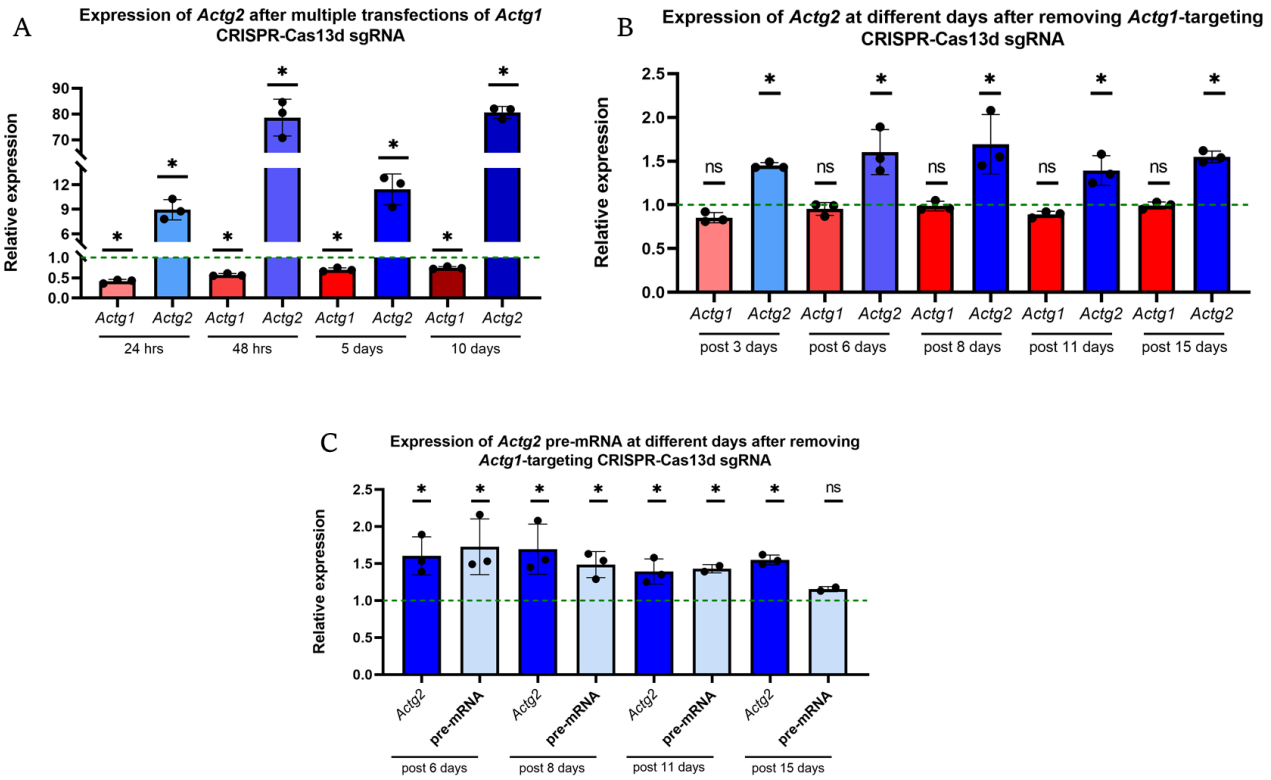

Figure 17. Cas13d-induced *Actg2* upregulation persists in the absence of the *Actg1* targeting sgRNA.

A: Cas13d-mediated *Actg1* mRNA cleavage and subsequent *Actg2* upregulation is maintained for several days after multiple rounds of cell passaging and sgRNA transfections. B: Cells were split after a 10-day treatment with *Actg1*-targeting sgRNAs, then were kept without sgRNAs, and collected at different time points. The upregulation of *Actg2* persisted throughout the 15-day period, even after the normalization of *Actg1* expression. C: Upregulation of *Actg2* is caused by increased transcription, rather than increased mRNA stability, as indicated by the upregulation of *Actg2* pre-mRNA levels at respective time points. Normalization performed to a GFP knockdown at a respective time point (dashed line set as 1).

I have then performed an ATAC-seq to evaluate the chromatin state at the *Actg2* locus during the Cas13d-mediated TA-like response. CRISPR-Cas13d-expressing NIH3T3 cells where treated with sgRNAs targeting *Actg1* mRNA for 5 days, and *Actg2* upregulation was established on regular basis. Samples for ATAC-seq were collected after 5 days of continuous *Actg1* targeting, assuming that 5 days is enough for chromatin remodeling to occur. However, ATAC-seq analysis did not identify any peaks that would correspond to regions of open

chromatin at the *Actg2* locus (Figure 18B). Significant peaks were not identified at any other *Actin* loci as well (Figure 19). Together, these data indicate that Cas13d induced TA-like response does not require chromatin remodeling, despite prominent transcriptional increase of adapting genes.

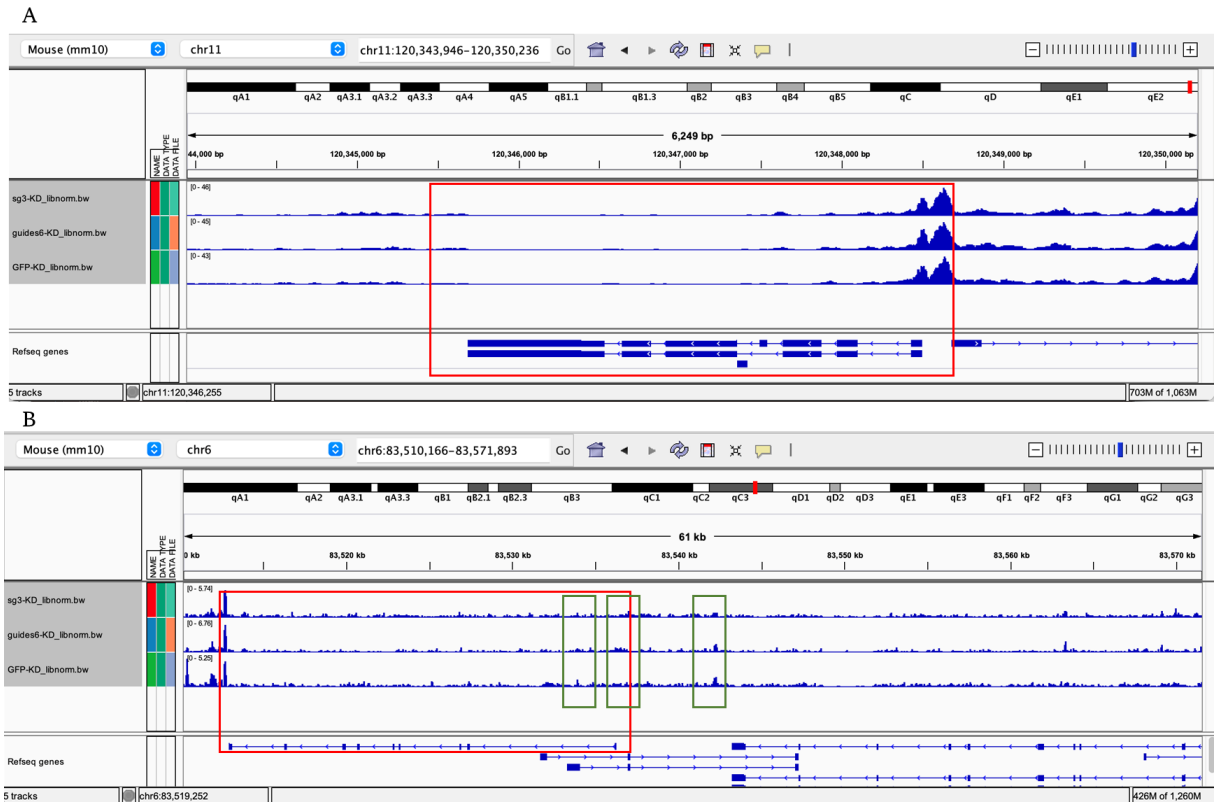

Figure 18. CRISPR-Cas13d-mediated transcriptional upregulation of *Actg2* does not require chromatin remodeling.

A: Image from the integrated genome viewer (IGV) browser showing the tracks of *Actg1* locus. Top track – *Actg1* mRNA cleavage by a single guide (sg_uniq), middle track - *Actg1* mRNA cleavage by a pool of guides (sg_pool), bottom track – control GFP mRNA cleavage. Cas13d-mediated cleavage of *Actg1* mRNA does not impact the chromatin architecture at the *Actg1* locus. B: Image from the IGV browser showing the tracks of *Actg2* locus. Top track – *Actg1* mRNA cleavage by a single guide (sg_uniq), middle track - *Actg1* mRNA cleavage by a pool of guides (sg_pool), bottom track – control GFP mRNA cleavage. Red square highlights the boundaries of *Actg2*. Green squares highlight the expected increased chromatin accessibility areas. Cas13d-mediated *Actg2* upregulation does not result from increased chromatin accessibility at the *Actg2* locus.

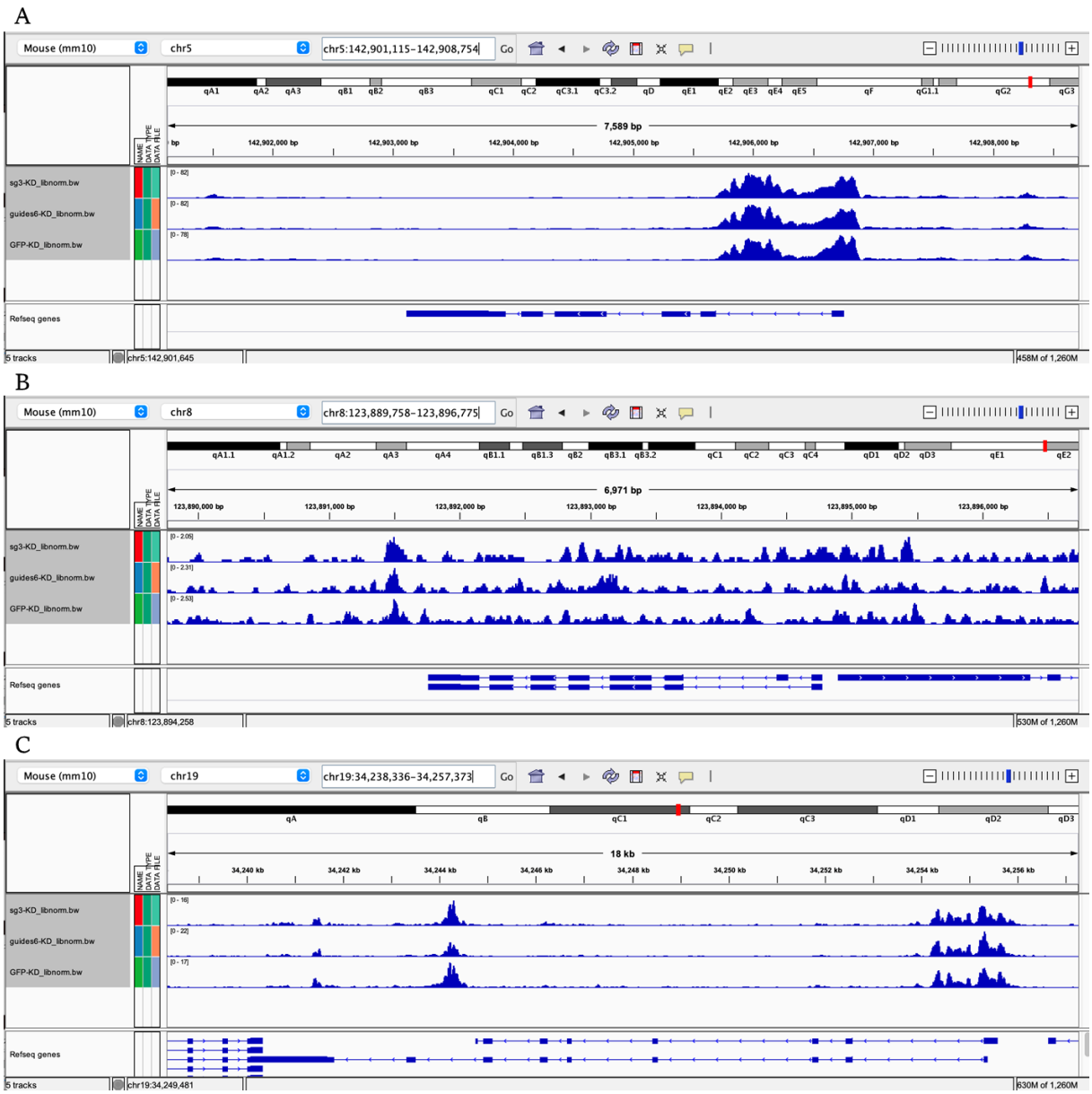

Figure 19. CRISPR-Cas13d-mediated *Actg1* mRNA cleavage does not lead to chromatin remodeling at any *Actin* locus.

A: Image from the integrated genome viewer (IGV) browser showing the tracks of *Actb* locus. Top track – *Actg1* mRNA cleavage by a single guide (sg_uniq), middle track - *Actg1* mRNA cleavage by a pool of guides (sg_pool), bottom track – control GFP mRNA cleavage. Cas13d-mediated cleavage of *Actg1* mRNA does not impact the chromatin architecture at the *Actb* locus. B: Image from the IGV browser showing the tracks of *Acta1* locus. Top track – *Actg1* mRNA cleavage by a single guide (sg_uniq), middle track - *Actg1* mRNA cleavage by a pool of guides (sg_pool), bottom track – control GFP mRNA cleavage. Cas13d-mediated cleavage of *Actg1* mRNA does not impact the chromatin architecture at the *Acta1* locus. C: Image from the IGV browser showing the tracks of *Acta2* locus. Top track – *Actg1* mRNA cleavage by a single guide (sg_uniq), middle track -

Actg1 mRNA cleavage by a pool of guides (sg_pool), bottom track – control GFP mRNA cleavage. Cas13d-mediated cleavage of *Actg1* mRNA does not impact the chromatin architecture at the *Acta2* locus.

4.2.7 Targeting different cleavage sites with CRISPR-Cas13d results in varying TA-like response

Multiple sgRNAs; i.e., 8 targeting *Ctnna1* mRNA and 6 targeting *Nckap1* mRNA, were tested to inspect whether using different guides to target different cleavage sites, thus potentially creating distinct mRNA degradation patterns, would result in varying or non-changing CRISPR-Cas13d-mediated TA-like response. sgRNA recognition sites were spaced out across the mRNAs' coding sequences (Figure 20A, 21A). The results indicate that separate guides have different efficiency which correlates, to some extent, with the degree of a TA-like response in *Ctnna1* and *Nckap1* knockdown (Figure 20B-C, 21B). In addition, although a certain level of mRNA degradation is achieved in each case, not all of them lead to a TA-like response (Figures 20, 21), meaning that the location where the initial mRNA cleavage occurs could be important in triggering the TA-like response. Curiously, the most efficient guides appear to be located at or in close proximity to exon-exon junctions.

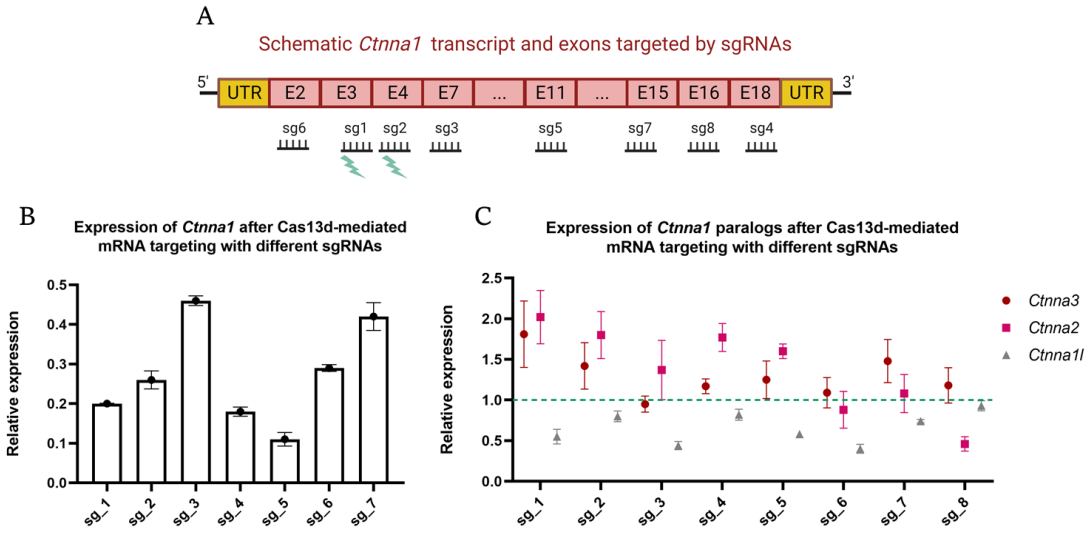

Figure 20. Different *Ctnna1* Cas13d cleavage sites lead to varying TA-like response. A: Schematic of the *Ctnna1* transcript and the locations of individual sgRNA recognition sites. sg1 and sg2, marked with lightning icons, demonstrate the most robust TA-like response. B: Each individual guide efficiently cleaves and downregulates *Ctnna1*.

C: *Ctnna1* mRNA cleavage with individual guides leads to varying upregulation of *Ctnna3* and *Ctnna2*. sg1 and sg2 demonstrate the most robust upregulation of both paralogs. Normalization performed to a GFP knockdown (dashed line set as 1).

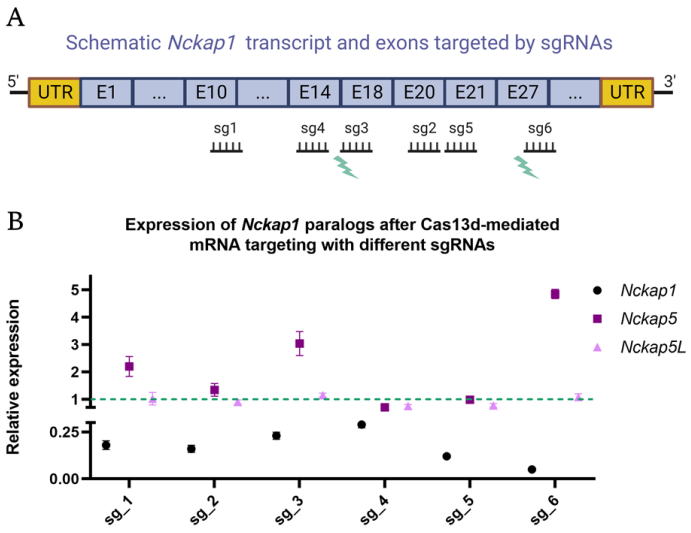

Figure 21. Different *Nckap1* Cas13d cleavage sites lead to varying TA-like response. A: Schematic of the *Nckap1* transcript and the locations of individual sgRNA recognition sites. sg3 and sg6, marked with lightning icons, demonstrate the most robust TA-like response. B: Each individual guide efficiently cleaves and downregulates *Nckap1*, but only cleavage using sg3 and sg6 leads to upregulation of *Nckap5*. Normalization performed to a GFP knockdown (dashed line set as 1).

4.2.8 Nuclear CRISPR-Cas13d-mediated pre-mRNA degradation does not trigger the TA-like response

I have designed intron-targeting CRISPR-Cas13d sgRNAs and used a nuclear-localized version of CRISPR-Cas13d (Cas13d-NLS) to evaluate whether targeting transcripts in the nucleus, namely pre-mRNAs, can trigger a TA-like response, or whether only cytoplasmic mRNA degradation leads to a TA-like response. Cells expressing Cas13d-NLS were subjected to transfection with sgRNAs aiming at the second intron within the *Actg1* pre-mRNA. RT-qPCR analyses have revealed low, but significant downregulation of *Actg1* pre-mRNA within the nucleus, while the levels of mature *Actg1* mRNA remained unaltered. Furthermore, there was no observed increase in *Actg2* pre-mRNA or mRNA within 24 hours (Figure 21A). I have also tested the same intron-targeting

sgRNA in a regular Cas13d cell line, in order to validate whether the intronic targeting is specific to nuclear Cas13d. RT-qPCR analyses have revealed no effect on *Actg1* pre-mRNA in the cytoplasmic Cas13d cell line (Figure 21B). In conclusion, these results indicate that nuclear pre-mRNA degradation alone does not appear to be sufficient and mRNA has to be degraded in the cytoplasm in order to trigger TA, or a TA-like response. In addition, these data suggest that certain factors, most likely proteins that perform their main functions in the cytoplasmic compartment, are required for TA.

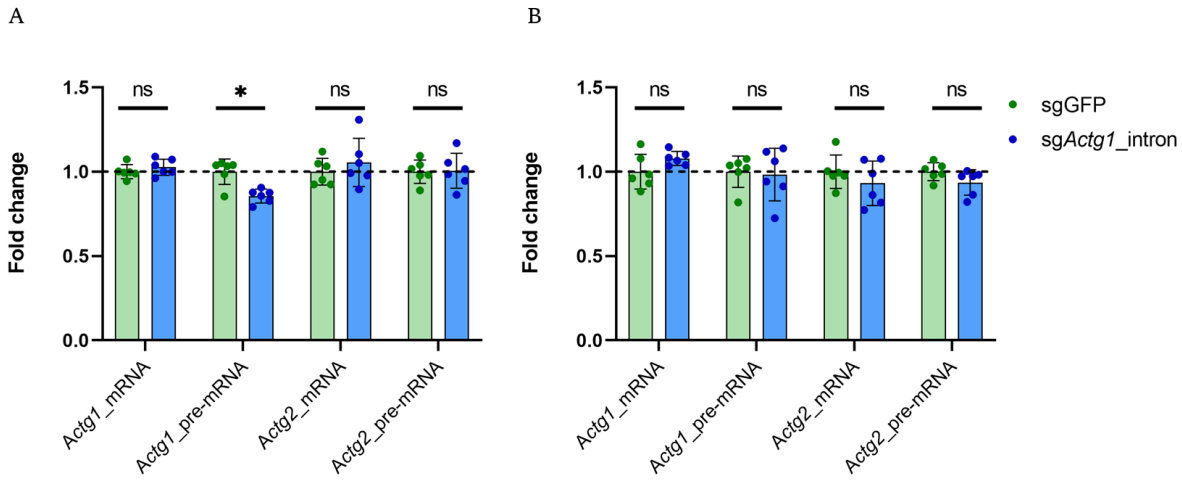

Figure 21. Nuclear pre-mRNA degradation does not trigger a TA-like response in NIH3T3 cells.

A: Targeting an *Actg1* intron with nuclear Cas13d results in low, but significant *Actg1* pre-RNA degradation; however, no upregulation of *Actg2* pre-mRNA or mRNA. B: Targeting an *Actg1* intron with regular Cas13d does not result in *Actg1* pre-RNA degradation, indicating that nuclear and cytoplasmic Cas13d effectors retain their activity in separate cellular compartments.

4.2.9 CRISPR-Cas13d-mediated mRNA degradation triggers the TA-like response in human cells

In order to investigate whether Cas13d-trigger TA-like response is not limited to a single mammalian system, in addition to experiments in murine NIH3T3 cells, I have also established a stable Cas13d-expressing HEK293T cell line. I have successfully demonstrated that Cas13d-mediated mRNA cleavage can be achieved in human cells and that such mRNA degradation results in a TA-like

response in HEK293T cells. I have transfected Cas13d-expressing HEK293T cells with sgRNAs targeting human *NCKAP1* transcript, triggered the degradation of *NCKAP1*, and observed the upregulation of *NCKAP5* and *NCKAP5L* (Figure 23).

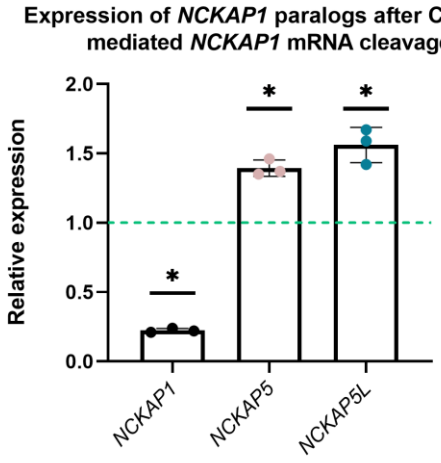

Figure 23. Cas13d-mediated mRNA cleavage triggers a TA-like response in human cells.

Cas13d-mediated cleavage of *NCKAP1* mRNA leads to *NCKAP5* and *NCKAP5L* upregulation in HEK293T cells.

4.3 Temporal profile of transcriptional adaptation

4.3.1 Higher degree of sequence similarity results in earlier transcriptional modulation of adapting genes

Finally, I was able to obtain some insight into how the TA response develops over time. I performed a CRISPR-Cas13d-mediated knockdown of *Nckap1*, followed by an RNA-seq experiment at two different time points. At 12 hours post knockdown, the downregulation of *Nckap1* is not yet at its maximum and only one, more highly similar related gene, *Nckap5l*, is upregulated (Table 21), whereas at 24 hours post knockdown another related gene, *Nckipsd*, becomes increased in expression (Table 22). In conclusion, these data suggest that the degree of sequence similarity might determine which adapting genes get upregulated first, and which get upregulated later during a TA response.

Ensembl gene	Full name	log2FoldChange	p adj
Nckap1	Nck-associated protein 1	-0.86	0.000005
Nckap5l (Cep169)	Nck-associated protein 5-like	0.41	0,000985

Table 21. Expression of *Nckap1* and potential adapting genes at 12 hours after sgRNA transfection; RNA-seq dataset.
At 12 hours after *Nckap1*-targeting sgRNA transfection, while the degradation is only at its initial stages, one similar gene, *Nckap5l*, with a sequence similarity of 43.35% (cDNA) or 45.25% (including promoter/enhancer region), is upregulated.

Ensembl gene	Full name	log2FoldChange	p adj
Nckap1 (Kiaa0587)	**Nck-associated protein 1**	**-1.46**	**0.000005**
Nckap5l (Cep169)	**Nck-associated protein 5-like**	**0.40**	**0.000167**
Nckipsd	**NCK-interacting protein with SH3 domain**	**0.22**	**0.014845**

Table 22. Expression of *Nckap1* and potential adapting genes at 24 hours after sgRNA transfection; RNA-seq dataset.
At 24 hours after *Nckap1*-targeting sgRNA transfection, while the degradation is high, two similar genes, *Nckap5l*, with a sequence similarity of 43.35% (cDNA) or 45.25% (including promoter/enhancer region), and *Nckipsd*, with a sequence similarity of 44.06% (cDNA) or 43.94% (including promoter/enhancer region), are upregulated.

4.3.2 Upregulation of adapting genes during TA occurs as soon as mRNA degradation is initiated

Finally, I have performed several time course experiments using different TA-induction systems to find out how quickly TA response develops after a proper trigger. Given the leakiness of the knocked-in inducible TA systems (Figure 9C,

9F), I have cloned the Tet-On system and an *Actb* PTC transgene in a new vector, and later transiently transfected and induced WT NIH3T3 cells in order to track how quickly TA can be observed. The WT background of the cells and the induction only upon transfection ensures the stability of *Actin* adapting gene expression at time point zero. After transfection, I induced the cells with 1000 ng/mL Doxycycline. RT-qPCR analyses have revealed that TA can be triggered almost as quickly as NMD of the PTC transcript is initiated. *Actb* adapting gene *Actg1* was upregulated as early as 15 minutes after Doxycycline induction (Figure 24A), whereas *Actg2*, the less sequence-wise similar adapting gene, became upregulated at 4-6 hours onwards (Figure 24B), once again indicating that the degree of sequence similarity might determine which adapting genes get upregulated first, and which get upregulated later during a TA response. It is, nevertheless, unclear why *Actg2* appeared to be downregulated at early time points (Figure 24A).

In addition, I have performed a time course experiment using the Cas13d-mediated mRNA cleavage system. I have transfected the Cas13d-expressing cells with sgRNAs targeting *Nckap1* mRNA and collected total RNA at several different time points in order to evaluate the expression of *Nckap1* paralogs. Similarly to previous observations, the TA-like response resulting from Cas13d-mediated mRNA cleavage is a rapid process, which could be observed as early as 6 hours after sgRNA transfection (Figure 24C).

In conclusion, these results indicate that TA is very rapid process, which is initiated practically as soon as mRNA degradation is triggered.

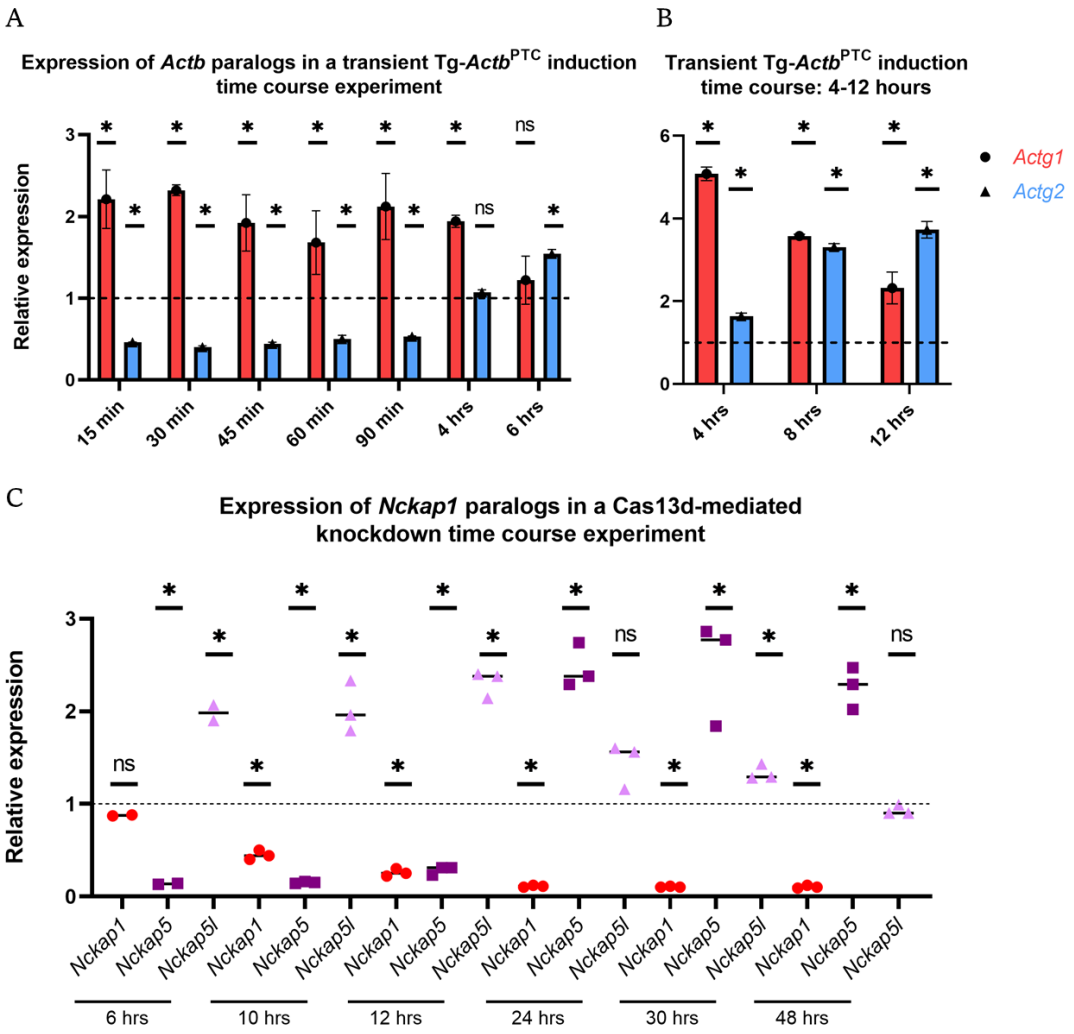

Figure 24. TA time course experiments using the *Actb*^{PTC} transgene overexpression and Cas13d-mediated mRNA cleavage systems.

A: *Actb*^{PTC} transgene overexpression and induction, early time points. *Actg1* is upregulated as early as 15 minutes after induction, whereas *Actg2* becomes upregulated at 6 hours after induction. B: *Actb*^{PTC} transgene overexpression and induction, late time points. *Actg1* and *Actg2* upregulation is maintained, *Actg2* upregulation increases gradually over time. Normalized to not induced *Actb*^{PTC} transgene transfected cells (dashed line set as 1). C: CRISPR-Cas13d-mediated *Nckap1* mRNA cleavage, total mRNA collected at different time points. *Nckap5* becomes upregulated at 24 hours after sgRNA transfection, whereas *Nckap5l* is upregulated as early as 6 hours after sgRNA transfection; however, decreases in expression from 24 hours onwards.

5. DISCUSSION

Despite over-the-years accumulated data on TA, its exact molecular mechanisms remain obscure. In this dissertation, firstly, I describe several new tools that can broaden research capabilities and help answer mechanistic questions about TA and, secondly, provide initial data on temporal aspects of TA. I demonstrate that a genomic perturbation, a DNA lesion, is not required for TA, rather – the degradation of cytoplasmic mRNAs alone plays a central role in triggering TA. Additionally, the initial transcriptional augmentation response, which manifests as upregulation of related genes, does not involve epigenetic changes as shown by Cas13d-mediated mRNA degradation. My data suggest that TA initiation is a two-step process, where mRNA degradation fragments initially serve as proxies for tuning transcriptional output before such information is reflected on the chromatin level. Furthermore, genes with higher degree of sequence similarity are transcriptionally modulated before genes with lower degree of sequence similarity.

5.1 CRISPR-Cas13d-mediated cytoplasmic wild-type mRNA degradation is sufficient to trigger TA

Molecular TA models, as proposed in 2019, still invigorate the debate whether mutant mRNA degradation alone is sufficient to trigger TA, or rather the recruitment of UPF3A, an antagonist of NMD pathway and thus mRNA degradation (Shum et al., 2016), onto the PTC-bearing mRNA promotes TA, or as it was called on that occasion – the genetic compensation response (GCR). The first model proposes that mutant mRNA degradation intermediates translocate into the nucleus, where they bind to specific loci and modulate the expression of the related gene(s) via transcriptional regulators including antisense RNAs, histone modifiers and/or chromatin remodelers (El-Brolosy et al., 2019). The second model focuses on the full-length PTC-containing mutant mRNA interacting with a histone modifier Wdr5-COMPASS complex, and guiding the polymer within the nucleus to upregulate the expression of the

related gene(s) (Ma et al., 2019). Both models suggest that the sequence similarity with the mutant mRNA determines which genes get upregulated during TA/GCR (the downregulation of related genes back when the models were proposed, had not been observed, or rather considered).

The data presented in this dissertation prove that the degradation of cytoplasmic mRNAs alone can trigger TA and that such process does not require the recruitment of various NMD factors, including UPF1 and UPF3A. One outstanding question remains – what is the exact mechanism of CRISPR-Cas13d-mediated mRNA degradation, and whether it could resemble, in any way, the degradation pathways of endogenous mRNA quality surveillance? Cas13d degrades mRNAs by forming an activated ternary complex composed of Cas13d bound to both crRNA and its complementary target RNA. The two Cas13d REC and NUC lobes contain the catalytic subunits that wrap around a spacer:protospacer duplex, whereas complementary nucleotides of the target mRNA base pair with that spacer within crRNA (C. Zhang et al., 2018). Upon activation, HEPN domains initiate mRNA hydrolysis and cleavage. Perhaps somewhat similarly, mRNA cleavage via the NMD pathway occurs at close proximity, approximately 5–40 nucleotides downstream, to a PTC (Eberle, Lykke-Andersen, Muhlemann, & Jensen, 2009), where a large decay-inducing (DECID) complex, surrounding the PTC and consisting of SMG1–UPF1–eRFs (SURF) complex, SMG6 or SMG5-7 heterodimer, UPF2 and UPF3X, associates with the mutant mRNA (Kurosaki, Popp, & Maquat, 2019). Although Cas13d and UPF1 proteins are similar in size (~100 kDa and ~130 kDa, respectively), Cas13d is considerably smaller than the whole DECID complex. Nevertheless, in both cases, structurally, certain portions of the mRNA sequence are expected to remain shielded from the activity of endo- and exonucleases, which could be key in preserving and producing TA-triggering mRNA degradation fragments. The importance of short motifs in eliciting TA was recently demonstrated in *C. elegans act-5*/*act-3* TA model, where a 25 base pair-length sequence in the regulatory region of the *act-3* locus, demonstrating a 60% identity to a

sequence in the *act-5* mRNA, was sufficient to induce TA (Welker, Serobyan, Zaker Esfahani, & Stainier, 2023).

In summary, the data presented in this dissertation firmly support the degradation-favoring mechanistic model of TA (El-Brolosy et al., 2019) and provide evidence for related gene(s) upregulation upon mRNA degradation without any dependence on a PTC. Ultimately, although the scientific field is still waiting for evidence how exactly mRNA degradation fragments translocate into the nucleus and find specific loci to bind and modulate, such mechanism seems theoretically more plausible than the nuclear reentry of full-length PTC-bearing mRNAs. Although possible (Goldstein & Trescott, 1970), few mechanisms have been described, mostly relying on retrotransposition, namely on the regulation of highly abundant in the mammalian genome (representing 17% of the human and 19% of the mouse genome) LINE-1 retrotransposons (Bodak, Yu, & Ciaudo, 2014). Finally, one should be careful and consider the possibility that the two TA/GCR scientist groups are looking at a pair of unrelated compensation mechanisms. The fact that we think of TA and GCR as perhaps the same pathway or at least somewhat intertwined processes with some molecular differences can be related to recency bias stimulated by the back-to-back publication dates as well as their perhaps accidental similarities.

5.2 CRISPR-Cas13d-mediated TA-like response does not require chromatin remodeling

Both El-Brolosy et al. and Ma et al. have demonstrated in their 2019 papers that TA involves chromatin remodeling, namely, both groups reported increased H3K4 trimethylation, rendering the DNA in the chromatin more accessible for transcription factors, at the adapting genes loci (El-Brolosy et al., 2019; Ma et al., 2019). However, in their follow-up work Ma et al. have reported that H3K4me3 enrichment is not required for GCR in zebrafish *leg1a–leg1b* model, while maintaining the Upf3a essentiality notion (Xie et al., 2023), whereas recent work from Stainier lab described an intergenerational and

transgenerational inheritance of TA, whereby wild-type offspring of TA-displaying heterozygous animals exhibit increased expression of the adapting genes (Jiang et al., 2022). The question of chromatin state involvement in TA remains fluid; yet, data tend to indicate that certain degree of epigenetics is at play, with a few exceptions, in CRISPR-Cas9 mutants.

Data presented in this dissertation propose a model where TA or a TA-like response can be rapidly triggered without chromatin remodeling. Extended yet temporary mRNA degradation by Cas13d leads to an increased adapting gene expression that persists even after targeted mRNA levels are restored, suggesting a certain level of epigenetic involvement; nevertheless, without enhanced chromatin opening in the Cas13d-triggered mRNA degradation context. Given that chromatin remodeling, as indicated by the H3K4me3 enrichment and newly formed chromatin peaks in the ATAC-seq analyses, has been reported in CRISPR-Cas9 generated mutants with degrading alleles (El-Brolosy et al., 2019), one plausible explanation for this discrepancy between Cas13d and Cas9 contexts could be linked to the fact that Cas13d approach is susceptible to fluctuating levels of trigger sgRNAs, resulting in an inherently transient state of target mRNA disruption. Supporting this hypothesis, similar occurrences have been documented during the development of flies and worms, where rapid gene activation and deactivation take place in the absence of the typical histone modifications associated with canonical gene regulation (Perez-Lluch et al., 2015). It is highly conceivable that alterations in chromatin accessibility unfold over several cell divisions, playing a role in the formation of an epigenetic TA memory (Jiang et al., 2022); yet, these alterations might not be necessary for the immediate TA response itself.

Another explanation could rely on different mRNA degradation fragments being generated and their varying ability to act as chromatin-remodeling sRNAs. As discussed in the previous section, it is possible that particular larger or smaller portions of the mRNA sequence remain shielded by a Cas13d or DECID complex, preserving and producing diverse TA-triggering mRNA degradation fragments in both scenarios. Nonetheless, even without this

hypothetical preservation, it is highly possible that different mRNA degradation pathways produce various decay intermediates, which are later separately processed into unique qualities-possessing sRNAs.

Numerous studies have reported the ability of sRNAs to modify the chromatin's structure and increase or repress transcription at target loci (reviewed in (L. C. Li, 2014)). However, small activating RNAs (saRNAs), a sub-class of dsRNA molecules, which can activate endogenous genes via an RNA-based promoter targeting mechanism, can also act through the assembly of an RNA-induced transcriptional activation (RITA) complex, which interacts with RNA polymerase II to stimulate transcription initiation and productive elongation, accompanied by monoubiquitination of histone 2B (H2Bub1) (Portnoy et al., 2016). Intriguingly, H2Bub1 mark, a regulator of transcription elongation, is not necessarily linked to more permissive chromatin, as several reports have suggested its ability to stabilize nucleosomes (Segala, Bennesch, Pandey, Hulo, & Picard, 2016). In addition, some saRNAs may operate at the post-transcriptional level; e.g., by enhancing mRNA stability or translation efficiency, without directly modifying chromatin.

In summary, Cas13d-triggered TA-like response, which manifests as transcriptional upregulation of adapting genes, does not involve chromatin remodeling. Epigenetics in TA: chromatin state alterations and chromatin mark implementation as a consequence of mRNA degradation remain one of the most intriguing questions in TA research. It appears that, at least in certain cases, TA-induced transcriptional augmentation does not require more permissive chromatin; therefore whether chromatin remodeling during the TA response is a cause or an effect of increased transcription remains to be resolved.

5.3 Implications for further TA and gene perturbation studies

Data presented in this dissertation clearly demonstrate that evaluating the effects of TA demands a meticulous approach and careful considerations. The key challenge lies in distinguishing between noise and signal within the

complex genetic landscape: both RNA-seq and ATAC-seq experiments demonstrate a multitude of differentially expressed genes or chromatin accessibility peaks in TA vs control conditions, irrespective of the TA-triggering method used. How many of those genes and peaks have a direct connection to TA, or, in other words, are the direct consequence of gene regulation via TA, remains obscure and not intuitive, despite a number of large datasets generated over time.

One of the greatest challenges in TA studies remains selecting and establishing appropriate controls that would not bias TA screens and offer the ability to impartially distinguish the primary and secondary effects of TA. Mutant mRNA non-transcribing – RNA-less – alleles: promoter- or full-locus deletion mutants, have been suggested to serve as the current gold standard in helping detect and account for TA effects (El-Brolosy et al., 2019; Serobyan et al., 2020) in various model organisms; however, one should not disregard the potential unwanted broad genomic effects perturbations such as large deletions may have on cellular transcriptional landscape. Firstly, large deletions can accidentally disrupt the expression of nearby genes by removing not only coding sequences but also less clearly annotated regulatory elements (Pulecio, Verma, Mejia-Ramirez, Huangfu, & Raya, 2017): promoters, enhancers, silencers, or insulators. Similarly, large deletions can affect the expression of non-coding RNAs, which play critical roles in gene regulation (Statello, Guo, Chen, & Huarte, 2021). In addition, generating large deletions can cause unpredictable chromosomal rearrangements (Chen et al., 2014; Choi & Meyerson, 2014; Kosicki, Tomberg, & Bradley, 2018), such as translocations or inversions, as well as unintended epigenetic changes (Arnould et al., 2021; Zou et al., 2022); e.g., alterations in DNA methylation patterns and histone modifications in the surrounding genomic regions, potentially influencing gene expression and cellular function. One should note that such effects have been tested, but not observed in less complex, traditional, CRISPR-Cas9 mutagenesis using a single guide at on- and off-target loci in plants (J. H. Lee et al., 2019).

Although completely abolishing mRNA expression is an efficient way to avoid genetic compensation via TA, generating such large deletions is a demanding and risky task, which sometimes might not even be feasible if the locus of interest is particularly complex. Therefore, despite such alleles being a sensible way to start genetic analysis of a gene function, they should be only one of many tools that help formulate firm conclusions.

Tools and RNA-targeting systems described in this dissertation, offer an attractive complementary approach to studying the direct effects of TA. CRISPR-Cas13d targets wild-type cytoplasmic mRNAs and does not induce DNA damage, which becomes handy for a fast and relatively clean approach to test whether one's intended mutant gene is potentially subjected to TA. As mentioned previously, the major drawback of Cas13d is its reported unspecific collateral activity upon activation. Although it still remains debated, whether collateral targeting is present in mammalian systems, regardless of the answer, it should not interfere with observing TA. For example, one recent report has suggested that Cas13d can lead to a global human transcriptome's downregulation nearly by a half, when normalized to proper internal control (Shi et al., 2023); nevertheless, TA has a proportional effect, thus the upregulation (or downregulation) of TA-related genes would still be observed in the context of whatever global impact Cas13d has on the transcriptome. Furthermore, the data in this dissertation suggest that Cas13d triggers TA very rapidly, typically, within the first 22 hours of eliciting mRNA degradation. Such timing safely accounts for the majority of cellular protein half-lives (Mathieson et al., 2018), thus the effects of intended mRNA degradation can be assessed without affecting the protein loss, which is central to establishing the presence of TA.

Another approach to explore the molecular mechanisms and gene targets of TA presented in this dissertation, the use of PTC-bearing transgenes, is arguably the cleanest way of studying TA or verifying whether creating certain LOF mutants is a viable and safe strategy. Such approach does not affect the expression of the endogenous protein, thus, with appropriate controls, all the transcriptomic effects evident after the degradation of PTC-bearing transgenes,

can be safely assumed not to be influenced by the protein-loss effects. Another advantage for using PTC-bearing transgenes in TA studies is comparing matching genetic backgrounds. E.g., comparing full-locus deletion vs. nonsense alleles, now a standard practice in TA research, runs into a caveat of contrasting two different genetic conditions, where both mutations can separately influence the genomic makeover and related gene expression. Although TA-related genes are defined as those genes that become dysregulated in PTC- (or other RNA degradation-eliciting alleles), but not RNA-less alleles, one is always left with a possibility that RNA-less alleles, being large and complex gene perturbations, can have their own influence on certain gene expression and obscure some TA-related genes. For example, RNA-less alleles are not immune to protein-loss effects, and some genes can be regulated via both robustness pathways: TA and protein-loss dependent compensation. In the case of *Actg2*, an *Acgt1*-related gene, it is upregulated in both PTC and RNA-less alleles; however, to a different extent: *Actg2* is highly upregulated, typically more than 10-fold, in *Actg1* PTC alleles, and less prominently upregulated, approximately 1.5-fold, in an *Actg1* RNA-less allele. It is a lucky scenario, but one can easily imagine a case where the related gene is upregulated to a more similar extent in both mutant conditions; in such situation, the analysis of sequencing data would likely deem such related gene as not significantly differentially expressed in a PTC versus RNA-less allele.

The importance of a genetic background in TA studies has been recently demonstrated in a *C. elegans* study, where multiple nonsense alleles were shown to upregulate different *clh* family genes, depending on which exons were removed from the *clh-1* gene (Fernandez-Abascal et al., 2022). Knowing that different mutations of the same gene can lead to different TA outcomes – up- or downregulation of the related genes – proves the importance of clean and thought-through experimental design in any TA experiment. Overexpressing PTC-bearing transgenes prevents being exposed to generating different genetic backgrounds. Using vectors with PTC-bearing transgenes is always done in the wild-type background; similarly, generating a knock-in line results in having

one safe harbor locus altered rather than tinkering a coding locus with unpredictable outcomes.

In summary, TA is a phenomenon that introduces an additional layer of intricacy into the already multifaceted world of gene perturbation research. Given the complexity of cellular RNA regulation processes and gene networks, it is imperative to exercise caution while interpreting both gene perturbation- and TA studies-related results. The potential for spurious correlations and seemingly significant outcomes due to noise or convoluted genetic backgrounds underscores the need for robust experimental design, rigorous statistical analysis, and functional validation in TA research. The path to unraveling the true biological significance, evolutionary role, and the scope of TA demands a judicious balance between exploration and skepticism, ensuring that the signal amidst the noise is genuinely reflective of the underlying biological mechanisms. This cautious approach is essential for advancing our understanding of TA and its role in shaping cellular responses to gene perturbations.

6. CONCLUSION

In conclusion, I have established several new approaches to advance the studies on transcriptional adaptation and provided comprehensive evidence that the degradation of cytoplasmic mRNAs plays a central role in triggering TA. I achieved my dissertation aims as follows:

Aim1: Study various mRNA degradation and transcriptional adaptation-inducing tools.

By creating inducible PTC-bearing transgene overexpression systems and utilizing CRISPR-Cas13d effector in targeting cytoplasmic wild-type mRNAs, I introduced two new approaches to model and study TA in mammalian cell culture systems.

Aim 2: Create an inducible model of transcriptional adaptation in mouse cell lines.

I have demonstrated that TA can be triggered on demand and that such approach, in principle, can be used to study the direct and indirect TA gene targets, as well as transcriptomic responses from the earliest onset of TA until its saturation time point.

Aim 3: Reveal the temporal profile of transcriptional adaptation and identifying the genes whose expression is directly upregulated during the transcriptional adaptation response.

I have demonstrated that related genes with higher degree of sequence similarity are upregulated faster than genes with lower degree of sequence similarity. Additionally, I have revealed that TA response has distinct epigenetic properties depending on how TA is triggered, namely, Cas13d-mediated degradation of wild-type mRNAs induces immediate transcriptional augmentation that is independent of epigenetic remodeling, whereas CRISPR-Cas9 mutants develop robust and measurable chromatin accessibility changes.

7. SUMMARIES

7.1 English summary

Inducible gene expression approaches to study the mechanism and cellular impact of transcriptional adaptation

Introduction

In the field of studying gene function by introducing various genetic manipulations, the discrepancies between knockdown and knockout animal models have long stood as a perplexing phenomenon (Kok et al., 2015). While gene knockout tools such as CRISPR-Cas9 have massively expanded the genetic manipulation capabilities (Gasiunas et al., 2012; Jinek et al., 2012), it was noticed that they often yielded milder phenotypic effects compared to knockdown methods. Several mechanisms explaining such observations have been proposed, namely the off-target effects (Jiang et al., 2020) or the toxicity of knockdown reagents (Zimmer et al., 2019), as well as, in certain cases, genetic robustness, described as an organism's ability to maintain its phenotype despite genetic changes (Kitano, 2007).

Classical mechanisms of genetic robustness include dosage compensation, compensation via redundant gene paralogs, and changes in gene regulatory networks, reviewed in (Jakutis & Stainier, 2021). In addition to these mechanisms, studies of discrepant *Egfl7* knockdown and knockout zebrafish phenotypes have led to the discovery of transcriptional adaptation (TA) (Rossi et al., 2015), a phenomenon whereby a mutation in one gene leads to a transcriptional augmentation of other, so-called adapting genes. First thought to be a novel genetic compensation mode, which surprisingly does not rely on protein loss and confers robustness solely on a transcriptional level, later it was discovered that TA can result in diverse phenotypic outcomes, from beneficial effects to potential harm, depending on the specific mutation or a gene model involved (Jakutis & Stainier, 2021; Kontarakis & Stainier, 2020). Therefore, TA is now viewed as a phenomenon that lies at the intersection of two conserved

gene regulation pathways: mRNA quality surveillance and gene regulation by small RNAs. These processes contribute equally to TA by generating small RNAs from mRNA degradation fragments and modulating adapting gene expression. A possible mechanistic explanation can be drawn from RNA activation, involving 21-bp RNA duplexes that enhance transcription by modifying repressive histone methylation (L. C. Li et al., 2006).

TA's precise mechanism remains a subject of ongoing research, but evidence suggests a central role for mutant mRNA degradation (El-Brolosy et al., 2019). Epigenetic remodeling is also thought to play a role, as evidenced by an increase in active histone marks at the transcription start sites of the adapting genes (El-Brolosy et al., 2019; Ma et al., 2019). Significant knowledge gaps surround the phenomenon of TA, necessitating further research for a comprehensive understanding and implications for studies that involve mutant generation. Many questions persist regarding the evolutionary and mechanistic aspects of TA. Firstly, it remains unclear if TA is a specialized form of genetic robustness or an evolution's by-product tied to genome duplication events. Limited documented instances raise questions about its prevalence, necessitating comparative phenotype analyses and unbiased detection methods. Additionally, mechanistic aspects need exploration, including uncovering the characteristics of degradation products from mutant mRNAs and the involvement of specific RNA-binding proteins and histone-modifying proteins in enabling those degradation intermediates to trigger TA. Finally, it is important to determine the required sequence similarity between the adapting genes for TA and its impact on the mutant cell transcriptome. On top of these questions, an argument between the proposed key TA trigger is ongoing: does mRNA degradation take the central role in inducing TA (El-Brolosy et al., 2019), or rather the recruitment of Upf3a together with a histone modifier Wdr5-COMPASS complex onto the full-length PTC-bearing mRNA promotes the TA response (Ma et al., 2019). An inducible TA system where TA can be triggered on demand and its effects on the cell's transcriptome followed through time, as well as an approach to target wild-type cytoplasmic RNAs without altering the

cell's genome could help provide answers to some of the aforementioned questions and disputes. Experiments and genetic tools described in this dissertation aim to investigate how TA develops from its earliest onset, how it affects the global transcriptome of the cell, as well as provide compelling evidence for an mRNA degradation-focused TA mechanism.

Results

Inducible degradation-prone transgene overexpression system triggers TA, but is unsuitable to study the temporal aspects of this phenomenon

With the aim to explore the temporal dynamics of adapting gene upregulation during TA, I have engineered and utilized an inducible, degradation-prone transgene overexpression system in NIH3T3 cells. The experiments began by assessing whether Doxycycline had any direct impact on *Actin* gene expression in wild-type NIH3T3 cells, revealing minimal influence on *Actb* and *Actg1* expression. Subsequently, degradation-prone transgenes-carrying NIH3T3 cells were induced, and the expression of Tg-*Actb*^{WT}, Tg-*Actg1*^{WT}, Tg-*Actb*^{PTC}, and Tg-*Actg1*^{PTC} was measured. RT-qPCR analyses confirmed efficient transgene expression upon Doxycycline treatment, with no significant changes depending on the induction strength. Importantly, the results established the safety of using Doxycycline in NIH3T3 cells to monitor *Actin* gene expression. The investigation then shifted to PTC-bearing transgenes (Tg-*Actb*^{PTC} or Tg-*Actg1*^{PTC}) to ascertain whether they were targeted by the mRNA surveillance mechanisms. RT-qPCR analyses indicated efficient downregulation of the PTC-bearing transgenes, pointing towards their likely degradation through the NMD pathway. Subsequent experiments aimed to explore whether the degradation of PTC-bearing transgenes led to the upregulation of known adapting genes. RT-qPCR analyses demonstrated the upregulation of *Actg1* and *Actg2* in Tg-*Actb*^{PTC}-expressing cells and *Actg2* in Tg-*Actg1*^{PTC}-expressing cells, suggesting that the overexpression of PTC-bearing transgenes triggered a TA response independently of protein loss. Finally, the study investigated the expression of adapting genes without Doxycycline induction, evaluating whether the inducible

TA system was not leaky under normal conditions. RT-qPCR analysis revealed the upregulation of adapting genes in PTC-bearing transgene-expressing cells without Doxycycline induction compared to both WT transgene-expressing and wild-type NIH3T3 cells. This unexpected transgene activation without induction rendered the inducible system less suitable for studying the TA response's earliest onset and its temporal effects on adapting gene expression. Despite the transgene limitations, I have also discovered TA in human cells, using a stable transgenic approach. Overexpression and degradation of *ACTB* transgenes with either a UAA or UAG PTCs resulted in the upregulation of *ACTG1*, *ACTG2*, and the endogenous *ACTB*. In summary, these findings highlight the nuanced dynamics of the inducible TA system and its implications for studying temporal aspects of TA response.

<u>CRISPR-Cas13-mediated wild-type mRNA degradation triggers a TA-like response without the presence of a DNA lesion</u>

With the aim to explore various methods of triggering mRNA degradation and assess their potential to induce TA, I have engineered and utilized CRISPR-Cas13d-expressing cells. In the first line of experiments, I have transfected those cells with sgRNAs targeting *Actg1* mRNA, employing both a pool of six *Actg1*-targeting sgRNAs and a specific *Actg1* sgRNA. The findings indicated that cytoplasmic mRNA degradation, importantly in these conditions – without genomic lesions – was sufficient to induce a TA-like response, manifesting as the upregulation of *Actg2*. Notably, similar outcomes were observed when applying this mRNA degradation approach to other gene models, namely *Ctnna1* and *Nckap1*. Further insights emerged from RNA-seq experiments that compared newly obtained CRISPR-Cas13d *Actg1* KD and older CRISPR-Cas9 *Actg1* KO datasets, revealing little overlap between the dysregulated genes and suggesting that diverse mRNA degradation modes led to distinct TA responses. The second line of experiments revolved around the investigation into the persistence of the TA-like response over time. *Actg1* mRNA was continuously targeted, resulting in sustained *Actg2* upregulation even after ceasing sgRNA

transfections. This observation suggested that cytoplasmic mRNA degradation could produce intermediaries capable of persistent modulation at the adapting gene loci. Nevertheless, an ATAC-seq experiment designed to evaluate changes in chromatin state revealed that such persistent *Actg2* upregulation did not require chromatin remodeling at the *Actg2* locus during the Cas13d-mediated TA-like response, challenging the notion that Cas13d-induced TA-like response necessitates chromatin remodeling despite significant transcriptional upregulation of adapting genes. Further experiments examined the impact of different sgRNAs targeting *Ctnna1* and *Nckap1*, revealing variations in efficiency and the degree of TA-like responses. Guides positioned near exon-exon junctions exhibited higher effectiveness, prompting consideration of the location of initial mRNA cleavage as a potentially important factor in triggering the TA-like response. The last set of experiments investigated the potential role of nuclear pre-mRNA degradation in triggering TA. Using a nuclear-localized version of CRISPR-Cas13d (Cas13d-NLS), I explored whether targeting *Actg1* transcripts in the nucleus, specifically *Actg1* pre-mRNAs, could induce a TA-like response. The findings indicated that nuclear pre-mRNA degradation alone was not sufficient to trigger an upregulation of *Actg2*, emphasizing the necessity for cytoplasmic mRNA degradation. This observation raised intriguing questions about the potential involvement of cytoplasmic factors, likely proteins with primary functions in the cytoplasmic compartment, in the TA process.

Temporal dynamics reveal that TA is a rapid process, which relies, at least partially, on the degree of sequence similarity and is initiated almost immediately after the onset of mRNA degradation

In an effort to understand the temporal dynamics of the TA response, I conducted CRISPR-Cas13d-mediated knockdown of *Nckap1* and performed RNA-seq experiments at two distinct time points. The results at 12 hours post-knockdown revealed that only the closely sequence-wise related gene *Nckap5l* showed increased expression. However, at 24 hours post-knockdown, another less similar related gene, *Nckipsd*, displayed elevated expression. This suggests

that the speed of the TA response may be influenced by the degree of sequence similarity, with certain adapting genes upregulated earlier than others. Additionally, various time course experiments using different TA-induction systems indicated that the TA response is a rapid process, initiated almost immediately upon triggering mRNA degradation.

Conclusion

In summary, this work has introduced innovative approaches to advance the understanding of TA and has provided substantial evidence highlighting the central role of cytoplasmic mRNA degradation in initiating TA. Data in this dissertation describe how novel tools for studying mRNA degradation and TA were developed, including inducible systems for overexpressing transgenes with premature termination codons and the utilization of CRISPR-Cas13d to target cytoplasmic wild-type mRNAs. These approaches expanded the possibilities for modeling and investigating TA in mammalian cell cultures. Moreover, I describe the creation of an inducible system for TA in mouse cell lines. This system demonstrated the ability to trigger TA as needed, enabling the study of both direct and indirect TA gene targets and the analysis of transcriptomic responses from the initial stages of TA through to its saturation point. Finally, the study unveiled important insights into the temporal dynamics of TA. Genes with higher sequence similarity were found to be upregulated more rapidly than those with lower similarity. Furthermore, it was revealed that the epigenetic properties of TA responses vary depending on the triggering mechanism. Cas13d-mediated degradation of wild-type mRNAs led to immediate transcriptional enhancement independent of epigenetic changes, while CRISPR-Cas9 mutants induced significant and measurable alterations in chromatin accessibility. This research has thus significantly advanced our knowledge of TA and provided valuable tools and findings that contribute to the broader understanding of gene expression regulation in response to physiological and supraphysiological mRNA degradation.

Zusammenfassung (German summary)

Induzierbare Genexpression-Ansätze zur Untersuchung des Mechanismus und der zellulären Auswirkungen der transkriptionellen Anpassung

Einleitung

Im Bereich der Erforschung der Genfunktion durch verschiedene genetische Manipulationen haben die Diskrepanzen zwischen Knockdown- und Knockout-Tiermodellen lange Zeit als verwirrendes Phänomen gegolten (Kok et al., 2015). Während Gen-Knockout-Tools wie CRISPR-Cas9 die genetischen Manipulationsmöglichkeiten massiv erweitert haben (Gasiunas et al., 2012; Jinek et al., 2012), wurde festgestellt, dass sie oft mildere phänotypische Effekte im Vergleich zu Knockdown-Methoden hervorrufen. Es wurden mehrere Mechanismen vorgeschlagen, um solche Beobachtungen zu erklären, nämlich die Off-Target-Effekte (Jiang et al., 2020) oder die Toxizität von Knockdown-Reagenzien (Zimmer et al., 2019) sowie, in bestimmten Fällen, die genetische Robustheit, die als die Fähigkeit eines Organismus beschrieben wird, sein Phänotyp trotz genetischer Veränderungen aufrechtzuerhalten (Kitano, 2007). Klassische Mechanismen der genetischen Robustheit umfassen Dosiskompensation, Kompensation durch redundante Genparaloge und Veränderungen in genregulatorischen Netzwerken, rezensiert in (Jakutis & Stainier, 2021). Neben diesen Mechanismen führten Studien zu diskrepanten Phänotypen von *Egfl7*-Knockdown- und Knockout-Zebrafisch-Modellen zur Entdeckung der transkriptionellen Anpassung (TA) (Rossi et al., 2015), einem Phänomen, bei dem eine Mutation in einem Gen zu einer transkriptionellen Steigerung anderer sogenannter anpassender Gene führt. Ursprünglich als eine neuartige Form der genetischen Kompensation angesehen, die überraschenderweise nicht auf Proteinverlust beruht und ausschließlich auf transkriptioneller Ebene Robustheit verleiht, wurde später entdeckt, dass TA zu vielfältigen phänotypischen Auswirkungen führen kann, von vorteilhaften Effekten bis hin zu potenziellen Schäden, abhängig von der spezifischen

Mutation oder dem beteiligten Genmodell (Jakutis & Stainier, 2021; Kontarakis & Stainier, 2020). Daher wird TA jetzt als ein Phänomen betrachtet, das an der Schnittstelle zweier konservierter Genregulationswege liegt: der Qualitätsüberwachung von mRNA und der Genregulation durch kleine RNAs. Diese Prozesse tragen gleichermaßen zur TA bei, indem sie kleine RNAs aus Fragmente des mRNA-Abbaus erzeugen und die Expression der anpassenden Gene modulieren. Eine mögliche mechanistische Erklärung kann aus der RNA-Aktivierung abgeleitet werden, bei der 21-BP-RNA-Duplexe die Transkription durch Modifikation repressiver Histonenmethylierung verbessern (L. C. Li et al., 2006).

Der genaue Mechanismus der TA bleibt Gegenstand laufender Forschung, aber es gibt Hinweise auf eine zentrale Rolle des Abbaus mutierter mRNA (El-Brolosy et al., 2019). Auch eine Rolle der epigenetischen Umgestaltung wird vermutet, wie durch eine Zunahme aktiver Histonmarkierungen an den Transkriptionsstartstellen der anpassenden Gene belegt ist (El-Brolosy et al., 2019; Ma et al., 2019). Es gibt noch erhebliche Wissenslücken hinsichtlich des Phänomens der TA, die weitere Forschung erfordern, um ein umfassendes Verständnis und Implikationen für Studien, die die Generierung von Mutationen beinhalten, zu erlangen. Viele Fragen bestehen bezüglich der evolutionären und mechanistischen Aspekte der TA. Zunächst bleibt unklar, ob TA eine spezialisierte Form der genetischen Robustheit ist oder ein Nebenprodukt der Evolution im Zusammenhang mit Genomduplikationsereignissen. Begrenzte dokumentierte Fälle werfen Fragen nach ihrer Verbreitung auf, was vergleichende Phänotypanalysen und unvoreingenommene Nachweismethoden erfordert. Darüber hinaus müssen mechanistische Aspekte erforscht werden, einschließlich der Aufdeckung der Eigenschaften von Abbauprodukten aus mutierten mRNAs und der Beteiligung spezifischer RNA-bindender Proteine und Histon-modifizierender Proteine, um diese Abbauintermediate zur Auslösung der TA zu befähigen. Schließlich ist es wichtig, die erforderliche Sequenzähnlichkeit zwischen den anpassenden Genen für die TA und deren Auswirkungen auf das Transkriptom der mutierten Zellen zu bestimmen. Neben

diesen Fragen läuft eine Diskussion über den vorgeschlagenen Schlüsselmechanismus der TA weiter: Nimmt der mRNA-Abbau die zentrale Rolle bei der Induktion der TA ein (El-Brolosy et al., 2019) oder fördert vielmehr die Rekrutierung von Upf3a zusammen mit einem Histon-Modifikator Wdr5-COMPASS-Komplex auf die mRNA mit vorzeitigen Terminationscodons die TA-Reaktion (Ma et al., 2019). Ein induzierbares TA-System, bei dem TA auf Anfrage ausgelöst werden kann und dessen Auswirkungen auf das Transkriptom der Zelle im Laufe der Zeit verfolgt werden können, sowie ein Ansatz zur gezielten Anvisierung von Wildtyp-zytoplasmatischen RNAs ohne Veränderung des Zellgenoms könnten dazu beitragen, einige der genannten Fragen und Streitigkeiten zu klären. Die in dieser Dissertation beschriebenen Experimente und genetischen Werkzeuge zielen darauf ab, wie TA sich von ihrem frühesten Beginn an entwickelt, wie sie das globale Transkriptom der Zelle beeinflusst und überzeugende Beweise für einen auf mRNA-Abbau ausgerichteten TA-Mechanismus liefern.

Ergebnisse

Induzierbares, degradationsanfälliges Transgenüberexpressionssystem löst TA aus, ist jedoch ungeeignet, die zeitlichen Aspekte dieses Phänomens zu untersuchen

Mit dem Ziel, die zeitliche Dynamik der Hochregulierung von Anpassungsgenen während der TA zu erkunden, habe ich ein induzierbares, degradationsanfälliges Transgenüberexpressionssystem in NIH3T3-Zellen konstruiert und verwendet. Die Experimente begannen mit der Bewertung, ob Doxycyclin einen direkten Einfluss auf die Expression der *Actin*-Gene in Wildtyp- NIH3T3-Zellen hat und zeigten minimale Auswirkungen auf die Expression von *Actb* und *Actg1*. Anschließend wurden NIH3T3-Zellen, die Transgene mit Neigung zur Degradation trugen, induziert, und die Expression von Tg-*Actb*^{WT}, Tg-*Actg1*^{WT}, Tg-*Actb*^{PTC} und Tg-*Actg1*^{PTC} wurde gemessen. RT-qPCR-Analysen bestätigten eine effiziente Transgenexpression nach Doxycyclin-Behandlung, ohne signifikante Veränderungen abhängig von der

Induktionsstärke. Die Ergebnisse etablierten die sichere Verwendung von Doxycyclin in NIH3T3-Zellen zur Überwachung der Expression von *Actin*-Genen. Die Untersuchung konzentrierte sich dann auf PTC-haltige Transgene (Tg-*Actb*^{PTC} oder Tg-*Actg1*^{PTC}), um festzustellen, ob sie von mRNA-Überwachungsmechanismen erfasst wurden. RT-qPCR-Analysen deuteten auf eine effiziente Herunterregulierung von PTC-haltigen Transgenen hin, was auf ihre wahrscheinliche Degradation durch den NMD-Weg hindeutete. Nachfolgende Experimente sollten untersuchen, ob die Degradation von PTC-haltigen Transgenen zu einer Hochregulierung bekannter Anpassungsgene führt. RT-qPCR-Analysen zeigten eine Hochregulierung von *Actg1* und *Actg2* in Tg-*Actb*^{PTC}-expressing-Zellen und *Actg2* in Tg-*Actg1*^{PTC}-expressing-Zellen, was darauf hindeutet, dass die Überexpression von PTC-haltigen Transgenen eine TA-Reaktion auslöste, die unabhängig vom Proteingewinnverlust war. Schließlich wurde die Expression von Anpassungsgenen ohne Doxycyclin-Induktion getestet, um festzustellen, ob das induzierbare TA-System unter normalen Bedingungen nicht undicht ist. RT-qPCR-Analysen zeigten eine Hochregulierung von Anpassungsgenen in PTC-haltigen Transgen-expressing-Zellen ohne Doxycyclin-Induktion im Vergleich zu WT-Transgen-expressing und Wildtyp-NIH3T3-Zellen. Diese unerwartete Transgenaktivierung ohne Induktion machte das induzierbare System weniger geeignet für die Untersuchung des frühesten Auftretens der TA-Reaktion und ihrer zeitlichen Auswirkungen auf die Expression von Anpassungsgenen. Trotz der Transgen-Beschränkungen habe ich auch TA in menschlichen Zellen mittels eines stabilen transgenen Ansatzes entdeckt. Die Überexpression und Degradation von *ACTB*-Transgenen mit UAA- oder UAG-PTCs führte zur Hochregulierung von *ACTG1*, *ACTG2* und dem endogenen *ACTB*. Zusammenfassend verdeutlichen diese Ergebnisse die nuancierte Dynamik des induzierbaren TA-Systems und seine Auswirkungen auf die zeitlichen Aspekte der TA-Reaktion.

CRISPR-Cas13-vermittelte Wildtyp-mRNA-Degradation löst eine TA-ähnliche Reaktion ohne Vorhandensein einer DNA-Läsion aus

Mit dem Ziel, verschiedene Methoden zur Auslösung der mRNA-Degradation zu untersuchen und ihre potenzielle Fähigkeit zur Induktion von TA zu bewerten, habe ich CRISPR-Cas13d-expressing-Zellen konstruiert und verwendet. In der ersten Reihe von Experimenten habe ich diese Zellen mit sgRNAs transfiziert, die auf *Actg1*-mRNA abzielten, wobei sowohl ein Pool von sechs *Actg1*-zielenden sgRNAs als auch ein spezifisches *Actg1*-sgRNA verwendet wurden. Die Ergebnisse zeigten, dass die cytoplasmatische mRNA-Degradation, insbesondere unter diesen Bedingungen - ohne genomische Läsionen -, ausreichte, um eine TA-ähnliche Reaktion auszulösen, die sich als Hochregulierung von *Actg2* manifestierte. Bemerkenswerterweise wurden ähnliche Ergebnisse beobachtet, als dieser Ansatz der mRNA-Degradation auf andere Genmodelle angewendet wurde, nämlich *Ctnna1* und *Nckap1*. Weitere Einblicke ergaben sich aus RNA-seq-Experimenten, die neu gewonnene CRISPR-Cas13d *Actg1* KD- und ältere CRISPR-Cas9 *Actg1* KO-Datensätze verglichen und wenig Überschneidung zwischen den dysregulierten Genen zeigten, was darauf hindeutet, dass verschiedene Modi der mRNA-Degradation zu unterschiedlichen TA-Reaktionen führten. Die zweite Reihe von Experimenten drehte sich um die Untersuchung der Persistenz der TA-ähnlichen Reaktion im Laufe der Zeit. *Actg1*-mRNA wurde kontinuierlich anvisiert, was zu einer anhaltenden Hochregulierung von *Actg2* führte, selbst nachdem die sgRNA-Transfektionen eingestellt wurden. Diese Beobachtung legt nahe, dass die cytoplasmische mRNA-Degradation Zwischenprodukte erzeugen könnte, die eine anhaltende Modulation an den sich anpassenden Genloci bewirken können. Dennoch zeigte ein ATAC-seq-Experiment, das Veränderungen im Chromatinzustand bewerten sollte, dass eine solche anhaltende *Actg2*-Hochregulierung keine Chromatinremodellierung am *Actg2*-Locus während der Cas13d-vermittelten TA-ähnlichen Reaktion erforderte. Dies stellt die Annahme in Frage, dass die Cas13d-vermittelte TA-ähnliche Reaktion Chromatinremodellierung erfordert, obwohl es zu einer signifikanten transkriptionellen Hochregulierung von sich anpassenden Genen

kommt. Weitere Experimente untersuchten den Einfluss verschiedener sgRNAs, die auf *Ctnna1* und *Nckap1* abzielten, und zeigten Variationen in Effizienz und Grad der TA-ähnlichen Reaktionen. Führungen in der Nähe von Exon-Exon-Verbindungen zeigten eine höhere Wirksamkeit und regten dazu an, die Lage des initialen mRNA-Spalts als potenziell wichtigen Faktor bei der Auslösung der TA-ähnlichen Reaktion zu betrachten. Der letzte Satz von Experimenten untersuchte die potenzielle Rolle der Kern-mRNA-Degradation bei der Auslösung der TA. Unter Verwendung einer nuklear-lokalisierten Version von CRISPR-Cas13d (Cas13d-NLS) wurde untersucht, ob das Zielen auf Transkripte im Kern, insbesondere auf prä-mRNAs von *Actg1*, eine TA-ähnliche Reaktion auslösen könnte. Die Ergebnisse zeigten, dass die nukleare prä-mRNA-Degradation allein nicht ausreichte, um eine Hochregulierung von *Actg2* auszulösen, was die Notwendigkeit der cytoplasmatischen mRNA-Degradation betonte. Diese Beobachtung wirft interessante Fragen nach der potenziellen Beteiligung von cytoplasmatischen Faktoren auf, höchstwahrscheinlich Proteinen mit Hauptfunktionen im cytoplasmatischen Kompartiment, am TA-Prozess auf.

Zeitliche Dynamiken zeigen, dass TA ein schneller Prozess ist, der zumindest teilweise auf dem Grad der Sequenzähnlichkeit beruht und praktisch sofort nach dem Beginn der mRNA-Degradation eingeleitet wird

Um die zeitlichen Dynamiken der TA-Reaktion zu verstehen, führte ich eine CRISPR-Cas13d-vermittelte Knockdown von *Nckap1* durch und führte RNA-seq-Experimente zu zwei unterschiedlichen Zeitpunkten durch. Die Ergebnisse nach 12 Stunden zeigten, dass nur das eng sequenzverwandte Gen *Nckap5l* eine erhöhte Expression zeigte. Bei 24 Stunden nach dem Knockdown zeigte jedoch ein weniger ähnlich verwandtes Gen, *Nckipsd*, eine erhöhte Expression. Dies legt nahe, dass die Geschwindigkeit der TA-Reaktion durch den Grad der Sequenzähnlichkeit beeinflusst werden kann, wobei bestimmte sich anpassende Gene früher hochreguliert werden als andere. Verschiedene Zeitverlaufs-Experimente mit verschiedenen TA-Induktions-Systemen deuteten darauf hin,

dass die TA-Reaktion ein schneller Prozess ist, der praktisch sofort nach Auslösung der mRNA-Degradation eingeleitet wird.

Schlussfolgerung

In dieser Arbeit wurden innovative Ansätze zur Weiterentwicklung des Verständnisses der TA vorgestellt und erhebliche Beweise für die zentrale Rolle des zytoplasmatischen mRNA-Abbaus bei der Initiierung der TA geliefert. Die Daten in dieser Dissertation beschreiben, wie neue Werkzeuge zur Untersuchung des mRNA-Abbaus und der TA entwickelt wurden, einschließlich induzierbarer Systeme zur Überexpression von Transgenen mit vorzeitigen Terminationscodons und der Verwendung von CRISPR-Cas13d zur gezielten Anvisierung zytoplasmatischer Wildtyp-mRNAs. Diese Ansätze erweiterten die Möglichkeiten zur Modellierung und Untersuchung der TA in Säugetierzellkulturen. Darüber hinaus beschreibe ich die Entwicklung eines induzierbaren Systems für die TA in Mauszelllinien. Dieses System zeigte die Fähigkeit, die TA nach Bedarf auszulösen und ermöglichte die Untersuchung sowohl direkter als auch indirekter TA-Gentargets sowie die Analyse der transkriptomischen Reaktionen von den Anfangsstadien der TA bis zu ihrem Sättigungspunkt. Schließlich brachte die Studie wichtige Erkenntnisse über die räumlich-zeitliche Dynamik der TA ans Licht. Es stellte sich heraus, dass Gene mit höherer Sequenzähnlichkeit schneller hochreguliert wurden als solche mit geringerer Ähnlichkeit. Darüber hinaus wurde festgestellt, dass die epigenetischen Eigenschaften der TA-Reaktionen je nach Auslösemechanismus variieren. Der Cas13d-vermittelte Abbau von Wildtyp-mRNAs führte zu sofortiger transkriptioneller Verbesserung unabhängig von epigenetischen Veränderungen, während CRISPR-Cas9-Mutanten signifikante und messbare Veränderungen in der Chromatinzugänglichkeit induzierten. Diese Forschung hat unser Wissen über TA erheblich erweitert und wertvolle Werkzeuge und Erkenntnisse geliefert, die zum umfassenderen Verständnis der Regulation der Genexpression in Reaktion auf physiologischen und supraphysiologischen mRNA-Abbau beitragen.

8. REFERENCE LIST

Aagaard, L., & Rossi, J. J. (2007). RNAi therapeutics: principles, prospects and challenges. *Adv Drug Deliv Rev, 59*(2-3), 75-86. doi:10.1016/j.addr.2007.03.005

Abudayyeh, O. O., Gootenberg, J. S., Essletzbichler, P., Han, S., Joung, J., Belanto, J. J., . . . Zhang, F. (2017). RNA targeting with CRISPR-Cas13. *Nature, 550*(7675), 280-284. doi:10.1038/nature24049

Aguti, S., Marrosu, E., Muntoni, F., & Zhou, H. (2020). Gapmer Antisense Oligonucleotides to Selectively Suppress the Mutant Allele in COL6A Genes in Dominant Ullrich Congenital Muscular Dystrophy. *Methods Mol Biol, 2176*, 221-230. doi:10.1007/978-1-0716-0771-8_16

Akay, A., Jordan, D., Navarro, I. C., Wrzesinski, T., Ponting, C. P., Miska, E. A., & Haerty, W. (2019). Identification of functional long non-coding RNAs in C. elegans. *BMC Biol, 17*(1), 14. doi:10.1186/s12915-019-0635-7

Anders, S., & Huber, W. (2010). Differential expression analysis for sequence count data. *Genome Biol, 11*(10), R106. doi:10.1186/gb-2010-11-10-r106

Apostolopoulos, A., Tsuiji, H., Shichino, Y., & Iwasaki, S. (2023). CRISPRδ: dCas13-mediated translational repression for accurate gene silencing in mammalian cells. *bioRxiv*, 2023.2005.2014.540671. doi:10.1101/2023.05.14.540671

Arnould, C., Rocher, V., Finoux, A. L., Clouaire, T., Li, K., Zhou, F., . . . Legube, G. (2021). Loop extrusion as a mechanism for formation of DNA damage repair foci. *Nature, 590*(7847), 660-665. doi:10.1038/s41586-021-03193-z

Badano, J. L., & Katsanis, N. (2002). Beyond Mendel: an evolving view of human genetic disease transmission. *Nat Rev Genet, 3*(10), 779-789. doi:10.1038/nrg910

Bibikova, M., Golic, M., Golic, K. G., & Carroll, D. (2002). Targeted chromosomal cleavage and mutagenesis in Drosophila using zinc-finger nucleases. *Genetics, 161*(3), 1169-1175. Retrieved from https://www.ncbi.nlm.nih.gov/pubmed/12136019

Blomen, V. A., Majek, P., Jae, L. T., Bigenzahn, J. W., Nieuwenhuis, J., Staring, J., . . . Brummelkamp, T. R. (2015). Gene essentiality and synthetic lethality in haploid human cells. *Science, 350*(6264), 1092-1096. doi:10.1126/science.aac7557

Bodak, M., Yu, J., & Ciaudo, C. (2014). Regulation of LINE-1 in mammals. *Biomol Concepts, 5*(5), 409-428. doi:10.1515/bmc-2014-0018

Boehm, V., Kueckelmann, S., Gerbracht, J. V., Kallabis, S., Britto-Borges, T., Altmuller, J., . . . Gehring, N. H. (2021). SMG5-SMG7 authorize nonsense-mediated mRNA decay by enabling SMG6 endonucleolytic activity. *Nat Commun, 12*(1), 3965. doi:10.1038/s41467-021-24046-3

Boer, E. F., Jette, C. A., & Stewart, R. A. (2016). Neural Crest Migration and Survival Are Susceptible to Morpholino-Induced Artifacts. *PLoS One, 11*(12), e0167278. doi:10.1371/journal.pone.0167278

Brockdorff, N., & Turner, B. M. (2015). Dosage compensation in mammals. *Cold Spring Harb Perspect Biol, 7*(3), a019406. doi:10.1101/cshperspect.a019406

Brouns, S. J., Jore, M. M., Lundgren, M., Westra, E. R., Slijkhuis, R. J., Snijders, A. P., . . . van der Oost, J. (2008). Small CRISPR RNAs guide antiviral defense in prokaryotes. *Science, 321*(5891), 960-964. doi:10.1126/science.1159689

Buenrostro, J. D., Giresi, P. G., Zaba, L. C., Chang, H. Y., & Greenleaf, W. J. (2013). Transposition of native chromatin for fast and sensitive epigenomic profiling of open chromatin, DNA-binding proteins and nucleosome position. *Nat Methods, 10*(12), 1213-1218. doi:10.1038/nmeth.2688

Carlson, D. F., Tan, W., Lillico, S. G., Stverakova, D., Proudfoot, C., Christian, M., . . . Fahrenkrug, S. C. (2012). Efficient TALEN-mediated gene knockout in livestock. *Proc Natl Acad Sci U S A, 109*(43), 17382-17387. doi:10.1073/pnas.1211446109

Carthew, R. W., & Sontheimer, E. J. (2009). Origins and Mechanisms of miRNAs and siRNAs. *Cell, 136*(4), 642-655. doi:10.1016/j.cell.2009.01.035

Chang, H. H. Y., Pannunzio, N. R., Adachi, N., & Lieber, M. R. (2017). Non-homologous DNA end joining and alternative pathways to double-strand break repair. *Nat Rev Mol Cell Biol, 18*(8), 495-506. doi:10.1038/nrm.2017.48

Charles, E. J., Kim, S. E., Knott, G. J., Smock, D., Doudna, J., & Savage, D. F. (2021). Engineering improved Cas13 effectors for targeted post-transcriptional regulation of gene expression. *bioRxiv*, 2021.2005.2026.445687. doi:10.1101/2021.05.26.445687

Chen, X., Xu, F., Zhu, C., Ji, J., Zhou, X., Feng, X., & Guang, S. (2014). Dual sgRNA-directed gene knockout using CRISPR/Cas9 technology in Caenorhabditis elegans. *Sci Rep, 4*, 7581. doi:10.1038/srep07581

Choi, P. S., & Meyerson, M. (2014). Targeted genomic rearrangements using CRISPR/Cas technology. *Nat Commun, 5*, 3728. doi:10.1038/ncomms4728

Christian, M., Cermak, T., Doyle, E. L., Schmidt, C., Zhang, F., Hummel, A., . . . Voytas, D. F. (2010). Targeting DNA double-strand breaks with TAL effector nucleases. *Genetics, 186*(2), 757-761. doi:10.1534/genetics.110.120717

Corey, D. R., & Abrams, J. M. (2001). Morpholino antisense oligonucleotides: tools for investigating vertebrate development. *Genome Biol, 2*(5), REVIEWS1015. doi:10.1186/gb-2001-2-5-reviews1015

Costello, A., Lao, N. T., Gallagher, C., Capella Roca, B., Julius, L. A. N., Suda, S., . . . Clynes, M. (2019). Leaky Expression of the TET-On System Hinders Control of Endogenous miRNA Abundance. *Biotechnol J, 14*(3), e1800219. doi:10.1002/biot.201800219

Davis, M. P., van Dongen, S., Abreu-Goodger, C., Bartonicek, N., & Enright, A. J. (2013). Kraken: a set of tools for quality control and analysis of high-throughput sequence data. *Methods, 63*(1), 41-49. doi:10.1016/j.ymeth.2013.06.027

De Souza, A. T., Dai, X., Spencer, A. G., Reppen, T., Menzie, A., Roesch, P. L., . . . Ulrich, R. G. (2006). Transcriptional and phenotypic comparisons of

Ppara knockout and siRNA knockdown mice. *Nucleic Acids Res, 34*(16), 4486-4494. doi:10.1093/nar/gkl609

Deng, X., Berletch, J. B., Ma, W., Nguyen, D. K., Hiatt, J. B., Noble, W. S., . . . Disteche, C. M. (2013). Mammalian X upregulation is associated with enhanced transcription initiation, RNA half-life, and MOF-mediated H4K16 acetylation. *Dev Cell, 25*(1), 55-68. doi:10.1016/j.devcel.2013.01.028

Deng, X., Hiatt, J. B., Nguyen, D. K., Ercan, S., Sturgill, D., Hillier, L. W., . . . Disteche, C. M. (2011). Evidence for compensatory upregulation of expressed X-linked genes in mammals, Caenorhabditis elegans and Drosophila melanogaster. *Nat Genet, 43*(12), 1179-1185. doi:10.1038/ng.948

Dietzl, G., Chen, D., Schnorrer, F., Su, K. C., Barinova, Y., Fellner, M., . . . Dickson, B. J. (2007). A genome-wide transgenic RNAi library for conditional gene inactivation in Drosophila. *Nature, 448*(7150), 151-156. doi:10.1038/nature05954

Dobin, A., Davis, C. A., Schlesinger, F., Drenkow, J., Zaleski, C., Jha, S., . . . Gingeras, T. R. (2013). STAR: ultrafast universal RNA-seq aligner. *Bioinformatics, 29*(1), 15-21. doi:10.1093/bioinformatics/bts635

Doman, J. L., Raguram, A., Newby, G. A., & Liu, D. R. (2020). Evaluation and minimization of Cas9-independent off-target DNA editing by cytosine base editors. *Nat Biotechnol, 38*(5), 620-628. doi:10.1038/s41587-020-0414-6

Dooley, C. M., Wali, N., Sealy, I. M., White, R. J., Stemple, D. L., Collins, J. E., & Busch-Nentwich, E. M. (2019). The gene regulatory basis of genetic compensation during neural crest induction. *PLoS Genet, 15*(6), e1008213. doi:10.1371/journal.pgen.1008213

Doudna, J. A., & Charpentier, E. (2014). Genome editing. The new frontier of genome engineering with CRISPR-Cas9. *Science, 346*(6213), 1258096. doi:10.1126/science.1258096

Eberle, A. B., Lykke-Andersen, S., Muhlemann, O., & Jensen, T. H. (2009). SMG6 promotes endonucleolytic cleavage of nonsense mRNA in human cells. *Nat Struct Mol Biol, 16*(1), 49-55. doi:10.1038/nsmb.1530

Edwards, J. S., & Palsson, B. O. (1999). Systems properties of the Haemophilus influenzae Rd metabolic genotype. *J Biol Chem, 274*(25), 17410-17416. doi:10.1074/jbc.274.25.17410

Eisen, J. S., & Smith, J. C. (2008). Controlling morpholino experiments: don't stop making antisense. *Development, 135*(10), 1735-1743. doi:10.1242/dev.001115

El-Brolosy, M. A., Kontarakis, Z., Rossi, A., Kuenne, C., Gunther, S., Fukuda, N., . . . Stainier, D. Y. R. (2019). Genetic compensation triggered by mutant mRNA degradation. *Nature, 568*(7751), 193-197. doi:10.1038/s41586-019-1064-z

Elena, S. F., & Sanjuan, R. (2008). The effect of genetic robustness on evolvability in digital organisms. *BMC Evol Biol, 8*, 284. doi:10.1186/1471-2148-8-284

Evers, B., Jastrzebski, K., Heijmans, J. P., Grernrum, W., Beijersbergen, R. L., & Bernards, R. (2016). CRISPR knockout screening outperforms shRNA and CRISPRi in identifying essential genes. *Nat Biotechnol, 34*(6), 631-633. doi:10.1038/nbt.3536

Fernandez-Abascal, J., Wang, L., Graziano, B., Johnson, C. K., & Bianchi, L. (2022). Exon-dependent transcriptional adaptation by exon-junction complex proteins Y14/RNP-4 and MAGOH/MAG-1 in Caenorhabditis elegans. *PLoS Genet, 18*(10), e1010488. doi:10.1371/journal.pgen.1010488

Fire, A., Xu, S., Montgomery, M. K., Kostas, S. A., Driver, S. E., & Mello, C. C. (1998). Potent and specific genetic interference by double-stranded RNA in Caenorhabditis elegans. *Nature, 391*(6669), 806-811. doi:10.1038/35888

Firnhaber, C., & Hammarlund, M. (2013). Neuron-specific feeding RNAi in C. elegans and its use in a screen for essential genes required for GABA

neuron function. *PLoS Genet, 9*(11), e1003921. doi:10.1371/journal.pgen.1003921

Fugger, K., & West, S. C. (2016). Keeping homologous recombination in check. *Cell Res, 26*(4), 397-398. doi:10.1038/cr.2016.25

Gao, Y., Zhang, Y., Zhang, D., Dai, X., Estelle, M., & Zhao, Y. (2015). Auxin binding protein 1 (ABP1) is not required for either auxin signaling or Arabidopsis development. *Proc Natl Acad Sci U S A, 112*(7), 2275-2280. doi:10.1073/pnas.1500365112

Gasiunas, G., Barrangou, R., Horvath, P., & Siksnys, V. (2012). Cas9-crRNA ribonucleoprotein complex mediates specific DNA cleavage for adaptive immunity in bacteria. *Proc Natl Acad Sci U S A, 109*(39), E2579-2586. doi:10.1073/pnas.1208507109

Gelbart, M. E., & Kuroda, M. I. (2009). Drosophila dosage compensation: a complex voyage to the X chromosome. *Development, 136*(9), 1399-1410. doi:10.1242/dev.029645

GenomeAsia, K. C. (2019). The GenomeAsia 100K Project enables genetic discoveries across Asia. *Nature, 576*(7785), 106-111. doi:10.1038/s41586-019-1793-z

Gerety, S. S., & Wilkinson, D. G. (2011). Morpholino artifacts provide pitfalls and reveal a novel role for pro-apoptotic genes in hindbrain boundary development. *Dev Biol, 350*(2), 279-289. doi:10.1016/j.ydbio.2010.11.030

Goldstein, L., & Trescott, O. H. (1970). Characterization of RNAs that do and do not migrate between cytoplasm and nucleus. *Proc Natl Acad Sci U S A, 67*(3), 1367-1374. doi:10.1073/pnas.67.3.1367

Gossen, M., & Bujard, H. (1992). Tight control of gene expression in mammalian cells by tetracycline-responsive promoters. *Proc Natl Acad Sci U S A, 89*(12), 5547-5551. doi:10.1073/pnas.89.12.5547

Grishok, A., Tabara, H., & Mello, C. C. (2000). Genetic requirements for inheritance of RNAi in C. elegans. *Science, 287*(5462), 2494-2497. doi:10.1126/science.287.5462.2494

Gu, Z., Steinmetz, L. M., Gu, X., Scharfe, C., Davis, R. W., & Li, W. H. (2003). Role of duplicate genes in genetic robustness against null mutations. *Nature, 421*(6918), 63-66. doi:10.1038/nature01198

Gupta, R., Ghosh, A., Chakravarti, R., Singh, R., Ravichandiran, V., Swarnakar, S., & Ghosh, D. (2022). Cas13d: A New Molecular Scissor for Transcriptome Engineering. *Front Cell Dev Biol, 10*, 866800. doi:10.3389/fcell.2022.866800

Hatkevich, T., Miller, D. E., Turcotte, C. A., Miller, M. C., & Sekelsky, J. (2021). A pathway for error-free non-homologous end joining of resected meiotic double-strand breaks. *Nucleic Acids Res*. doi:10.1093/nar/gkaa1205

Hietpas, R. T., Jensen, J. D., & Bolon, D. N. (2011). Experimental illumination of a fitness landscape. *Proc Natl Acad Sci U S A, 108*(19), 7896-7901. doi:10.1073/pnas.1016024108

Hillary, V. E., & Ceasar, S. A. (2023). A Review on the Mechanism and Applications of CRISPR/Cas9/Cas12/Cas13/Cas14 Proteins Utilized for Genome Engineering. *Mol Biotechnol, 65*(3), 311-325. doi:10.1007/s12033-022-00567-0

Hippenmeyer, S., Youn, Y. H., Moon, H. M., Miyamichi, K., Zong, H., Wynshaw-Boris, A., & Luo, L. (2010). Genetic mosaic dissection of Lis1 and Ndel1 in neuronal migration. *Neuron, 68*(4), 695-709. doi:10.1016/j.neuron.2010.09.027

Hosoya, O., Chung, M., Ansai, S., Takeuchi, H., & Miyaji, M. (2021). A modified Tet-ON system minimizing leaky expression for cell-type specific gene induction in medaka fish. *Dev Growth Differ, 63*(8), 397-405. doi:10.1111/dgd.12743

Hsiao, T. L., & Vitkup, D. (2008). Role of duplicate genes in robustness against deleterious human mutations. *PLoS Genet, 4*(3), e1000014. doi:10.1371/journal.pgen.1000014

Hsu, P. D., Scott, D. A., Weinstein, J. A., Ran, F. A., Konermann, S., Agarwala, V., . . . Zhang, F. (2013). DNA targeting specificity of RNA-guided Cas9 nucleases. *Nat Biotechnol, 31*(9), 827-832. doi:10.1038/nbt.2647

Huang, P. Y., Kandyba, E., Jabouille, A., Sjolund, J., Kumar, A., Halliwill, K., . . . Balmain, A. (2017). Lgr6 is a stem cell marker in mouse skin squamous cell carcinoma. *Nat Genet, 49*(11), 1624-1632. doi:10.1038/ng.3957

Ideue, T., Hino, K., Kitao, S., Yokoi, T., & Hirose, T. (2009). Efficient oligonucleotide-mediated degradation of nuclear noncoding RNAs in mammalian cultured cells. *RNA, 15*(8), 1578-1587. doi:10.1261/rna.1657609

Ishino, Y., Shinagawa, H., Makino, K., Amemura, M., & Nakata, A. (1987). Nucleotide sequence of the iap gene, responsible for alkaline phosphatase isozyme conversion in Escherichia coli, and identification of the gene product. *J Bacteriol, 169*(12), 5429-5433. doi:10.1128/jb.169.12.5429-5433.1987

Jackson, A. L., & Linsley, P. S. (2010). Recognizing and avoiding siRNA off-target effects for target identification and therapeutic application. *Nat Rev Drug Discov, 9*(1), 57-67. doi:10.1038/nrd3010

Jakutis, G., & Stainier, D. Y. R. (2021). Genotype-Phenotype Relationships in the Context of Transcriptional Adaptation and Genetic Robustness. *Annu Rev Genet, 55*, 71-91. doi:10.1146/annurev-genet-071719-020342

Jiang, Z., Carlantoni, C., Allanki, S., Ebersberger, I., & Stainier, D. Y. R. (2020). Tek (Tie2) is not required for cardiovascular development in zebrafish. *Development, 147*(19). doi:10.1242/dev.193029

Jiang, Z., El-Brolosy, M. A., Serobyan, V., Welker, J. M., Retzer, N., Dooley, C. M., . . . Stainier, D. Y. R. (2022). Parental mutations influence wild-type offspring via transcriptional adaptation. *Sci Adv, 8*(47), eabj2029. doi:10.1126/sciadv.abj2029

Jinek, M., Chylinski, K., Fonfara, I., Hauer, M., Doudna, J. A., & Charpentier, E. (2012). A programmable dual-RNA-guided DNA endonuclease in adaptive bacterial immunity. *Science, 337*(6096), 816-821. doi:10.1126/science.1225829

Johnson, R. D., & Jasin, M. (2000). Sister chromatid gene conversion is a prominent double-strand break repair pathway in mammalian cells. *EMBO J, 19*(13), 3398-3407. doi:10.1093/emboj/19.13.3398

Kallunki, T., Barisic, M., Jaattela, M., & Liu, B. (2019). How to Choose the Right Inducible Gene Expression System for Mammalian Studies? *Cells, 8*(8). doi:10.3390/cells8080796

Kamath, R. S., Fraser, A. G., Dong, Y., Poulin, G., Durbin, R., Gotta, M., . . . Ahringer, J. (2003). Systematic functional analysis of the Caenorhabditis elegans genome using RNAi. *Nature, 421*(6920), 231-237. doi:10.1038/nature01278

Karczewski, K. J., Francioli, L. C., Tiao, G., Cummings, B. B., Alfoldi, J., Wang, Q., . . . MacArthur, D. G. (2020). The mutational constraint spectrum quantified from variation in 141,456 humans. *Nature, 581*(7809), 434-443. doi:10.1038/s41586-020-2308-7

Kemble, H., Nghe, P., & Tenaillon, O. (2019). Recent insights into the genotype-phenotype relationship from massively parallel genetic assays. *Evol Appl, 12*(9), 1721-1742. doi:10.1111/eva.12846

Khan, A. A., Betel, D., Miller, M. L., Sander, C., Leslie, C. S., & Marks, D. S. (2009). Transfection of small RNAs globally perturbs gene regulation by endogenous microRNAs. *Nat Biotechnol, 27*(6), 549-555. doi:10.1038/nbt.1543

Kitano, H. (2007). Towards a theory of biological robustness. *Mol Syst Biol, 3*, 137. doi:10.1038/msb4100179

Klattenhoff, C., & Theurkauf, W. (2008). Biogenesis and germline functions of piRNAs. *Development, 135*(1), 3-9. doi:10.1242/dev.006486

Kok, F. O., Shin, M., Ni, C. W., Gupta, A., Grosse, A. S., van Impel, A., . . . Lawson, N. D. (2015). Reverse genetic screening reveals poor correlation between morpholino-induced and mutant phenotypes in zebrafish. *Dev Cell, 32*(1), 97-108. doi:10.1016/j.devcel.2014.11.018

Kontarakis, Z., & Stainier, D. Y. R. (2020). Genetics in Light of Transcriptional Adaptation. *Trends Genet, 36*(12), 926-935. doi:10.1016/j.tig.2020.08.008

Kosicki, M., Tomberg, K., & Bradley, A. (2018). Repair of double-strand breaks induced by CRISPR-Cas9 leads to large deletions and complex rearrangements. *Nat Biotechnol, 36*(8), 765-771. doi:10.1038/nbt.4192

Kurosaki, T., & Maquat, L. E. (2016). Nonsense-mediated mRNA decay in humans at a glance. *J Cell Sci, 129*(3), 461-467. doi:10.1242/jcs.181008

Kurosaki, T., Popp, M. W., & Maquat, L. E. (2019). Quality and quantity control of gene expression by nonsense-mediated mRNA decay. *Nat Rev Mol Cell Biol, 20*(7), 406-420. doi:10.1038/s41580-019-0126-2

Kushawah, G., Hernandez-Huertas, L., Abugattas-Nunez Del Prado, J., Martinez-Morales, J. R., DeVore, M. L., Hassan, H., . . . Moreno-Mateos, M. A. (2020). CRISPR-Cas13d Induces Efficient mRNA Knockdown in Animal Embryos. *Dev Cell, 54*(6), 805-817 e807. doi:10.1016/j.devcel.2020.07.013

Lai, J. K. H., Gagalova, K. K., Kuenne, C., El-Brolosy, M. A., & Stainier, D. Y. R. (2019). Induction of interferon-stimulated genes and cellular stress pathways by morpholinos in zebrafish. *Dev Biol, 454*(1), 21-28. doi:10.1016/j.ydbio.2019.06.008

Lander, E. S., Linton, L. M., Birren, B., Nusbaum, C., Zody, M. C., Baldwin, J., . . . International Human Genome Sequencing, C. (2001). Initial sequencing and analysis of the human genome. *Nature, 409*(6822), 860-921. doi:10.1038/35057062

Lee, J. H., Mazarei, M., Pfotenhauer, A. C., Dorrough, A. B., Poindexter, M. R., Hewezi, T., . . . Stewart, C. N., Jr. (2019). Epigenetic Footprints of CRISPR/Cas9-Mediated Genome Editing in Plants. *Front Plant Sci, 10*, 1720. doi:10.3389/fpls.2019.01720

Lee, J. S., Yu, Q., Shin, J. T., Sebzda, E., Bertozzi, C., Chen, M., . . . Kahn, M. L. (2006). Klf2 is an essential regulator of vascular hemodynamic forces in vivo. *Dev Cell, 11*(6), 845-857. doi:10.1016/j.devcel.2006.09.006

Lee, R. C., Feinbaum, R. L., & Ambros, V. (1993). The C. elegans heterochronic gene lin-4 encodes small RNAs with antisense complementarity to lin-14. *Cell, 75*(5), 843-854. doi:10.1016/0092-8674(93)90529-y

Lehner, B. (2011). Molecular mechanisms of epistasis within and between genes. *Trends Genet, 27*(8), 323-331. doi:10.1016/j.tig.2011.05.007

Li, F. J., Xu, Z. S., Aye, H. M., Brasseur, A., Lun, Z. R., Tan, K. S. W., & He, C. Y. (2017). An efficient cumate-inducible system for procyclic and bloodstream form Trypanosoma brucei. *Mol Biochem Parasitol, 214*, 101-104. doi:10.1016/j.molbiopara.2017.04.007

Li, L. C. (2014). Chromatin remodeling by the small RNA machinery in mammalian cells. *Epigenetics, 9*(1), 45-52. doi:10.4161/epi.26830

Li, L. C., Okino, S. T., Zhao, H., Pookot, D., Place, R. F., Urakami, S., . . . Dahiya, R. (2006). Small dsRNAs induce transcriptional activation in human cells. *Proc Natl Acad Sci U S A, 103*(46), 17337-17342. doi:10.1073/pnas.0607015103

Li, Y., Xu, J., Guo, X., Li, Z., Cao, L., Liu, S., . . . You, F. (2023). The collateral activity of RfxCas13d can induce lethality in a RfxCas13d knock-in mouse model. *Genome Biol, 24*(1), 20. doi:10.1186/s13059-023-02860-w

Li, Y. S., Meng, R. R., Chen, X., Shang, C. L., Li, H. B., Zhang, T. J., . . . Wang, F. C. (2019). Generation of H11-albumin-rtTA Transgenic Mice: A Tool for Inducible Gene Expression in the Liver. *G3 (Bethesda), 9*(2), 591-599. doi:10.1534/g3.118.200963

Lindahl, T. (1974). An N-glycosidase from Escherichia coli that releases free uracil from DNA containing deaminated cytosine residues. *Proc Natl Acad Sci U S A, 71*(9), 3649-3653. doi:10.1073/pnas.71.9.3649

Livesey, B. J., & Marsh, J. A. (2020). Using deep mutational scanning to benchmark variant effect predictors and identify disease mutations. *Mol Syst Biol, 16*(7), e9380. doi:10.15252/msb.20199380

Loew, R., Heinz, N., Hampf, M., Bujard, H., & Gossen, M. (2010). Improved Tet-responsive promoters with minimized background expression. *BMC Biotechnol, 10*, 81. doi:10.1186/1472-6750-10-81

Longman, D., Johnstone, I. L., & Caceres, J. F. (2000). Functional characterization of SR and SR-related genes in Caenorhabditis elegans. *EMBO J, 19*(7), 1625-1637. doi:10.1093/emboj/19.7.1625

Lopez-Perrote, A., Castano, R., Melero, R., Zamarro, T., Kurosawa, H., Ohnishi, T., . . . Llorca, O. (2016). Human nonsense-mediated mRNA decay factor UPF2 interacts directly with eRF3 and the SURF complex. *Nucleic Acids Res, 44*(4), 1909-1923. doi:10.1093/nar/gkv1527

Love, M. I., Huber, W., & Anders, S. (2014). Moderated estimation of fold change and dispersion for RNA-seq data with DESeq2. *Genome Biol, 15*(12), 550. doi:10.1186/s13059-014-0550-8

Lu, A. L., Clark, S., & Modrich, P. (1983). Methyl-directed repair of DNA base-pair mismatches in vitro. *Proc Natl Acad Sci U S A, 80*(15), 4639-4643. doi:10.1073/pnas.80.15.4639

Lu, J., & Deutsch, C. (2008). Electrostatics in the ribosomal tunnel modulate chain elongation rates. *J Mol Biol, 384*(1), 73-86. doi:10.1016/j.jmb.2008.08.089

Lykke-Andersen, S., & Jensen, T. H. (2015). Nonsense-mediated mRNA decay: an intricate machinery that shapes transcriptomes. *Nat Rev Mol Cell Biol, 16*(11), 665-677. doi:10.1038/nrm4063

Ma, Z., Zhu, P., Shi, H., Guo, L., Zhang, Q., Chen, Y., . . . Chen, J. (2019). PTC-bearing mRNA elicits a genetic compensation response via Upf3a and COMPASS components. *Nature, 568*(7751), 259-263. doi:10.1038/s41586-019-1057-y

MacArthur, D. G., Balasubramanian, S., Frankish, A., Huang, N., Morris, J., Walter, K., . . . Tyler-Smith, C. (2012). A systematic survey of loss-of-function variants in human protein-coding genes. *Science, 335*(6070), 823-828. doi:10.1126/science.1215040

Macneil, L. T., & Walhout, A. J. (2011). Gene regulatory networks and the role of robustness and stochasticity in the control of gene expression. *Genome Res, 21*(5), 645-657. doi:10.1101/gr.097378.109

Majithia, A. R., Tsuda, B., Agostini, M., Gnanapradeepan, K., Rice, R., Peloso, G., . . . Altshuler, D. (2016). Prospective functional classification of all possible missense variants in PPARG. *Nat Genet, 48*(12), 1570-1575. doi:10.1038/ng.3700

Makarova, K. S., Aravind, L., Wolf, Y. I., & Koonin, E. V. (2011). Unification of Cas protein families and a simple scenario for the origin and evolution of CRISPR-Cas systems. *Biol Direct, 6*, 38. doi:10.1186/1745-6150-6-38

Makarova, K. S., Grishin, N. V., Shabalina, S. A., Wolf, Y. I., & Koonin, E. V. (2006). A putative RNA-interference-based immune system in prokaryotes: computational analysis of the predicted enzymatic machinery, functional analogies with eukaryotic RNAi, and hypothetical mechanisms of action. *Biol Direct, 1*, 7. doi:10.1186/1745-6150-1-7

Makarova, K. S., Wolf, Y. I., Iranzo, J., Shmakov, S. A., Alkhnbashi, O. S., Brouns, S. J. J., . . . Koonin, E. V. (2020). Evolutionary classification of CRISPR-Cas systems: a burst of class 2 and derived variants. *Nat Rev Microbiol, 18*(2), 67-83. doi:10.1038/s41579-019-0299-x

Maquat, L. E., Tarn, W. Y., & Isken, O. (2010). The pioneer round of translation: features and functions. *Cell, 142*(3), 368-374. doi:10.1016/j.cell.2010.07.022

Masel, J., & Siegal, M. L. (2009). Robustness: mechanisms and consequences. *Trends Genet, 25*(9), 395-403. doi:10.1016/j.tig.2009.07.005

Masel, J., & Trotter, M. V. (2010). Robustness and evolvability. *Trends Genet, 26*(9), 406-414. doi:10.1016/j.tig.2010.06.002

Mathieson, T., Franken, H., Kosinski, J., Kurzawa, N., Zinn, N., Sweetman, G., . . . Savitski, M. M. (2018). Systematic analysis of protein turnover in primary cells. *Nat Commun, 9*(1), 689. doi:10.1038/s41467-018-03106-1

Meyer, B. J. (2005). X-Chromosome dosage compensation. *WormBook*, 1-14. doi:10.1895/wormbook.1.8.1

Miller, S. M., Wang, T., Randolph, P. B., Arbab, M., Shen, M. W., Huang, T. P., . . . Liu, D. R. (2020). Continuous evolution of SpCas9 variants compatible with non-G PAMs. *Nat Biotechnol, 38*(4), 471-481. doi:10.1038/s41587-020-0412-8

Moraes, F., & Goes, A. (2016). A decade of human genome project conclusion: Scientific diffusion about our genome knowledge. *Biochem Mol Biol Educ, 44*(3), 215-223. doi:10.1002/bmb.20952

Moresco, E. M., Li, X., & Beutler, B. (2013). Going forward with genetics: recent technological advances and forward genetics in mice. *Am J Pathol, 182*(5), 1462-1473. doi:10.1016/j.ajpath.2013.02.002

Morgens, D. W., Deans, R. M., Li, A., & Bassik, M. C. (2016). Systematic comparison of CRISPR/Cas9 and RNAi screens for essential genes. *Nat Biotechnol, 34*(6), 634-636. doi:10.1038/nbt.3567

Morris, J. A. (2015). The genomic load of deleterious mutations: relevance to death in infancy and childhood. *Front Immunol, 6*, 105. doi:10.3389/fimmu.2015.00105

Navickas, A., Chamois, S., Saint-Fort, R., Henri, J., Torchet, C., & Benard, L. (2020). No-Go Decay mRNA cleavage in the ribosome exit tunnel produces 5'-OH ends phosphorylated by Trl1. *Nat Commun, 11*(1), 122. doi:10.1038/s41467-019-13991-9

Nicoli, S., Standley, C., Walker, P., Hurlstone, A., Fogarty, K. E., & Lawson, N. D. (2010). MicroRNA-mediated integration of haemodynamics and Vegf signalling during angiogenesis. *Nature, 464*(7292), 1196-1200. doi:10.1038/nature08889

Novodvorsky, P., Watson, O., Gray, C., Wilkinson, R. N., Reeve, S., Smythe, C., . . . Chico, T. J. (2015). klf2ash317 Mutant Zebrafish Do Not Recapitulate Morpholino-Induced Vascular and Haematopoietic Phenotypes. *PLoS One, 10*(10), e0141611. doi:10.1371/journal.pone.0141611

O'Leary, M. N., Schreiber, K. H., Zhang, Y., Duc, A. C., Rao, S., Hale, J. S., . . . Kennedy, B. K. (2013). The ribosomal protein Rpl22 controls ribosome composition by directly repressing expression of its own paralog, Rpl22l1. *PLoS Genet, 9*(8), e1003708. doi:10.1371/journal.pgen.1003708

Oehme, I., Bosser, S., & Zornig, M. (2006). Agonists of an ecdysone-inducible mammalian expression system inhibit Fas Ligand- and TRAIL-induced apoptosis in the human colon carcinoma cell line RKO. *Cell Death Differ, 13*(2), 189-201. doi:10.1038/sj.cdd.4401730

Ozata, D. M., Gainetdinov, I., Zoch, A., O'Carroll, D., & Zamore, P. D. (2019). PIWI-interacting RNAs: small RNAs with big functions. *Nat Rev Genet, 20*(2), 89-108. doi:10.1038/s41576-018-0073-3

Pauli, A., Montague, T. G., Lennox, K. A., Behlke, M. A., & Schier, A. F. (2015). Antisense Oligonucleotide-Mediated Transcript Knockdown in Zebrafish. *PLoS One, 10*(10), e0139504. doi:10.1371/journal.pone.0139504

Payne, J. L., & Wagner, A. (2019). The causes of evolvability and their evolution. *Nat Rev Genet, 20*(1), 24-38. doi:10.1038/s41576-018-0069-z

Peng, W., Song, R., & Acar, M. (2016). Noise reduction facilitated by dosage compensation in gene networks. *Nat Commun, 7*, 12959. doi:10.1038/ncomms12959

Perez-Lluch, S., Blanco, E., Tilgner, H., Curado, J., Ruiz-Romero, M., Corominas, M., & Guigo, R. (2015). Absence of canonical marks of active chromatin in developmentally regulated genes. *Nat Genet, 47*(10), 1158-1167. doi:10.1038/ng.3381

Portnoy, V., Lin, S. H., Li, K. H., Burlingame, A., Hu, Z. H., Li, H., & Li, L. C. (2016). saRNA-guided Ago2 targets the RITA complex to promoters to stimulate transcription. *Cell Res, 26*(3), 320-335. doi:10.1038/cr.2016.22

Pulecio, J., Verma, N., Mejia-Ramirez, E., Huangfu, D., & Raya, A. (2017). CRISPR/Cas9-Based Engineering of the Epigenome. *Cell Stem Cell, 21*(4), 431-447. doi:10.1016/j.stem.2017.09.006

Qiu, S., Adema, C. M., & Lane, T. (2005). A computational study of off-target effects of RNA interference. *Nucleic Acids Res, 33*(6), 1834-1847. doi:10.1093/nar/gki324

Quinlan, A. R., & Hall, I. M. (2010). BEDTools: a flexible suite of utilities for comparing genomic features. *Bioinformatics, 26*(6), 841-842. doi:10.1093/bioinformatics/btq033

Ramirez, F., Dundar, F., Diehl, S., Gruning, B. A., & Manke, T. (2014). deepTools: a flexible platform for exploring deep-sequencing data. *Nucleic Acids Res, 42*(Web Server issue), W187-191. doi:10.1093/nar/gku365

Robinson, J. T., Thorvaldsdottir, H., Winckler, W., Guttman, M., Lander, E. S., Getz, G., & Mesirov, J. P. (2011). Integrative genomics viewer. *Nat Biotechnol, 29*(1), 24-26. doi:10.1038/nbt.1754

Robu, M. E., Larson, J. D., Nasevicius, A., Beiraghi, S., Brenner, C., Farber, S. A., & Ekker, S. C. (2007). p53 activation by knockdown technologies. *PLoS Genet, 3*(5), e78. doi:10.1371/journal.pgen.0030078

Rossi, A., Kontarakis, Z., Gerri, C., Nolte, H., Holper, S., Kruger, M., & Stainier, D. Y. (2015). Genetic compensation induced by deleterious mutations but not gene knockdowns. *Nature, 524*(7564), 230-233. doi:10.1038/nature14580

Sancar, A., & Rupp, W. D. (1983). A novel repair enzyme: UVRABC excision nuclease of Escherichia coli cuts a DNA strand on both sides of the damaged region. *Cell, 33*(1), 249-260. doi:10.1016/0092-8674(83)90354-9

Saredi, G., Huang, H., Hammond, C. M., Alabert, C., Bekker-Jensen, S., Forne, I., . . . Groth, A. (2016). H4K20me0 marks post-replicative chromatin and recruits the TONSL-MMS22L DNA repair complex. *Nature, 534*(7609), 714-718. doi:10.1038/nature18312

Schneeberger, K. (2014). Using next-generation sequencing to isolate mutant genes from forward genetic screens. *Nat Rev Genet, 15*(10), 662-676. doi:10.1038/nrg3745

Schulte-Merker, S., & Stainier, D. Y. (2014). Out with the old, in with the new: reassessing morpholino knockdowns in light of genome editing technology. *Development, 141*(16), 3103-3104. doi:10.1242/dev.112003

Segala, G., Bennesch, M. A., Pandey, D. P., Hulo, N., & Picard, D. (2016). Monoubiquitination of Histone H2B Blocks Eviction of Histone Variant H2A.Z from Inducible Enhancers. *Mol Cell, 64*(2), 334-346. doi:10.1016/j.molcel.2016.08.034

Seok, H., Lee, H., Jang, E. S., & Chi, S. W. (2018). Evaluation and control of miRNA-like off-target repression for RNA interference. *Cell Mol Life Sci, 75*(5), 797-814. doi:10.1007/s00018-017-2656-0

Serobyan, V., Kontarakis, Z., El-Brolosy, M. A., Welker, J. M., Tolstenkov, O., Saadeldein, A. M., . . . Stainier, D. Y. (2020). Transcriptional adaptation in Caenorhabditis elegans. *Elife, 9*. doi:10.7554/eLife.50014

Shabalina, S. A., & Koonin, E. V. (2008). Origins and evolution of eukaryotic RNA interference. *Trends Ecol Evol, 23*(10), 578-587. doi:10.1016/j.tree.2008.06.005

Shi, P., Murphy, M. R., Aparicio, A. O., Kesner, J. S., Fang, Z., Chen, Z., . . . Wu, X. (2023). Collateral activity of the CRISPR/RfxCas13d system in human cells. *Commun Biol, 6*(1), 334. doi:10.1038/s42003-023-04708-2

Shoemaker, C. J., & Green, R. (2012). Translation drives mRNA quality control. *Nat Struct Mol Biol, 19*(6), 594-601. doi:10.1038/nsmb.2301

Shum, E. Y., Jones, S. H., Shao, A., Chousal, J. N., Krause, M. D., Chan, W. K., . . . Wilkinson, M. F. (2016). The Antagonistic Gene Paralogs Upf3a and Upf3b Govern Nonsense-Mediated RNA Decay. *Cell, 165*(2), 382-395. doi:10.1016/j.cell.2016.02.046

Snead, N. M., & Rossi, J. J. (2010). Biogenesis and function of endogenous and exogenous siRNAs. *Wiley Interdiscip Rev RNA, 1*(1), 117-131. doi:10.1002/wrna.14

Statello, L., Guo, C. J., Chen, L. L., & Huarte, M. (2021). Gene regulation by long non-coding RNAs and its biological functions. *Nat Rev Mol Cell Biol, 22*(2), 96-118. doi:10.1038/s41580-020-00315-9

Stoeger, T., Gerlach, M., Morimoto, R. I., & Nunes Amaral, L. A. (2018). Large-scale investigation of the reasons why potentially important genes are ignored. *PLoS Biol, 16*(9), e2006643. doi:10.1371/journal.pbio.2006643

Sulem, P., Helgason, H., Oddson, A., Stefansson, H., Gudjonsson, S. A., Zink, F., . . . Stefansson, K. (2015). Identification of a large set of rare complete human knockouts. *Nat Genet, 47*(5), 448-452. doi:10.1038/ng.3243

Sunter, J. D. (2016). A vanillic acid inducible expression system for Trypanosoma brucei. *Mol Biochem Parasitol, 207*(1), 45-48. doi:10.1016/j.molbiopara.2016.04.001

Sztal, T. E., McKaige, E. A., Williams, C., Ruparelia, A. A., & Bryson-Richardson, R. J. (2018). Genetic compensation triggered by actin mutation prevents the muscle damage caused by loss of actin protein. *PLoS Genet, 14*(2), e1007212. doi:10.1371/journal.pgen.1007212

Theodosiou, M., Widmaier, M., Bottcher, R. T., Rognoni, E., Veelders, M., Bharadwaj, M., . . . Fassler, R. (2016). Kindlin-2 cooperates with talin to activate integrins and induces cell spreading by directly binding paxillin. *Elife, 5*, e10130. doi:10.7554/eLife.10130

Topczewska, J. M., Topczewski, J., Shostak, A., Kume, T., Solnica-Krezel, L., & Hogan, B. L. (2001). The winged helix transcription factor Foxc1a is essential for somitogenesis in zebrafish. *Genes Dev, 15*(18), 2483-2493. doi:10.1101/gad.907401

Vitor, A. C., Huertas, P., Legube, G., & de Almeida, S. F. (2020). Studying DNA Double-Strand Break Repair: An Ever-Growing Toolbox. *Front Mol Biosci, 7*, 24. doi:10.3389/fmolb.2020.00024

Wagner, A. (2000). Robustness against mutations in genetic networks of yeast. *Nat Genet, 24*(4), 355-361. doi:10.1038/74174

Wang, T., Birsoy, K., Hughes, N. W., Krupczak, K. M., Post, Y., Wei, J. J., . . . Sabatini, D. M. (2015). Identification and characterization of essential genes in the human genome. *Science, 350*(6264), 1096-1101. doi:10.1126/science.aac7041

Welker, J. M., Serobyan, V., Zaker Esfahani, E., & Stainier, D. Y. R. (2023). Partial sequence identity in a 25-nucleotide long element is sufficient for transcriptional adaptation in the Caenorhabditis elegans act-5/act-3 model. *PLoS Genet, 19*(6), e1010806. doi:10.1371/journal.pgen.1010806

White, J. K., Gerdin, A. K., Karp, N. A., Ryder, E., Buljan, M., Bussell, J. N., . . . Steel, K. P. (2013). Genome-wide generation and systematic phenotyping of knockout mice reveals new roles for many genes. *Cell, 154*(2), 452-464. doi:10.1016/j.cell.2013.06.022

Wienholds, E., Koudijs, M. J., van Eeden, F. J., Cuppen, E., & Plasterk, R. H. (2003). The microRNA-producing enzyme Dicer1 is essential for zebrafish development. *Nat Genet, 35*(3), 217-218. doi:10.1038/ng1251

Wilson, R. C., & Doudna, J. A. (2013). Molecular mechanisms of RNA interference. *Annu Rev Biophys, 42*, 217-239. doi:10.1146/annurev-biophys-083012-130404

Wolter, F., & Puchta, H. (2018). The CRISPR/Cas revolution reaches the RNA world: Cas13, a new Swiss Army knife for plant biologists. *Plant J, 94*(5), 767-775. doi:10.1111/tpj.13899

Wood, V., Lock, A., Harris, M. A., Rutherford, K., Bahler, J., & Oliver, S. G. (2019). Hidden in plain sight: what remains to be discovered in the eukaryotic proteome? *Open Biol, 9*(2), 180241. doi:10.1098/rsob.180241

Xie, A., Ma, Z., Wang, J., Zhang, Y., Chen, Y., Yang, C., . . . Peng, J. (2023). Upf3a but not Upf1 mediates the genetic compensation response induced by leg1 deleterious mutations in an H3K4me3-independent manner. *Cell Discov, 9*(1), 63. doi:10.1038/s41421-023-00550-2

Xu, C., Zhou, Y., Xiao, Q., He, B., Geng, G., Wang, Z., . . . Yang, H. (2021). Programmable RNA editing with compact CRISPR-Cas13 systems from uncultivated microbes. *Nat Methods, 18*(5), 499-506. doi:10.1038/s41592-021-01124-4

Yamamoto, S., Jaiswal, M., Charng, W. L., Gambin, T., Karaca, E., Mirzaa, G., . . . Bellen, H. J. (2014). A drosophila genetic resource of mutants to study mechanisms underlying human genetic diseases. *Cell, 159*(1), 200-214. doi:10.1016/j.cell.2014.09.002

Yang, N., MacArthur, D. G., Gulbin, J. P., Hahn, A. G., Beggs, A. H., Easteal, S., & North, K. (2003). ACTN3 genotype is associated with human elite athletic performance. *Am J Hum Genet, 73*(3), 627-631. doi:10.1086/377590

Ye, D., Wang, X., Wei, C., He, M., Wang, H., Wang, Y., . . . Sun, Y. (2019). Marcksb plays a key role in the secretory pathway of zebrafish Bmp2b. *PLoS Genet, 15*(9), e1008306. doi:10.1371/journal.pgen.1008306

Zabinsky, R. A., Mason, G. A., Queitsch, C., & Jarosz, D. F. (2019). It's not magic - Hsp90 and its effects on genetic and epigenetic variation. *Semin Cell Dev Biol, 88*, 21-35. doi:10.1016/j.semcdb.2018.05.015

Zhang, B., Ye, Y., Ye, W., Perculija, V., Jiang, H., Chen, Y., . . . Ouyang, S. (2019). Two HEPN domains dictate CRISPR RNA maturation and target cleavage in Cas13d. *Nat Commun, 10*(1), 2544. doi:10.1038/s41467-019-10507-3

Zhang, C., Konermann, S., Brideau, N. J., Lotfy, P., Wu, X., Novick, S. J., . . . Lyumkis, D. (2018). Structural Basis for the RNA-Guided Ribonuclease Activity of CRISPR-Cas13d. *Cell, 175*(1), 212-223 e217. doi:10.1016/j.cell.2018.09.001

Zhao, X. F., Fjose, A., Larsen, N., Helvik, J. V., & Drivenes, O. (2008). Treatment with small interfering RNA affects the microRNA pathway and causes unspecific defects in zebrafish embryos. *FEBS J, 275*(9), 2177-2184. doi:10.1111/j.1742-4658.2008.06371.x

Zhou, X., Vink, M., Klaver, B., Berkhout, B., & Das, A. T. (2006). Optimization of the Tet-On system for regulated gene expression through viral evolution. *Gene Ther, 13*(19), 1382-1390. doi:10.1038/sj.gt.3302780

Zhou, Y., Lei, C., & Zhu, Z. (2020). A low-background Tet-On system based on post-transcriptional regulation using Csy4. *PLoS One, 15*(12), e0244732. doi:10.1371/journal.pone.0244732

Zimmer, A. M., Pan, Y. K., Chandrapalan, T., Kwong, R. W. M., & Perry, S. F. (2019). Loss-of-function approaches in comparative physiology: is there a future for knockdown experiments in the era of genome editing? *J Exp Biol, 222*(Pt 7). doi:10.1242/jeb.175737

Zou, R. S., Marin-Gonzalez, A., Liu, Y., Liu, H. B., Shen, L., Dveirin, R. K., . . . Ha, T. (2022). Massively parallel genomic perturbations with multi-target CRISPR interrogates Cas9 activity and DNA repair at endogenous sites. *Nat Cell Biol, 24*(9), 1433-1444. doi:10.1038/s41556-022-00975-z

9. ACKNOWLEDGEMENT

Throughout the 5-year PhD journey, I have met and subsequently was taught, supervised, mentored, lectured, encouraged, and sometimes tortured by many people who deserve to be mentioned in gratitude and honor, and in exceptional cases – longing.

First, I would like to express my deepest gratitude to my supervisor, Prof. Dr. Didier Stainier, for his unwavering guidance, support, and mentorship throughout the course of my research. Didier's insightful feedback and encouragement have been invaluable in shaping the direction of this work. I believe Didier took a big risk accepting me, a fresh medical student without much real fundamental research experience, into his lab, whereas I, personally, would not have been so valorous in his shoes. Nevertheless, looking back, it seems to have been a solid decision, and I thank Didier for being able to spot something auspicious in me those 5 years ago.

I am also immensely grateful to my PostDoc mentor Dr. Zacharias Kontarakis, Zach, especially for the first year and a half of the PhD, during which he taught me all the techniques and skills I was lacking, but needed for a successful completion of my project. The personal meetings with him, initially, gave me nothing but headache; however, overtime they proved to be the best testing ground for a young and inexperienced me. Finally, shooting hoops on Saturday evenings or grilling in his balcony remain some of the best memories of the PhD time.

Although I had stopped working with zebrafish faster that any German gets a sunburn on the first day of summer (that is usually early August in Germany), I thank my zebrafish PhD mentor Sri Teja Mullapudi for explaining and demonstrating, both in theory and practice, how smart shortcuts in lab, and in life, work.

Before starting a PhD, one thing I did not expect to happen, was finding some true and lasting friendships. A very exceptional thank-you goes to Alessandra Gentile, Giulia Boezio, and Srinivas Allanki, with who my PhD

started and with the departure of whom – ended. The remaining 20 months revolved about filling several voids, mostly being listened to ranting about aliens, conspiracy theories, geopolitics, and experiencing a sincere laugh or common source of annoyance; however, sharing dark Instagram reels and occasional travels to London helped like good medicine.

My heartfelt appreciation extends to the closest replacements of the aforementioned trio: Savita Gupta, Agatha Ribeiro da Silva, Pinelopi Goumenaki, Christopher 'Chris' Dooley, Lihan Xie, Shengnan Zhao, Mridula Balakrishnan, and Eleanor Vail, who are caring and encouraging friends, never putting themselves first. I am thankful for [too] long lunch sessions, weekend hikes, chess at work and board game nights, all of which helped maintain sanity and high spirit.

Thank you to other fellow PhD and PostDoc colleagues: Mohamed El-Brolosy, Hadil El-Sammak, Vahan Serobyan, Paolo Panza, Simon Perathoner, whose camaraderie, [occasional] intellectual and [mostly] too-dangerous-to-disclose discussions, as well as rare glimpses of good humor have created a stimulating environment that has not impoverished, and sometimes even enriched, my academic journey.

I would like to extend my thanks to the lab's technical staff, particularly Sharon Meaney-Gardian, technicians Petra Neeb, Carmen Büttner, Justin Martinez, FACS facility managers Kikhi Khrievono and Ann Atzberger, Stefan Günther from the Deep Sequencing Platform Scientific Service Group and once again Simon Perathoner for their invaluable assistance in laboratory work, equipment maintenance, technical support, and scientific documentation. Their professionalism has significantly contributed to the smooth execution of my experiments.

I wish to acknowledge the financial and educational support provided by Boehringer Ingelheim Fonds (BIF). Their support in helping me travel and present my research abroad, as well seminars, BIF fellows' gatherings and

coursework have been pivotal in enabling the successful completion of this research and deciding on my future career steps.

Lastly, to my family, my significant other Gintarė, brother Kristijonas, father Mindaugas, grandparents Lilijana, Jonas, Regina, Rimvydas, but most importantly mother Eitautė, who was, excluding my supervisors and me, the most interested, but the least informed person about my project progress, I am deeply grateful for your boundless encouragement, patience, and love. Your belief in me has been the driving force behind my pursuit of academic excellence.

In conclusion, the journey towards completing this study has been a collective effort, and I am sincerely grateful to each and every individual who has played a part, no matter how big or small, in making this accomplishment possible.